EDGEWOOD

CHEMICAL BIOLOGICAL CENTER

U.S. ARMY RESEARCH, DEVELOPMENT AND ENGINEERING COMMAND

ECBC-CR-085

RESPIRATOR FILTER EFFICIENCY TESTING AGAINST PARTICULATE AND BIOLOGICAL AEROSOLS UNDER MODERATE TO HIGH FLOW RATES

Aaron W. Richardson
Jonathan P. Eshbaugh
Kent C. Hofacre

BATTELLE MEMORIAL INSTITUTE
Columbus, OH 43201-2693

Paul D. Gardner

RESEARCH AND TECHNOLOGY DIRECTORATE

August 2006

ABERDEEN PROVING GROUND, MD 21010-5424

Disclaimer

The findings in this report are not to be construed as an official Department of the Army position unless so designated by other authorizing documents.

REPORT DOCUMENTATION PAGE

Public reporting burden for this collection of information is estimated to average 1 hour per response, including the time for reviewing instructions, searching existing data sources, gathering and maintaining the data needed, and completing and reviewing this collection of information. Send comments regarding this burden estimate or any other aspect of this collection of information, including suggestions for reducing this burden to Department of Defense, Washington Headquarters Services, Directorate for Information Operations and Reports (0704-0188), 1215 Jefferson Davis Highway, Suite 1204, Arlington, VA 22202-4302. Respondents should be aware that notwithstanding any other provision of law, no person shall be subject to any penalty for failing to comply with a collection of information if it does not display a currently valid OMB control number. **PLEASE DO NOT RETURN YOUR FORM TO THE ABOVE ADDRESS.**

1. REPORT DATE (DD-MM-YYYY)	2. REPORT TYPE	3. DATES COVERED (From - To)
XX-08-2006	Final	Dec 2003 - Oct 2005

4. TITLE AND SUBTITLE	5a. CONTRACT NUMBER
Respirator Filter Efficiency Testing against Particulate and Biological Aerosols under Moderate to High Flow Rates	SPO700-00-D-3180
	5b. GRANT NUMBER
	5c. PROGRAM ELEMENT NUMBER

6. AUTHOR(S)	5d. PROJECT NUMBER
Richardson, Aaron W.; Eshbaugh, Jonathan P.; Hofacre, Kent C. (Battelle Memorial Institute); and Gardner, Paul D. (ECBC)	
	5e. TASK NUMBER
	335
	5f. WORK UNIT NUMBER

7. PERFORMING ORGANIZATION NAME(S) AND ADDRESS(ES) AND ADDRESS(ES)	8. PERFORMING ORGANIZATION REPORT NUMBER
Battelle Memorial Institute, 505 King Avenue, Columbus, OH 43201-2693 DIR, ECBC, ATTN: AMSRD-ECB-RT-PR, APG, MD 21010-5424	ECBC-CR-085

9. SPONSORING / MONITORING AGENCY NAME(S) AND ADDRESS(ES)	10. SPONSOR/MONITOR'S ACRONYM(S)
DIR, ECBC, ATTN: AMSRD-ECB-RT-PR, APG, MD 21010-5424	
	11. SPONSOR/MONITOR'S REPORT NUMBER(S)

12. DISTRIBUTION / AVAILABILITY STATEMENT
Approved for public release; distribution is unlimited.

13. SUPPLEMENTARY NOTES
COR: Paul Gardner, AMSRD-ECB-RT-PR, (410) 436-6692

14. ABSTRACT
The growing terrorism threat associated with biological and chemical agents presents a challenge to emergency responders, healthcare workers, and the civilian population. Currently, National Institute for Occupational Safety and Health (NIOSH)-approved respirators are used in various workplace settings to provide protection against harmful aerosols. The primary objective of this project was to evaluate and compare the aerosol filtration performance of NIOSH-approved respirator filters with non-biological (inert) and biological test aerosols under breather flow rates associated with high work rates. The inert test challenges consisted of solid and oil aerosols having nominal diameters ranging from 0.02 to 3.02 μm, spanning the spectrum of potential biological threat agents. As expected, penetration of submicron aerosols was found to increase under increased cyclic and constant flow conditions. The magnitude and significance of this increase was dependent on the specific filter type and design. The most penetrating particle size was generally between 0.1 and 0.2 μm for the P100 filters and 0.05 and 0.10 μm for the N95 filters. Inert aerosols of similar aerodynamic diameter were shown to provide a reasonable estimate of performance against the biological aerosols tested, Bg spores and MS2 phage. The second objective was to assess the extent of reaerosolization of surrogate biological agents from NIOSH-approved filtering facepieces. The extent of reaerosolization was dependent on the particle size, particle type, and loading level.

15. SUBJECT TERMS

Filtration efficiency	Bioaerosol	Biological aerosol	Cyclic	High flow
Aerosol penetration	Filter	Reaerosolization	Breathing	Reentrainment

16. SECURITY CLASSIFICATION OF:			17. LIMITATION OF ABSTRACT	18. NUMBER OF PAGES	19a. NAME OF RESPONSIBLE PERSON
					Sandra J. Johnson
a. REPORT	b. ABSTRACT	c. THIS PAGE			19b. TELEPHONE NUMBER (include area code)
U	U	U	UL	181	(410) 436-2914

Blank

EXECUTIVE SUMMARY

The growing terrorism threat associated with biological and chemical agents presents a challenge to emergency responders, healthcare workers, and the civilian population. The use of National Institute for Occupational Safety and Health (NIOSH)-approved respirators, if used according to recommended practices, provides protection against harmful agents in different workplace settings. Currently, NIOSH certifies respirators based on an inert aerosol test at a constant flow rate of 85 L/min. However, measurements of physiological parameters of workers show peak inhalation flow rates for short durations in the 300 to 400 L/min range for certain activities that demand high work loads. One objective of this study was to investigate the effects of high volumetric and peak flow rates on respirator filtration performance. In addition, although NIOSH-approved respirator filters have been shown to provide adequate protection against inert aerosols, their performance with respect to protection against bioaerosols has not been extensively assessed. Thus, another objective of this study was to evaluate and compare the aerosol filtration performance of NIOSH-approved respirator filters with non-biological (inert) and biological test aerosols.

Four cyclic and three constant flow conditions were selected based on an analysis completed by the U.S. Army's Edgewood Chemical Biological Center (ECBC) to assess the relationship between work load and ventilation rate. The cyclic flow conditions have minute volumes ranging from moderate (40 L/min) to high (135 L/min) with peak flows up to 430 L/min. The respirator filters were selected in coordination with NIOSH and included two N95 and two P100 filtering facepieces, and two N95 and two P100 cartridges. The inert aerosol challenges had nominal diameters ranging from 0.05 to 3.0 μm and were selected to span a range of potential bioaerosol threat agent sizes to include nanoparticles well below the size of bioaerosol threat agents. Oil aerosols were used with the P100 filters and solids with the N95 filters. The biological aerosols included bacterial *B. globigii* (Bg) spores and the virus MS2 phage.

The most penetrating particle size was generally between 0.1 and 0.2 μm for the P100 filters and 0.05 and 0.10 μm for the N95 filters. The inert testing demonstrated that the penetration of submicron particles tends to increase with flow rate or filtration velocity. The magnitude and significance of this increase was dependent on the specific filter design. For example, the SEA HE-T P100 cartridge met the P100 requirement (less than 0.03 percent penetration) even at the highest cyclic flow conditions. In comparison, the Survivair 1050 P100 cartridge, which has approximately half of the available surface area, had a penetration in excess of 0.1 percent. Although several of the filters had penetrations in excess of the NIOSH requirement at the highest flow conditions, the intended use and assigned protection factor of the respirator must be considered to determine whether the increase in penetration is significant.

Comparison of the penetrations measured under constant and cyclic flow conditions showed that the mean and peak inhalation flow (PIF) rates were important parameters. For the P100 cartridges, similar penetrations were measured under constant and cyclic flow if the constant flow was equivalent to the mean inhalation flow rate. In contrast to the P100 cartridges, it may be more important to consider the PIF when testing filtering facepieces or N95 cartridges, especially at the high volumetric flow rates that can be experienced during heavy work loads.

The N95 filters are not as suitable for the high volumetric flow rate applications as evidenced by their lower surface area as compared to the P100 cartridges. Selecting a constant flow equivalent to the peak inhalation flow generally provides a conservative estimate of filter performance under cyclic flow conditions.

The filtration efficiency of the N95 and P100 filters was also assessed against bioaerosol challenges, Bg spores and MS2 phage, aerosolized both from liquid suspension and a dry powder. The performance of NIOSH-approved N95 and P100 respirator filters was assessed against the bioaerosol challenges under high volumetric flow conditions. Mean penetrations were below the penetration requirements for the respective filter types (i.e., penetration less than 5 percent for N95 and less than 0.03 percent for P100 filters) under all flow conditions tested. Penetrations of Bg spores through the P100 filters were typically below detectable limits, thus, penetrations were at least an order-of-magnitude below the P100 requirement. The N95 filters also were very efficient at removing the bacterial aerosol challenges as average penetrations were less than 0.5 percent. There were no practical differences in the penetrations measured using the "wet" and "dry" Bg spore aerosolization methods. The most penetrating of the biological aerosols tested was the "wet" MS2 phage as the particle size was closest to the most penetrating particle size (MPPS) as measured using inert aerosol challenges. Average penetrations through the N95 and P100 filters were typically less than 2 and 0.03 percent, respectively, under all flow conditions. Inert aerosols of similar aerodynamic diameter were shown to provide a good estimate of performance against biological aerosols. The Bg spore "wet" and "dry" aerosol penetration was generally within a factor of five of the penetrations measured using the 1.3 μm PSL. Similarly, the MS2 "wet" aerosol penetration through the cartridges was within a factor of five of the inert aerosol penetrations measured using the 0.3 μm PSL. Comparisons were not made with the MS2 "dry" as aerosol penetration was typically below detectable limits. However, this is in agreement with the penetrations measured for the 2.3 μm PSL. The results demonstrated that testing with inert particles in the MPPS range provide a conservative estimate of biological aerosol penetration for those biological aerosols assessed in this study. Finally, the results demonstrated that using an optical light scattering instrument such as the LAS to measure bacterial aerosol penetration provides a conservative estimate of filter performance. This is notable due to the labor intensive nature of the bioassay method.

A test method was developed to quantify the extent of reaerosolization from a filtering facepiece loaded with either an inert or biological aerosol. Tests were performed to assess the effect of particle size, particle type, and loading level. Two brands of filtering facepieces were tested, the MSA Affinity Plus and Gerson 1730. The levels and trends of reaerosolization were similar for both brands. For the inert aerosols, reaerosolization was observed to increase with increased particle size over the range tested (0.8 to 2.2 μm). This trend was consistent with that observed by Qian et al. (1997) who attributed this to increased drag force on the larger particles.

The extent of reaerosolization of 0.8 μm particles from filtering facepieces without exhalation valves was very low (less than 0.002 percent or 1 in every 50,000 particles loaded). Reaerosolization was observed to increase by an order of magnitude when the same brands of filtering facepieces were tested with exhalation valves. This was attributed to the movement of the valve and localized high velocity air that could re-entrain particles collected on the surface of

the valve or valve housing. Specifically for the 0.8 μm PSL, the number of particles reaerosolized was observed to increase with increased loading over the range from 1×10^4 to 1×10^6 particles/cm^2. However, the number of particles did not increase proportionally to the increased loading. Increasing the loading by a factor of 10 only increased the number of particles reaerosolized by a factor of 5. Further work is recommended to determine whether similar trends hold for larger particles.

The percent reaerosolization of the biological aerosols was greater than that observed for the inert aerosols with a similar AMMD. For example, reaerosolization of the 0.8 μm PSL was minimal (~0.002 percent) while reaerosolization of the similarly-sized Bg spores was typically 0.05 to 0.1 percent. Similarly, reaerosolization of the 2.2 μm PSL was only 0.01 percent while reaerosolization of the comparably-sized MS2 "dry" was 0.5 percent. The higher reaerosolization for the biological aerosols was attributed to their broader size distribution. For example, the MS2 "dry" aerosol had significant mass between 2.5 and 5.0 μm that contained viable particles. As described above, the extent of reaerosolization was shown to increase with increased particle size. Thus, it is important to consider the entire size distribution and not just the nominal particle size when selecting an inert simulant.

In conclusion, the performance of NIOSH-approved N95 and P100 cartridges and filtering facepieces has been assessed against both inert and biological aerosols under high flow conditions representative of ventilation rates during heavy activity. All filters tested were very efficient against the bioaerosols tested in this study as measured penetrations were below NIOSH requirements for all flow conditions tested. The penetrations of inert particles provided a good indication of filter performance against bioaerosols with a similar aerodynamic diameter. When comparing penetrations measured under constant and cyclic flow, those measured at a constant flow equivalent to the cyclic flow MIF provided a good estimate of performance under cyclic flow conditions (i.e., generally within a factor of 2 to 4). Testing at a constant flow equivalent to the PIF results in higher penetrations than measured under the cyclic flow condition and, thus, would provide a more conservative estimate of performance. All cyclic flow testing performed in this task was done using a sinusoidal flow profile. Additional testing is recommended with alternative waveforms such as a trapezoidal waveform to assess the effect of flow profile. Finally, a method was developed to assess reaerosolization of inert and biological aerosols loaded onto a filtering facepiece due to a cough. The extent of reaerosolization was shown to be dependent on particle type, particle size, and loading level. Further work is recommended to assess the effect of varying the reentrainment flow profile (e.g., sneeze or cough profiles with different peak flows) and to assess the effect of loading level of particles greater than 1 μm.

Blank

PREFACE

Acknowledgments

Blank

CONTENTS

FIGURES

TABLES

RESPIRATOR FILTER EFFICIENCY TESTING AGAINST PARTICULATE AND BIOLOGICAL AEROSOLS UNDER MODERATE TO HIGH FLOW RATES

1.0 INTRODUCTION

1.1 Background

The growing terrorism threat associated with biological and chemical agents presents a challenge to emergency responders, healthcare workers, and the civilian population. Currently, National Institute for Occupational Safety and Health (NIOSH)-approved respirators are used in various workplace settings to provide protection against harmful aerosols. Particulate respirator filters are certified using an inert aerosol at a flow rate of 85 L/min. While this is sufficient to ensure protection in most situations when used according to recommended practices, it is unknown how these filters would perform at higher flow rates or against a biological aerosol that could be encountered in an act of terrorism. A rigorous, definitive study assessing respirator filter performance challenged with bioaerosols has not yet been conducted to fully address particle size dependence. In addition, investigations on the effects of high volumetric and peak flow rates on respirator filtration performance associated with high work rates are lacking.

1.2 Objective

The primary objective of this task was to evaluate and compare the aerosol filtration performance of NIOSH-approved respirator filters with non-biological (inert) and biological test aerosols under high breather flow rates. In addition, penetrations measured under constant and cyclic flow conditions were compared. Finally, the extent of reaerosolization of surrogate biological agents from NIOSH-approved filtering facepiece masks was characterized.

1.3 Scope

The literature review completed to identify previous efforts to assess the effects of particle size, particle type, and/or flow condition on the performance of particulate respirator

1

filters is described in Section 2.0. Section 3.0 describes the test matrices, methods, and results of the inert filtration efficiency testing performed at the U.S. Army's Edgewood Chemical Biological Center (ECBC). A similar summary of the bioaerosol testing performed at Battelle follows in Section 4.0. The test method developed for reaersolization and the results are discussed in Section 5.0. Conclusions and recommendations are provided in Section 6.0.

2.0 LITERATURE REVIEW

2.1 Search Strategy

A literature search was completed to identify previous efforts to assess the effects of particle size, particle type, and/or flow condition on the performance of particulate respirator filters. The purpose of the search was to help define the test parameters and matrices for this task. The search included the open literature, test standards, and the Chemical Biological Information Analysis Center (CBIAC) and Defense Technical Information Center (DTIC) databases. A partial list of search terms included: filter, respirator, efficiency, penetration, cyclic, breather, aerosol, and biological. In addition, a search of the open literature was completed to identify previous work assessing reaerosolization of biological aerosols from filtering facepieces. A partial list of key words used in the search included: filter, respirator, bioaerosol, reaerosolization, and reentrainment. Limited information was identified on the reaerosolization of particles from filter materials. The title, author, and abstract of each record were reviewed to identify the potentially relevant articles.

2.2 Inert Filtration Efficiency

The most relevant studies are summarized below following a brief overview of the primary mechanisms for aerosol collection and the influence of filtration velocity and aerosol size on each mechanism (Section 2.2.1). A number of studies that assessed the effect of both particle size and constant flow rate on measured penetration are reviewed in Section 2.2.2. Two studies that compare penetrations measured under constant and cyclic flow are reviewed in Section 2.2.3.

2.2.1 Aerosol Collection Mechanisms

Particle penetration is dependent on several parameters including the aerosol particle size, filtration velocity (based on flow rate and available surface area), and several filter parameters including the thickness, fiber diameter, and solidity or fiber packing density (i.e., ratio of solid fiber volume to gross filter volume). The four primary collection mechanisms, illustrated in Figure 1, for aerosol filtration are: (1) inertial impaction, (2) interception, (3) diffusion, and (4) electrostatic (Hinds, 1999). The general trends regarding the influence of filtration velocity and aerosol size on the mechanisms are summarized in Table 1. Particles less than 0.1 μm are most effectively collected by the diffusion mechanism. Diffusion occurs when the random (Brownian) motion of a particle causes that particle to contact a fiber. As velocity is increased, collection by diffusion is reduced. Interception occurs when a particle does not deviate from the stream line but is intercepted by the fiber (i.e., streamline passes within one particle radius of fiber). Interception is the most important collection mechanism for particles in the most penetrating particle size (MPPS) and is independent of velocity. Inertial impaction occurs when a particle deviates from the streamline around the fiber and collides with the fiber. This mechanism is most effective for larger particles and is enhanced by higher particle velocities. The electrostatic mechanism is an enhancement to mechanical filtration. Electret media are made of dielectric materials that have a significant microscopic bipolar charge on the fibers with a low net macroscopic charge. Charged particles are attracted to oppositely charged fibers by the Coulombic force. Neutral particles are collected by the polarization force induced by local electric fields within the filter media.
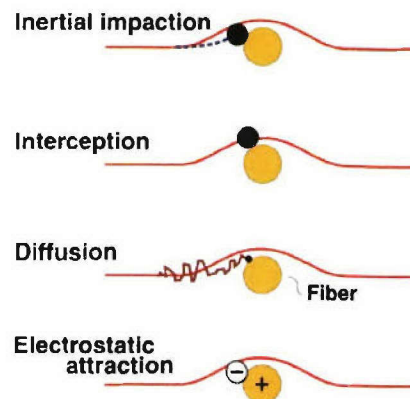
Figure 1. Four Mechanisms of Particle Capture (DHHS, 2003)

3

Table 1. Influence of Filtration Velocity and Aerosol Size on Collection Mechanisms

Mechanism	Increased Filtration Velocity	Increased Aerosol Size
Inertial Impaction	Collection Increased	Collection Increased
Interception	Independent of Velocity	Collection Increased
Diffusion	Collection Reduced	Collection Reduced
Electrostatic	Collection Reduced	Collection Reduced

The three primary collection mechanisms, diffusion, interception, and impaction, are effective over different particle sizes. The MPP through a filter exists where none of the mechanisms is dominant. This generally occurs between 0.05 and 0.5 µm depending on the filter properties and filtration velocity (Hinds, 1999). A generic illustration of the effect of particle size on filtration efficiency is provided in Figure 2. The figure also indicates where each collection mechanism is predominant over the particle size range. Penetration generally increases with increased flow rate or velocity in the region of the MPPS because the diffusion collection mechanism is reduced. This also generally leads to a shift in the MPPS toward smaller particles. Collection efficiency of larger particles can actually increase with increased velocity as the inertial impaction mechanism is enhanced.
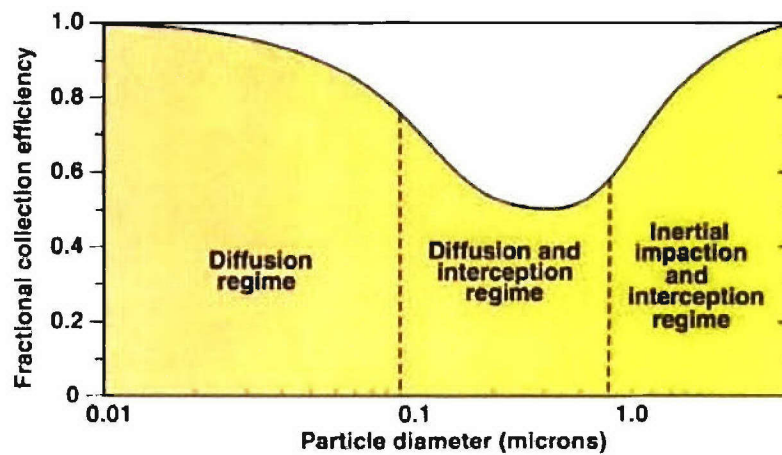
Figure 2. Primary Mechanism of Capture for Various Particle Diameters Indicating MPPS (DHHS, 2003)

2.2.2 Effect of Particle Size/Flow Rate

Several published studies have assessed the effect of particle size and/or flow rate on the measured efficiency of respirator filters including: Ruuskanen et al. (1988), Brosseau et al.

(1989); Stevens and Moyer (1989), Fardi and Lui (1991), Chen et al. (1992), Qian et al. (1998), Hanley and Foarde (2003). The challenge aerosols employed consisted mainly of charge-neutralized dioctyl phthalate (DOP), sodium chloride (NaCl), corn oil, or polystyrene latex (PSL) spheres. The aerosol concentrations upstream and downstream of the filter were typically analyzed using a laser aerosol spectrometer (LAS) or condensation nucleus counter (CNC) for particle sizes in the submicrometer range. For particles larger than 1 μm, researchers frequently used an aerodynamic particle sizer (APS, TSI Inc., Shoreview, MN) or aerodynamic size spectrometer (Aerosizer®, Amherst Process Instruments Inc., Hadley, MA). In general, the studies were conducted at constant flow rates ranging from 16 to 85 L/min using a variety of disposable dust-mist (DM), dust-fume-mist (DFM), and high-efficiency particulate air (HEPA) respirator filters. These respirator filters were certified under the requirements of 30 CFR 11 (1972), which has since been replaced by 42 CFR 84 (1995).

Stevens and Moyer (1989) evaluated the effect of a "worst-case" aerosol on the filtration efficiency of a variety of DM, DFM, and high-efficiency respirator filters. The most penetrating particle sizes were determined as a function of test flow rate. Filters were challenged with either solid NaCl aerosol or liquid DOP aerosol with numerical median diameters (NMDs) ranging from 0.03 to 0.3 μm and constant flow rates ranging from 16 to 85 L/min. The particle size of maximum penetration varied with filter type and flow rate, and was less than 0.25 μm NMD in all cases. As the flow rate was increased, the magnitude of penetration increased and a shift towards a smaller particle size for maximum penetration was observed. This is consistent with the mechanisms described above. At the most penetrating conditions, the high-efficiency filters provided greater than 99.97 percent efficiency, while the DM and DFM respirators had efficiencies ranging from 67 to 89 percent and 85 to 99 percent, respectively.

Brosseau et al. (1989) evaluated electrostatic DM respirators from ten manufacturers challenged with monodisperse PSL particles ranging in size from 0.102 to 2.02 μm. Filter penetration was greatest for particles 0.1 μm in diameter, which was consistent with the results of Stevens and Moyer (1989). In addition, appreciable differences were found in the performances of filters distributed by the ten different manufacturers, where filter penetration ranged from about 5 to 15 percent for the most penetrating particle sizes.

Fardi and Liu (1991) challenged DM and DFM respirators composed of charged and uncharged fibers using monodisperse NaCl and DOP particles with diameters in the range of

0.035 to 0.4 µm. Tests were conducted at constant flow rates ranging from 16 to 48 L/min, and aerosol penetration measurements were made using a condensation nucleus counter, aerodynamic particle sizer, and laser optical particle counter for purposes of comparison. Results obtained by these instruments were in agreement with each other in the overlapping size range of the instruments. The most penetrating particle size was found to be approximately 0.1 µm for filters containing charged fibers and 0.3 to 0.4 µm for mechanical filters. Consistent with Stevens and Moyer (1989), for all filters tested there was an increase in penetration with increasing particle size for small particles until a maximum was reached, and then penetration decreased with particle size for larger particles. For the range of respirator filters tested, the peak penetration varied from 1.2 to 30 percent at 16 L/min, 3.5 to 37 percent at 28 L/min, and 6 to 45 percent at 48 L/min. There was no significant difference in penetration between solid NaCl and liquid DOP particles of the same size.

Chen et al. (1992) assessed aerosol penetration as a function of particle size for several filtering facepieces and DM, DFM, and HEPA respirator cartridges using corn oil particles over a size range of 0.1 to 15 µm. Tests were conducted at constant flow rates ranging from 5 to 100 L/min. The respirators were sealed to a mannequin head form during testing. Results showed an increase in aerosol penetration with increasing flow rate in the submicrometer size range, leading the authors to concede that the primary removal mechanisms are diffusion and electrostatic attraction within this size range. The penetration of supermicrometer-sized aerosol particles decreased with mask flow, indicating removal of large particles by impaction.

Only a limited number of recent studies were identified that have evaluated N-, R-, and P-type respirators certified under 42 CFR 84. Qian et al. (1998) compared the measured filtration efficiency of NIOSH-approved N95 respirators with that of DM and DFM respirators using challenge aerosols of NaCl and PSL particles with sizes ranging from 0.1 to 5.10 µm. Tests were conducted at constant flow rates of 32 and 85 L/min. N95 respirators were found to have higher filtration efficiencies than DM and DFM respirators, showing at least 95 percent efficiency against particles at the most penetrating particle size (0.1 to 0.3 µm). The filtration efficiency increased with size, reaching approximately 99.5 percent or higher at about 0.75 µm.

In a more recent study, Hanley and Foarde (2003) assessed the filtration efficiency provided by the C2A1 canister against an inert potassium chloride aerosol (0.3 to 10 µm) over a range of constant flow rates (30, 50, and 80 L/min). The results demonstrated that the

penetration rapidly decreased as the particle size increased above 0.3 μm, and penetration of particles ranging from 0.3 to 0.7 μm increased with higher flow rate. Penetrations could not be accurately measured for particles greater than 0.7 μm as the downstream aerosol concentrations were below the detection limit of the aerosol particle counter, demonstrating the difficulty in generating sufficient challenge concentrations of the larger particles to accurately measure penetrations of high-efficiency filters.

Martin and Moyer (2000) evaluated several N95, N99, R95 and P100 electrostatic respirator filters to determine filter efficiency and most penetrating particle size. Challenge aerosols included NaCl (0.075 μm NMD, 1.86 GSD) and DOP (0.185 μm NMD, 1.60 GSD), and a constant flow rate of 85 L/min was used for N95 filters and 42.5 L/min for N99, R95, and P100 filters. Tests involved comparing "as received" filters to those dipped in isopropanol to remove the electrical charge associated with the filter fibers. All of the filters tested which had the electrostatic charge removed showed a dramatic increase in filter penetration. For the NaCl aerosol, N-series filters increased in maximum penetration from less than 5 percent up to 35 to 55 percent. Similarly, the maximum penetration increase with the R95 filters was from 0.03 percent up to 50 percent and for the P100 filters from 0.001 to 4 percent. In addition, there was a shift in the most penetrating particle size from approximately 0.05 to 0.10 μm for the new filters toward larger sizes in the 0.25 to 0.35 μm range once the electrostatic charge was removed.

2.2.3 Comparison of Constant/Cyclic Flow Penetrations

A limited number of studies were identified that assessed the effect of cyclic flow on filter performance. The two most relevant studies were by Stafford et al. (1973) and Brosseau et al. (1990).

Stafford et al. (1973) measured the penetration of monodisperse PSL (0.176 to 2.02 μm) and DOP (0.3 μm) aerosols through respirator filter cartridges at three cyclic flows with mean flow rates of 30, 35, and 53 L/min. These flows were selected to correspond to work rates of 415, 622, and 830 kg-m/min. Tests were also conducted at a constant flow rate of 16 L/min (equivalent to 32 L/min through a pair of cartridges). At steady-flow conditions, the maximum penetration occurred at a particle size of 0.3 μm, which is consistent with theoretical single-fiber predictions. However, during cyclic flow the particle size that produced maximum penetration

varied between filters, in one case less then 0.3 μm and in the other approximately 0.5 μm. Also, the maximum penetration was considerably higher than corresponding steady-flow values, suggesting that tests conducted under steady-flow conditions may provide a considerable overestimate of filter performance.

Brosseau et al. (1990) compared the collection of silica and asbestos aerosols by DM respirators under breathing and constant flows. The cyclic flow was sinusoidal with a mean flow of 76 L/min and a peak flow of 100 L/min, and represented a work rate of 622 kg-m/min. The constant flow rate was 32 L/min. In general, the silica penetration under cyclic flow conditions was about one and a half times as great as that measured under steady flow conditions, which is consistent with the results of Stafford et al. (1973). The asbestos results were inconclusive as the results varied by filter.

2.3 Biological Filtration Efficiency

The majority of research published in the open literature has focused on evaluation of surgical masks and a variety of disposable dust-mist (DM), dust-fume-mist (DFM), and high-efficiency particulate air (HEPA) respirator filters for protection against bacterial aerosols (Brosseau et al., 1994; Chen et al., 1994; Johnson et al., 1994; Willeke et al., 1996; Brosseau et al., 1997; McCullough et al., 1997; Wake et al., 1997; Qian et al., 1998).

2.3.1 Test Methods

Previous studies were largely conducted to assess use of respirators in controlling healthcare-worker exposures to infectious biological aerosols, namely *Mycobacterium tuberculosis*, the organism which causes tuberculosis. The studies used bacterial test aerosols including *M. chelonae*, *M. abscessus*, *Bacillus subtilis*, *B. megatherium*, *B. alcalophilus*, *Streptococcus salivarius*, *Staphylococcus epidermidis*, *Pseudomonas fluorescens*, *P. alcaligenes*, and *Micrococcus luteus* to simulate pathogenic organisms such as *M. tuberculosis*. No studies were identified in the open literature that assessed viral aerosol penetration through respirator filters.

8

Test system designs and methodologies employed for evaluating mask and respirator filter efficiency against biological aerosols varied between different research groups. Brousseau et al. (1994) used a column apparatus with vertical airflow to minimize aerosol losses to the duct walls by sedimentation. The mask or respirator filter was sealed with wax onto a metal plate within the duct. Measurements upstream and downstream of the filter were corroborated with Andersen cascade impactors and an aerodynamic particle sizer (APS, TSI Inc.), which measures the aerosol concentrations of viable and total particles, respectively. By comparison, Willeke et al. (1996) conducted tests using a rectangular test chamber with perforated metal sheets at the top and bottom of the chamber to ensure a uniform aerosol concentration in the vicinity of the test mannequin. The mask or respirator was sealed to the mannequin head form with silicone adhesive or petroleum jelly. Upstream and downstream particle concentrations were measured with an aerodynamic size spectrometer (Aerosizer®, Amherst Process Instruments Inc.) Finally, Wake et al. (1997) designed a test system which was comprised of two aerodynamically identical flow lines, one of which contained the mask or respirator filter while the other served as a reference line. The mask or filter was sealed with PVC tape or hot-melt adhesive within the flow line, and the downstream aerosol concentrations were measured using all glass impingers (AGI) for both the filtered and reference lines. The penetration through the filter was obtained from the ratio of the filtered and reference lines.

The bacterial aerosols were typically aerosolized using a 6-jet Collison nebulizer (BGI Inc.) operated at pressures ranging from 7 to 15 psi. McCullough et al. (1998) found that reducing the nebulizer operating pressure to 3 psi increased the percentage of culturable particles of *M. abscessus* from 15 to 45 percent. Generated challenge concentrations, if reported, were generally in the range of 10^4 to 10^6 colony forming units (CFU)/m^3 air, the higher concentration being used to provide a sufficient downstream concentration when testing the most efficient filters. Most studies were conducted under constant airflow rates ranging from 16 to 85 L/min. As alluded to above, a variety of techniques have been used to measure the challenge and filtered aerosol concentrations. Total particle analyzers used include the APS, Aerosizer®, and LAS. Viable particle samplers include the Andersen six-stage impactor, membrane filters, and AGIs. Viable sampling involves collecting and transferring the sampled organisms onto growth media to allow the organism to replicate for enumeration. Organism viability can be reduced due to aerosolization, transport, and sampling. Total particle analyzers measure both viable and

9

non-viable particles, therefore aerosol concentration measurements are higher than those determined by viable samplers. Strong correlation of filter penetration measured by viable samplers and the APS has been reported (Brousseau et al., 1994; Chen et al., 1994; McCullough et al., 1997; Johnson and Andersen, 1996). In some cases, it was noted that the filter penetrations were slightly lower for the Andersen impactor (Chen et al., 1994) and AGI (Johnson and Andersen, 1996) compared to the APS. However, because of the strong correlation, researchers suggest that a total particle analyzer may be used in place of more labor-intensive viable sampling techniques for determining bioaerosol penetration.

A single test standard was identified for evaluating the filtration efficiency of medical face mask materials using a biological aerosol (ASTM F 2101-01, 2001). A bacterial aerosol of *S. aureus* is generated from a suspension using a nebulizer, with a target mean particle size of 3.0 μm. Tests are conducted under a constant flow rate of 28.3 L/min. A six-stage Cascade impactor is used to measure the aerosol penetration downstream of the filter. The reported maximum filtration efficiency that can be measured using this method is 99.9 percent.

2.3.2 Inert/Biological Penetration Comparison

Several studies have compared measured penetrations of inert and biological aerosols through masks and respirator filters. Qian et al. (1998) evaluated the unloaded filtration efficiency of NIOSH-approved N95 respirators using challenge aerosols of polydisperse NaCl particles (0.1 to 0.7 μm), monodisperse polystyrene latex (PSL) spheres (0.60, 1.02, 2.94, 3.96, and 5.10 μm), and two bioaerosols, *B. subtilis* (mean aerodynamic diameter 0.8 μm) and *B. megatherium* (mean aerodynamic diameter 1.2 μm). Tests were conducted at a constant flow rate of 85 L/min. For both bacteria, the filtration efficiency of the N95 respirator was 99.5 percent or higher, equivalent to the data for the inert particles of the same aerodynamic diameter.

Brousseau et al. (1994) compared filtration efficiencies of the bioaerosol *M. chelonae* (0.78 μm NMAD, 1.2 GSD) to inert aerosols containing either monodisperse PSL particles (0.804 μm) or dioctyl phthalate (DOP) particles (0.12 μm NMAD, 1.5 GSD) for various layers of fiberglass flatsheet filter media. Tests were conducted at a steady flow rate of 46 L/min. Results indicated no significant difference in penetration through flatsheet fiberglass filter media

when challenged with *M. chelonae* and PSL particles of the same aerodynamic size. In addition, penetration of DOP particles as measured with an optical particle counter were closely correlated with the penetration of *M. chelonae* measured by the Andersen impactor and APS, as well as PSL particles measured by the APS. Based on their results, Brousseau et al. suggest that an inert aerosol with aerodynamic particle size similar to a bioaerosol of interest is an appropriate test aerosol to predict bioaerosol filter collection.

Under equivalent test conditions, Chen et al. (1994) report this same conclusion for experiments with a surgical mask and several disposable DM, DFM, and HEPA respirators against challenge aerosols of *M. chelonae* and PSL particles. Mean efficiencies for viable *M. chelonae* ranged from 97 percent for the surgical mask and DM respirator to more than 99.99 percent for the HEPA respirator. Mean efficiencies for the PSL particles were slightly lower in some cases, ranging from 96 percent for the surgical mask and DM respirator to more than 99.99 percent for the HEPA respirator. Chen et al. raised the question about practical significance of the measured differences between the filters tested in their study (less than 3 percent), when it has been estimated that at least 10 to 20 percent leakage occurs in masks not properly fitted to the wearer's face.

Wake et al. (1997) evaluated the filter efficiency of several respirator filters, disposable dust masks, and surgical masks against the bioaerosols *B. globigii*, *M. luteus*, and *P. alcaligenes*, monodisperse urea aerosols (1.5, 3, 5, 7, and 9 μm), and a NaCl aerosol (0.6 μm MMAD, 2.3 GSD). Bacterial penetration generally corresponded to those of non-biological aerosols of similar size, but no direct comparisons were made. Bacterial penetration ranged from less than 0.01 percent to 0.88 percent for various glass fiber and wool resin respirator filters, compared to up to 1.56 percent for the 1.5 μm urea particles and up to 0.31 percent for the NaCl particles.

Hanley and Foarde (2003) assessed the filtration efficiency provided by the C2A1 canister against a bioaerosol of *B. globigii* (Bg) spores over a range of constant flow rates (30, 50, and 80 L/min). For comparison, tests were also completed with a polydisperse potassium chloride aerosol with particles ranging in size from 0.3 to 10.0 μm. Samples of the challenge and downstream aerosol were collected on polycarbonate membrane filters with a pore size of 0.4 μm. Downstream samples were collected on filters with a diameter of 142 mm to allow the full canister flow to be passed through the filter without excessive pressure drop. All measured efficiencies with the bioaerosol challenge exceeded 99.99997 percent. In 31 of 33 tests, no Bg

spores were detected downstream of the C2A1 canister. The results demonstrated that inert aerosol penetration in the 0.7 to 1.0 μm size range were consistent with those measured using the Bg spore challenge.

Previous reports on filter performance against particles of various sizes, shapes and aspect ratios contain conflicting results. Willeke et al. (1996) compared penetrations through surgical masks and DM respirators of several rod-shaped bacteria (*B. megatherium*, *P. fluorescens*, *B. alcalophilus*) of varying aspect ratios with that of spherical *S. salivarius* and inert corn oil particles. Results indicate the penetration of spherical *S. salivarius* bacteria were approximately the same as spherical corn oil particles in the aerodynamic size range from 0.9 to 1.7 μm. The penetration of rod-shaped bacteria was lower than *S. salivarius*, and decreased with increase of aspect ratio showing that filter penetration of bacteria is a strong function of their shape. As an example, *Pseudomonas fluorescens*, with an average aspect ratio of 3, was found to penetrate 50 to 60 percent less than spherical particles of the same aerodynamic diameter. Willeke et al. postulated that due to greater surface area of non-spherical particles compared to spherical ones, interception and electrostatic attraction cause greater removal (i.e., less penetration) for rod-shaped bacteria compared to spherical particles of the same aerodynamic size.

In comparison, McCullough et al. (1997) evaluated the penetration of *M. abscessus* (mean aerodynamic diameter 0.69 μm), *B. subtilis* (mean aerodynamic diameter 0.88 μm), and *S. epidermidis* (mean aerodynamic diameter 0.87 μm) bioaerosols, along with a monodisperse PSL aerosol (0.55 μm) through a variety of DM and DFM respirator filters and surgical masks. In all cases, penetration of the PSL aerosol was greater than any of the biological aerosols due to its smaller aerodynamic diameter. However, the penetration of *B. subtilis* (a rod) was found greater than *S. epidermidis* (a sphere) at approximately the same aerodynamic diameter. Contrary to Willeke et al. (1996), the authors suggested that the aerodynamic diameter of the bacteria may not be an accurate predictor of aerosol penetration for non-spherical particles in these filters, particularly when electrostatic forces are dominant.

Particle shape was also found to influence penetration through fibrous filters. Tuinman and Steeenweg (1998) compared aerosols with several shapes including rod-shaped caffeine particles, angular urea particles, plate-like eicosanoic acid particles, and needle-shaped arachidic acid particles to spherical oil particles with an equivalent particle size distribution

12

(approximately 0.04 to 0.8 μm). The penetration decreased from spherical particles to angular particles and rods to the lowest penetration for plates. The reduction in penetration for rod-shaped particles compared to spherical particles was consistent with the findings of Willeke et al. (1996) for rod-shaped bacteria with aspect ratio similar to the caffeine particles.

2.3.3 Effect of Flow Rate

Several studies have been conducted assessing the effects of flow rate on filter efficiency of biological aerosols. Willeke et al. (1996) evaluated constant air flow rates ranging from 16 to 80 L/min to simulate breathing rates representative of conditions ranging from rest to strenuous work. Increasing the flow to 50 and 80 L/min resulted in increased penetrations of *P. fluorescens* through a DM respirator of 6 and 8 percent, respectively. The effect was most significant for particles less than 1 μm in aerodynamic diameter. Brosseau et al. (1997) assessed the effect of flow rate (45 and 85 L/min) and relative humidity (30 and 70 percent) on the penetration of *M. abscessus* aerosol through 16 respirator filters and 5 surgical masks. The median penetration of *M. abscessus* at 45 L/min was 2, 0.4, and 0.02 percent for DM, DFM, and HEPA filters, respectively. Increasing the flow rate to 85 L/min resulted in greater penetration, and changes in relative humidity caused minimal effects on bioaerosol collection. McCullough et al. (1997) reported similar results for a variety of respirator filters and surgical masks against three bacterial aerosols (*M. abscessus, S. epidermidis, B. subtilis*) under the same flow rate and relative humidity conditions. Only one study, conducted by Johnson et al. (1994), was identified in the open literature that tested a biological aerosol using cyclic rather than constant flow conditions. Johnson et al. simulated normal breathing during light exertion using an automated breathing simulator (TSI Inc.) operated at a breathing rate of 15 breaths/min, tidal volume of 1.5 L/breath, and minute volume of 22.5 L/min.

2.3.4 Viral Filtration Efficiency

Research efforts on respirator filter efficiency have largely focused on bacterial aerosols, thus limited information on viral aerosols was found. Harstad and Filler (1969) evaluated the performance of ultra-high-efficiency filter papers against the submicron viral aerosol of T1

bacteriophage (0.12 μm NMD) and the bacterial aerosol of *B. globigii* spores (1.0 μm NMD). Submicron phage aerosols were generated using a Dautrebande aerosol generator, Bg spore aerosols using a vaponefrin nebulizer, and aerosol concentration was measured upstream and downstream of the test filter using AGIs. Phage penetration through filters averaged 0.00095 percent, and increased markedly (up to 0.39 percent) with an increase in velocity up to 150 ft/min and neutralizing with bipolar air ions. Penetration of bacterial spore aerosols through the filter papers was essentially zero.

Hofacre et al. (1996) measured the penetration of a viral aerosol of MS2 phage and a monodisperse PSL aerosol (0.173 μm) through a HEPA filter used for collective protection. The MS2 phage aerosol concentrations upstream and downstream of the filter were measured using both a bioassay enumeration technique and a light scattering instrument. The inert aerosol concentrations were measured using the light scattering instrument. Aerosol penetration measured using the light scattering technique was statistically equivalent for both the MS2 phage and PSL particles, while the penetration of MS2 phage measured using the bioassay method was consistently lower. The study concluded that inert aerosols of similar size provided a conservative indication of HEPA filter performance against a bioaerosol.

2.3.5 Reaerosolization

Qian et al. (1997a) evaluated the reaerosolization of inert and biological aerosols from three different models of N95 half-mask respirators at velocities up to 300 cm/sec, intended to represent violent sneezing or coughing. The filters were loaded with aerosols of either NaCl (0.15 to 1.0 μm), PSL (0.60, 1.02, 2.94, 3.96, and 5.10 μm), or the bacterium *B. subtilis* or *B. megatherium*. The flow rate during loading was a constant 85 L/min and the environmental conditions were ambient (T=25°C, RH=22%). The particle loading (1×10^5 particles/cm^2) was the same for both the inert and biological aerosols. A quick release valve was used to pulse the airflow in the opposite direction of loading to simulate the cough or sneeze. An aerosol size spectrometer (Aerosizer®, Amherst Process Instruments, Hadley, MA) was used to measure the concentration up- and downstream of the filter. For each filter model, NaCl particle penetration was less than 5 percent, thus satisfying the certification requirement of 95 percent or more collection efficiency. Reaerosolization was found insignificant for particles less than 1.0 μm,

with less than 0.025 percent becoming reentrained. For the condition of violent sneezing or coughing, only larger particles were reaerosolized in significant amounts, with about 1 percent of 3 μm and 6 percent of 5 μm PSL particles. This is of importance as single bacteria may aggregate or attach to inert particles to form larger clusters, increasing their risk of potential reaerosolization. In addition, results indicate that bacteria become reentrained at high air velocities more easily than the NaCl particles of similar size, which the authors reason may signify a weaker bond to the filter fibers or more surface area exposed to the airflow. Finally, no reaerosolization of particles was observed when the relative humidity was increased to 35 percent, which the authors attribute to liquid bridging between particles and filter fibers that increases the adhesion force.

In a related study, Qian et al. (1997b) assessed the effects of particle size, inert particle type, filter type, and reentrainment velocity on reaerosolization of inert aerosols including NaCl, PSL, corn oil, and dust. Similar test methods were used as described above. Flat sheets of three types of fibrous filter media used in half-mask respirators were evaluated. The collection efficiency of the filters ranged from approximately 93 percent for 0.6 μm particles to 99.8 percent for 5.1 μm particles. Reaerosolization trends were in agreement with the previous study as reaerosolization of 0.6 to 5.1 μm particles increased approximately with the square of particle size and the square of reentrainment velocity, and decreased with relative humidity. Reaerosolization was also found to be a function of the particle type as dust was found to have the highest reentrainment, while corn oil was not reentrained at any of the test conditions. This was attributed to differences in interaction with the filter fibers of oily particles compared to solid, irregularly shaped particles. Consistent with previous studies, electrostatic charges on the filter fibers significantly increased the collection of submicrometer particles; however, particle reaerosolization was only slightly impeded by the embedded charges. Finally, filter properties were found to significantly affect particle reaerosolization. The number of reaerosolized particles decreased slightly with filter thickness, which supports the concept that most of the particles are reentrained from the front layer of the filter. Essentially no particle reentrainment was observed from charged felt, compared with up to 5 to 15 percent from glass fiber HEPA and polypropylene filters.

Reentrainment of bioaerosols from air ventilation filters has also recently been studied. Jankowska et al. (2000) compared the collection efficiency and reentrainment rate of the fungal

spores *Penicillium brevicompactum* and *P. melinii* against that of inert potassium chloride (KCl) particles using a medium prefilter and a higher efficiency fine filter. The fungal spores were aerosolized from an agar surface, simulating dry spore dispersion. Solid KCl particles were aerosolized from an aqueous solution using a Collison nebulizer. The aerosol concentrations up- and downstream of the filter were measured using an Aerosizer®. Filter loading ranged from approximately 10^5 to 10^6 particles/cm². The collection efficiency was found to be slightly lower for fungal spores than for KCl particles of the equivalent aerodynamic size. Reaerosolization increased with reentrainment velocity for all test particles. When the reentrainment velocity was the same as the loading velocity, the reaerosolization was less than 0.4 percent. When the reentrainment velocity was increased to 3.0 m/s, the reaerosolization of fungal spores was higher than that of KCl particles, ranging from 2 to 6 percent for *P. brevicompactum*, 5 to 12 percent for *P. melinii*, and 0.2 to 0.6 percent for KCl particles. The higher reentrainment of fungal spores was attributed to the presence of aggregated spores, such that the reentrainment velocity may become sufficient to break up the aggregates and reentrain the spores. The differences between fungal spores were attributed to surface structure, where *P. melinii* spores have a spiny surface imparting weaker contact with the filter fibers.

2.4 Summary

This section provides a brief summary of the trends observed in the literature and the impact on the current study. In addition, it identifies the data gaps in the literature and how they pertain to goals of the current study.

2.4.1 Filter Efficiency Testing

2.4.1.1 Inert Testing. Numerous studies were identified in the literature review that assessed the effect of flow rate and particle size on the measured aerosol penetration through particulate respirator filters. However, no studies were identified that assess the effect of high volumetric flow rates that may be encountered during heavy work rates on filter performance. Few studies in the literature assessed filtration performance above 85 L/min constant flow and none above 100 L/min. The results have shown that penetration of submicron particles,

16

specifically those in the MPPS range, tend to increase with increased flow rate. The MPPS is generally in the range of 0.1 to 0.3 μm depending on the type of filter. Particles larger than 1 μm have been shown to be collected more efficiently at higher flow rates as inertial impaction is enhanced. Previous studies have also demonstrated that even N95 filters are very efficient (>99.5%) at removing particles above 0.7 μm. To this end, the particle sizes tested in this study were focused on those in the MPPS region. Five particle sizes were tested over the range from 0.02 to 0.3 μm and only three particle sizes greater than 0.3 μm.

Few studies were identified that assessed aerosol filtration performance under cyclic flow conditions. The studies that were reviewed concluded that higher penetrations were measured under cyclic flow conditions, corresponding to various work rates, than measured under constant flow rates used in test standards (i.e., 32 or 85 L/min). There is considerable debate regarding the impact of the peak inhalation flow on filter performance, both from an aerosol and gas/vapor filtration perspective. No conclusions could be drawn from the literature as to the impact of peak flow or what an appropriate constant flow rate is to provide an estimate of performance under cyclic flow. As this is an important objective of the current study, the constant flows were matched to the cyclic flow minute volume, mean inhalation flow, or peak inhalation flow to permit comparisons.

2.4.1.2 Biological Testing. In summary, appreciable differences were found in the performance of respirator filters when challenged with biological aerosols. Overall, studies have confirmed that N95 and HEPA respirators are substantially more efficient than DM and DFM respirators and surgical masks against biological aerosols. Consistently, no significant difference in filter penetration was found between spherical inert and spherical bioaerosol particles of similar aerodynamic diameter, suggesting that inert particles of the same size may be used to predict bioaerosol efficiency. In some cases, the penetration of rod-shaped bacteria was lower than that of spherical organisms of the same aerodynamic diameter, indicating that in addition to particle size, particle shape may also affect penetration through respirator filters. Finally, increases in flow rates to levels representative of heavy working conditions were found to increase biological aerosol penetration, particularly for submicrometer particles. This becomes critically important when considering that a certain number of pathogenic organisms of

17

submicrometer size may be sufficient to cause a serious health risk. No studies were identified in the literature that assessed viral penetration through particulate respirator filters.

2.4.1.3 Reaerosolization. Particle size, shape and composition, air velocity, humidity, and filter properties were all factors found to significantly affect particle reentrainment from filter materials. Large particles of approximately 5.0 μm diameter and greater were found to be most susceptible to reaerosolization. Biological particles were found to become reentrained more easily than inert particles of comparable size, which is suspected to result from weaker contact with filter fibers due to irregular shapes and surface characteristics. In addition, aggregation of bacteria and fungal spores to form larger clusters was determined to also increase potential reaerosolization.

3.0 INERT PARTICULATE FILTRATION EFFICIENCY TESTING

Currently, NIOSH-approved particulate air purifying respirator filters are tested against salt or oil aerosols at a constant flow rate of 85 L/min for certification per 42 CFR Part 84 (1995). However, measurements of physiological parameters of workers show peak inhalation flow rates from 300 to 400 L/min for short durations during certain high work load activities (Caretti et al., 2004). As discussed in Section 2.0, studies to determine the effect of high breather flows on the filtration efficiency of NIOSH-approved particulate filters are lacking in the open literature. This section describes the testing completed to assess the effect of particle size, flow rate, and flow condition (i.e., cyclic versus constant) on filtration of inert aerosols. The two primary objectives of the inert testing were: (1) assess the effect of high volumetric flow conditions on the performance of NIOSH-approved particulate respirator filters and (2) compare performance under constant and cyclic flow conditions.

3.1 Test Parameters

The filters, summarized in Table 2, were selected in consultation with NIOSH and included two N95 filtering facepieces, two P100 filtering facepieces, two N95 cartridges, and two P100 cartridges. The two brands of commercial P100 filtering facepieces used in the study

had exhalation valves. The valves were not sealed during the inert filtration efficiency testing. Photographs of each filter are provided in Appendix A. The filters were not preconditioned prior to testing (i.e., tested as-received). The environmental conditions during testing were maintained at ambient temperature (25 ± 3°C) and relative humidity (40 ± 10%). Table 3 summarizes the challenge aerosols and the target particle sizes. Solid aerosols (i.e, salt and PSL) were used with the N95 filters and oil aerosols (i.e., Emery 3004 and DOP) were used with the P100 filters. This approach is consistent with how certification testing is performed by NIOSH (42 CFR 84, 1995). For each particle size, the challenge aerosol concentration was adequate to measure efficiencies of at least 99.97 percent.

Table 2. Summary of Cartridges and Filtering Facepieces

Filter Type	Rating	Model	Manufacturer
Cartridge	N95	Flexi-Filter	MSA (Pittsburgh, PA)
	N95	7506	North Safety Products (Cranston, RI)
	P100	HE-T	SEA (Branford, CT)
	P100	1050	Survivair (Santa Ana, CA)
Filtering Facepiece	N95	1730	Louis M. Gerson, Co., Inc. (Middleboro, MA)
	N95	Affinity Plus	MSA (Pittsburgh, PA)
	P100	8293	3M (St. Paul, MN)
	P100	2360	Moldex-Metric, Inc. (Culver City, CA)

Table 3. Summary of Challenge Aerosols for Testing N95 and P100 Filters

Filter Type	N95	P100
Target NMAD (µm)	Challenge Aerosol	
0.02, 0.05, 0.1, 0.2, 0.3	NaCl	DOP
0.7, 1.3, 2.9	PSL	Emery 3004

Tests were performed over a range of constant and cyclic flow conditions. The rationale for selection of the flow conditions is provided in Appendix B. As noted in the appendix, the cyclic flow conditions were selected to simulate work intensities ranging from moderate to exhaustive. The selected flow conditions are based on studies performed with unmasked subjects and, thus, are likely extreme under conditions of respirator wear. The breathing machine used in this study produced a sinusoidal waveform. The cyclic flow conditions with corresponding peak inhalation flow (PIF) and mean inhalation flow (MIF) are summarized in Table 4 and compared graphically in Figure 3. The MIF is the average flow rate over the

inhalation portion of the breathing cycle. The PIF represents the maximum flow rate obtained over the inhalation cycle. For a sinusoidal waveform, the PIF is π times the minute volume. The constant flow rates were selected to match a cyclic flow minute volume, MIF, or PIF for comparison purposes. These were 85 ± 5, 270 ± 15, and 360 ± 20 L/min. For example, the 85 L/min constant flow matches a cyclic flow minute volume (2.3 L tidal volume, 37 breaths/min) and a MIF (1.6 L tidal volume, 25 breaths/min). Since all single cartridges were from dual-cartridge respirators, they were tested at half of the tidal volume or constant flow rate stated previously.

Table 4. Summary of Cyclic Flows Used for Testing with the Inert Aerosol Challenges

Breathing Rate (breaths/min)	Tidal Volume (L)	Minute Volume (L/min)	PIF[a] (L/min)	MIF[b] (L/min)
25	1.6	40	130	85[c]
37	2.3	85	270[c]	175
42	2.7	115	360[c]	230
44	3.1	135	430	270[c]

(a) Peak inspiratory flow rate assuming ideal sinusoidal waveform
(b) Mean inspiratory flow rate assuming ideal sinusoidal waveform
(c) Selected for constant flow testing
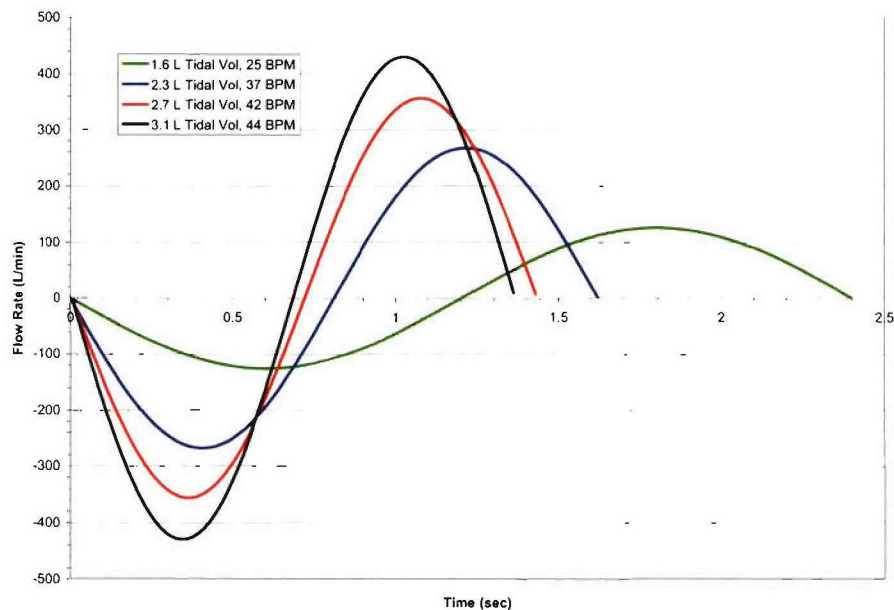
Figure 3. Comparison of Sinusoidal Waveforms Used to Assess the Effect of Moderate to High Breather Flows on Filter Performance

3.2 Test Matrix

The test matrices for the cartridges and filtering facepieces are provided in Tables 5 and 6, respectively. The tables indicate the number of tests performed at each combination of filter, particle size, and flow condition. The 0.02 to 0.3 µm aerosol challenges have been grouped since the efficiencies were measured sequentially using the same cartridge or filtering facepiece, as will be described in Section 2.3.1. Similarly, the 0.7 and 1.3 µm particle sizes have been grouped. Only two replicates were performed with the 2.9 µm challenge at each flow condition due to the high efficiency of the filters. The results demonstrated that the penetration of 2.9 µm particles was less than 0.001 percent for all conditions tested. Tests were not performed with the filtering facepieces at the highest cyclic flow condition for particle sizes ranging from 0.02 to 0.3 µm due to problems generating a stable challenge with the proper aerosol size distribution at this flow condition.

Table 5. Test Matrix Completed to Assess the Effect of High Cyclic Flows on Filtration Performance of Cartridge Respirator Filters

Filter	Target NMAD (µm)	Constant Flow (L/min)			Cyclic Flow (L/min)			
		42.5	135	180	20	42.5	57.5	67.5
		# Tests Completed						
North N95	0.02, 0.05, 0.1, 0.2, 0.3	3	3	3	3	3	3	3
	0.7, 1.3	3	3	3	3	3	3	3
	2.9	2	2	2	2	2	2	2
MSA N95	0.02, 0.05, 0.1, 0.2, 0.3	3	3	3	3	3	4	3
	0.7, 1.3	3	3	3	3	3	3	3
	2.9	2	2	2	2	2	2	2
SEA P100	0.02, 0.05, 0.1, 0.2, 0.3	3	3	3	3	3	3	3
	0.7, 1.3	3	4	3	3	3	4	3
	2.9	2	2	3	2	2	2	2
Survivair P100	0.02, 0.05, 0.1, 0.2, 0.3	3	3	3	3	3	3	3
	0.7, 1.3	3	3	3	3	3	3	3
	2.9	2	2	2	2	2	3	3

Table 6. Test Matrix Completed to Assess the Effect of High Cyclic Flows on Filtration Performance of Filtering Facepieces

Filter	Target NMAD (μm)	Constant Flow (L/min)			Cyclic Flow (L/min)			
		85	270	360	40	85	115	135
		# Tests Completed						
MSA N95	0.02, 0.05, 0.1, 0.2, 0.3	3	5	6	3	3	3	0[a]
	0.7, 1.3	3	3	3	3	3	3	3
	2.9	2	2	2	2	2	2	2
Gerson N95	0.02, 0.05, 0.1, 0.2, 0.3	3	3	3	3	3	3	0[a]
	0.7, 1.3	3	3	3	3	3	3	3
	2.9	2	2	2	2	2	2	2
3M P100	0.02, 0.05, 0.1, 0.2, 0.3	3	3	3	3	1	3	0[a]
	0.7, 1.3	3	3	3	3	3	3	3
	2.9	3	3	3	3	3	3	3
Moldex P100	0.02, 0.05, 0.1, 0.2, 0.3	3	3	3	3	3	0[a]	0[a]
	0.7, 1.3	3	3	3	3	3	3	3
	2.9	3	4	4	4	3	3	3

(a) Stable challenge could not be generated using TSI Model 3160 Automated Filter Tester.

3.3 Technical Approach

This section describes the test systems and procedures that were used to measure the inert filtration efficiencies. A modified Model 3160 Automated Filter Tester (TSI, Shoreview, MN) was used for testing with the 0.02 to 0.3 μm aerosols, and is described in Section 3.3.1. Due to limitations with the Model 3160, a separate test system was used for the 0.7, 1.3, and 2.9 μm aerosols, and is described in Section 3.3.2.

3.3.1 Model 3160 Automated Filter Tester

3.3.1.1 System Description. The Model 3160 consisted of four primary components: (1) aerosol generation system, (2) aerosol sensing devices, (3) filter holder, and (4) vacuum pump or breathing machine. The aerosol generation system consisted of an atomizer and electrostatic classifier (EC). The atomizer generated a polydisperse oil or salt aerosol that was passed through the EC to generate the desired monodisperse aerosol at the desired particle size. The aerosol exiting the EC was diluted with HEPA-filtered room air. The aerosol number concentrations up- and downstream of the test filter were measured simultaneously using two condensation particle counters (CPCs). The upstream CPC (Model 3760A, TSI, Shoreview,

MN) sampled at 1.5 L/min and the downstream CPC (Model 3762, TSI, Shoreview, MN) sampled at 3.0 L/min. The higher sample flow rate on the downstream CPC increased the sensitivity of the Model 3160 and allowed shorter sample durations. The upstream sample was diluted by a factor of approximately 100 prior to measurement using a diluter (Model 3302A, TSI). The dilution factor was adjustable based on the expected challenge concentration. A vacuum pump was used to pull the desired constant flow rate through the test filter. The flow rate was measured using a mass flow meter (Series 4000, TSI, Shoreview, MN).

Several modifications were made to the Model 3160 to permit efficiency measurements over the range of flow conditions. First, additional HEPA filters were installed at the dilution air inlet, as shown in Figure 4. Second, a 1.5 hp vacuum pump was added for testing at constant flows in excess of 150 L/min, and a breathing machine was adapted for cyclic flow testing. Finally, the test filters were housed in a Lucite® chamber, measuring approximately 22x18x10 cm, that was sealed between the filter chucks as shown in Figure 5. The aerosol entered the chamber through a 7.5-cm hole on top of the chamber. The filtering facepieces were placed over a similar sized hole in the bottom of the chamber and sealed using an adhesive. Threaded fittings were machined to mate with the cartridges.
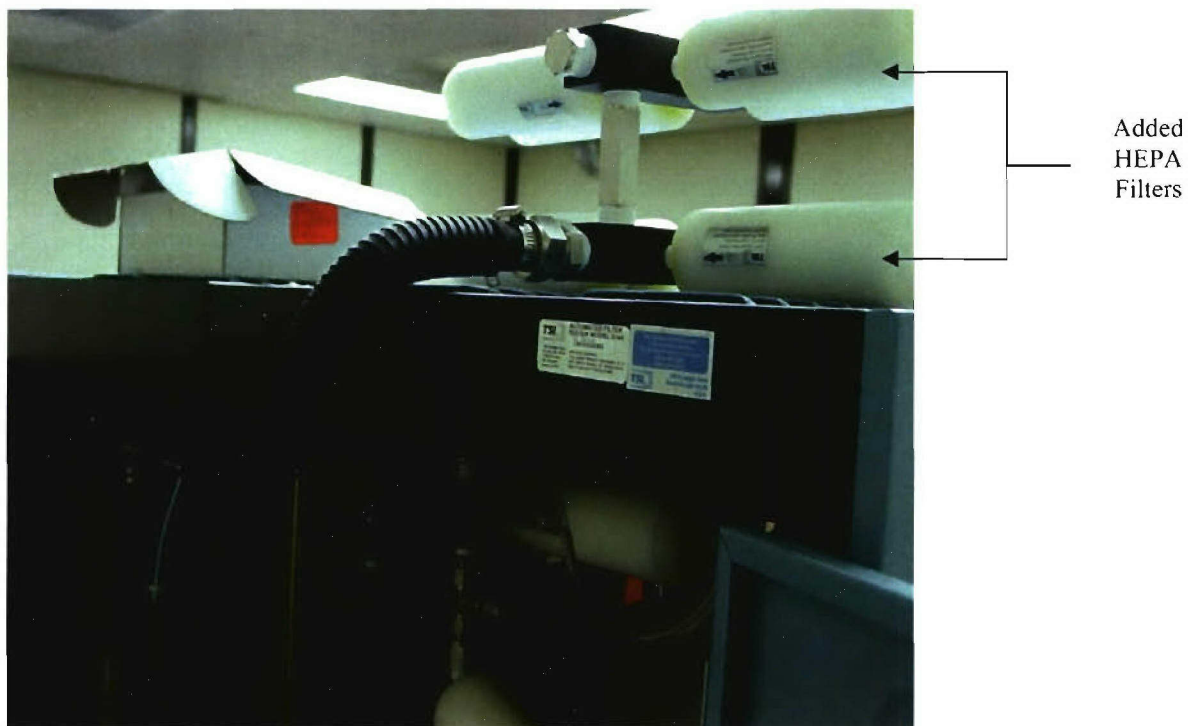
Figure 4. Additional HEPA Filters on Dilution Air Inlet of Model 3160
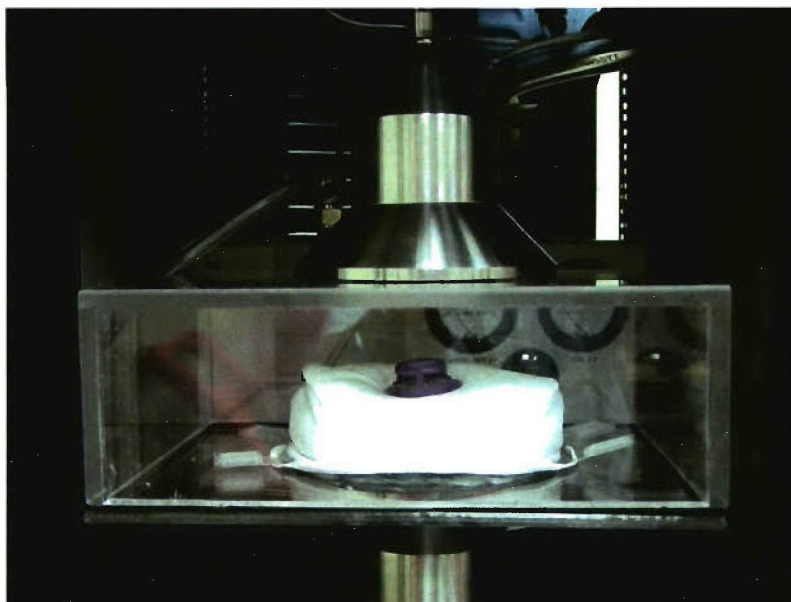
Figure 5. Lucite® Chamber Used to House and Seal Test Filters to the Model 3160

3.3.1.2 System Characterization. Shakedown tests were conducted to characterize the test system and establish the proper operating conditions. This included assessing the effect of non-isokinetic sampling, flow calibrations, and characterization of the challenge particle size distribution. The shakedown testing is detailed in Appendix C.

3.3.1.3 Test Procedure. Prior to testing a filter, the dilution ratio on the upstream CPC was verified at a specific particle size and flow condition. This was done without a test filter (i.e., cartridge or filtering facepiece) to ensure no sampling bias between the up and downstream samples (i.e., measured penetration was 100 percent indicating agreement between the up- and downstream CPCs). The sample bias test results are provided in Appendix C. With the dilution ratio set, the cartridge or filtering facepiece was mounted to the Lucite® chamber and the chamber sealed to the Model 3160. The vacuum pump or breathing machine was connected to the test system and set to the proper conditions. The Model 3160 was programmed to sequentially measure efficiencies at the following particle sizes: 0.02, 0.05, 0.1, 0.2, and 0.3 μm. The Model 3160 was started and automatically stepped through the particle sizes and measured the efficiencies. When complete, the vacuum pump or breathing machine was stopped and the filter removed from the test system and discarded.

24

3.3.2 Large Particle Test System

The Model 3160 was unable to produce particles greater than 0.4 μm under high flow conditions due to limitations of the system. This section describes the test system and approach used to measure filter efficiencies with challenge aerosols ranging from 0.7 to 2.9 μm.

3.3.2.1 System Description. The test system, pictured in Figure 6, consisted of an aerosol generation system, exposure chamber, filter holder, breathing machine (or vacuum pump), and aerosol sampling/classification system. For the N95 filters, a Collison nebulizer was
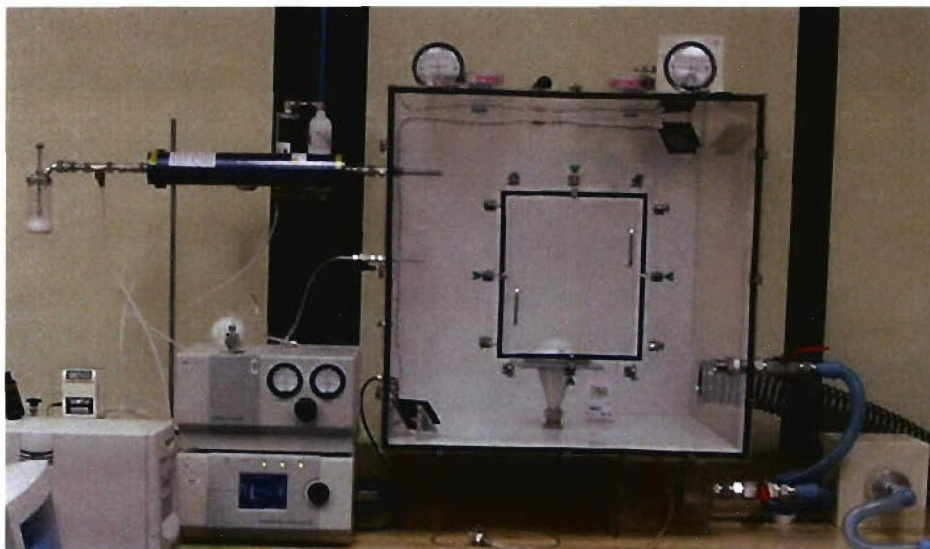
Figure 6. Test System Used to Measure Penetration of 0.7, 1.3, and 2.9 μm PSL through the N95 Filters

used to aerosolize PSL particles suspended in distilled water. A 24-jet Collison (BGI Inc., Waltham, MA) was used to aerosolize the 2.9 μm PSL and a 6-jet Collison (BGI Inc., Waltham, MA) was used to aerosolize the 0.7 and 1.3 μm PSL. For the P100 filters, a 6-jet Collison nebulizer was used to aerosolize Emery 3004 oil. The nebulizer produced a polydisperse oil aerosol with sufficient numbers of 0.7, 1.3, and 2.9 μm particles to measure efficiencies of at least 99.97 percent. The aerosol exiting the nebulizer was mixed with filtered house air before passing through a neutralizer (Model 3012, TSI, Shoreview, MN). The generator continuously delivered aerosol-laden air to the exposure chamber to ensure a stable aerosol challenge was

maintained. Additional dilution air was pulled, as needed, through two HEPA filters located on top of the chamber. The chamber contained mixing fans to ensure a well-mixed challenge atmosphere. Chamber pressure was measured using a magnehelic® pressure gauge. Excess challenge was vented through HEPA filters and exhausted into the room.

The filter holder was mounted on the bottom of the chamber. The design of the filter holder was specific to the filter being tested. For the filtering facepieces, the holder consisted of a cone with a flat plate at the top. The filtering facepiece was sealed to the flat plate using rope caulk. For the cartridges, threaded fittings were machined. The filter holder was mounted to a 2.5-cm OD stainless steel bulkhead fitting that passed through the bottom of the chamber. The filter holder was connected to the breathing machine with large diameter (~2.5 cm OD) flexible tubing. The breathing machine allowed for the adjustment of the tidal volume and breathing rate. The challenge-laden atmosphere was pulled through the test filter during inhalation. The breathing machine was equipped with a check valve such that the exhaled air was exhausted into the room after being filtered. The test system was also set up such that the test filter (i.e., cartridge or filtering facepiece) was bypassed during system startup to minimize loading since the objective of this effort was to measure the initial penetration.

The aerodynamic particle sizer (APS, Model 3321, TSI, Shoreview, MN) and diluter (Model 3302A, TSI, Shoreview, MN) were used to measure the challenge and downstream aerosol concentrations. The chamber contained a stainless steel probe that extended 10 cm beyond the chamber wall for collecting samples of the challenge atmosphere. The downstream aerosol concentration was sampled from a small chamber (cylindrical in shape with 15 cm diameter and 25 cm length) equipped with a stainless steel sample probe that extended approximately 7.5 cm into the chamber. Testing without a filter in the holder was completed to assess potential sampling bias on the measured penetrations due to the non-isokinetic sampling downstream.

3.3.2.2 System Characterization. Shakedown tests were completed to verify the proper operating conditions of the system. This included no-filter testing to identify any potential sampling bias between the up- and downstream samples and characterizing the challenge aerosol. The shakedown testing is detailed in Appendix D.

3.3.2.3 Test Procedure. The filter was mounted to the test fixture. The outlet valves on the P100 filtering facepieces were not sealed during testing. The test chamber was sealed and the breathing or vacuum pump, as appropriate, was started. The challenge generation system was started and permitted to operate for 10 to 20 minutes depending on the flow condition to allow the aerosol to reach a steady state concentration. During this time, the cartridge or filtering facepiece was bypassed to minimize filter loading. When steady state was reached, the valves were adjusted such that flow was pulled through the test filter. A sample of the challenge aerosol was collected with the APS for two minutes. Next, the sampling line was switched to sample downstream of the filter and adequate time was given for the instrument to stabilize. The downstream sample duration was varied to provide adequate time to permit efficiency measurements of at least 99.97 percent based on the challenge concentration. For the N95 filters, the sample duration was five minutes when testing 0.7 and 1.3 μm particles and 15 minutes during testing with the 2.9 μm particles. The longer sample duration was needed with the 2.9 μm PSL particles because the challenge concentration was lower. The P100 filters required 15 minutes of downstream sampling when testing with the 0.7, 1.3, and 2.9 μm oil challenge particles. After sampling downstream was complete, the sample line was switched to the upstream and a second two minute sample of the challenge concentration was collected. If the two challenge samples (i.e., before and after downstream sampling) were not within 20 percent of each other, the test was repeated as the challenge aerosol was not stable. After the challenge sample was collected, the aerosol generation system was stopped and the chamber flushed. The filter was removed from the test system and discarded, and a new filter was tested.

3.4 Calculation of Aerosol Penetration

The percent aerosol penetration (P) was defined as the ratio of the downstream aerosol concentration (C_{Down}) to the challenge aerosol concentration (C_{Chal}):

$$P(\%) = \frac{C_{Down}}{C_{Chal}} \times 100$$

Alternatively, the filtration efficiency (η) was defined as:

$$\eta(\%) = 100 - P = \left(1 - \frac{C_{Down}}{C_{Chal}}\right) \times 100$$

The concentrations were the average number concentrations measured by the aerosol sensing instrument (i.e., APS or CPC). The challenge concentration was the average of the challenge measurements made before and after the downstream sample.

3.5 Inert Results

The inert testing had two primary objectives: (1) assess the effect of high volumetric flow rates on performance of NIOSH-approved respirator filters over a range of particle sizes and (2) compare performance under constant and cyclic flow conditions. The results that address each objective are discussed in Sections 3.5.1 and 3.5.2, respectively.

3.5.1 Effect of High Volumetric Flow Rate

This section summarizes the results of the inert testing. Penetrations were measured as a function of both flow rate and particle size. The cartridge results are summarized in Section 3.5.1.1 and the filtering facepieces follow in Section 3.5.1.2. A complete summary of the measured penetrations for each trial is provided in Appendix E.

3.5.1.1 Cartridge Filters. The effects of particle size and flow condition on measured penetrations for the SEA HE-T and the Survivair® P100 cartridges are shown in Figures 7 through 10. The constant and cyclic flow conditions are provided in separate figures. The horizontal red line identifies the maximum allowable penetration based on the NIOSH P100 requirement (0.03%). Each data point represents the mean penetration and the error bars represent the 95 percent confidence intervals. The solid lines represent the best fit regressions. Both filters were extremely efficient for particles between 0.7 and 2.9 μm as penetrations were typically less than the minimum detection limit of 0.0001 percent at all flow conditions. Thus, the regressions provided are based on the particle sizes ranging from 0.02 to 0.3 μm. The most penetrating particle size (MPPS) was between 0.1 to 0.2 μm for both filters under both constant and cyclic flow. The MPPS shifted toward the lower end of this range as the flow rate increased. This observation is consistent with the literature (Stevens and Moyer, 1989). The primary collection mechanisms for particles in this range are interception and diffusion. The diffusion

mechanism becomes less efficient as the filtration velocity increases leading to a decrease in the MPPS.
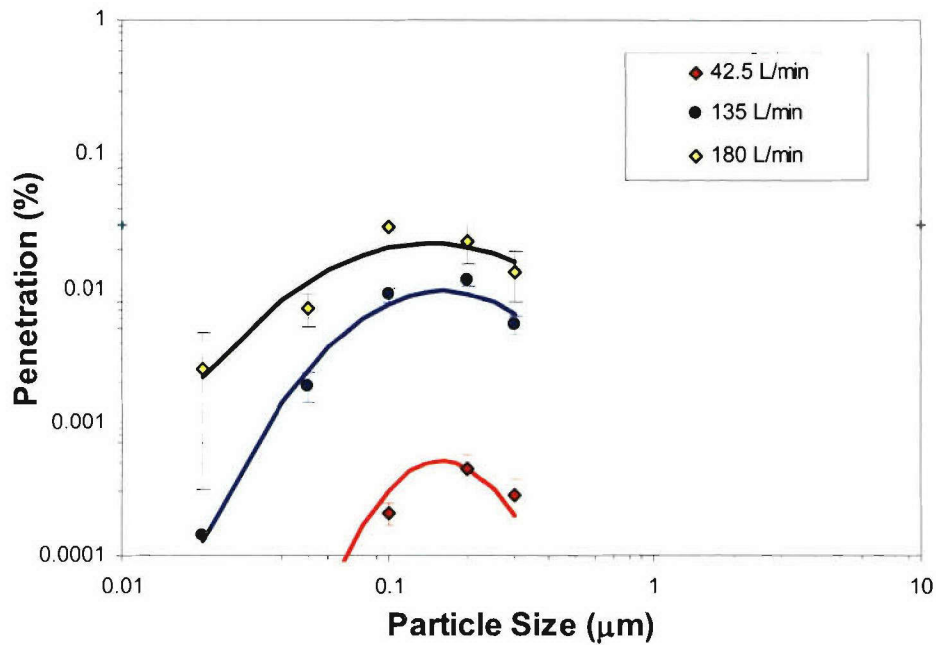
Figure 7. Effect of Particle Size and Constant Flow Rate on Measured Penetration through SEA HE-T P100 Cartridge
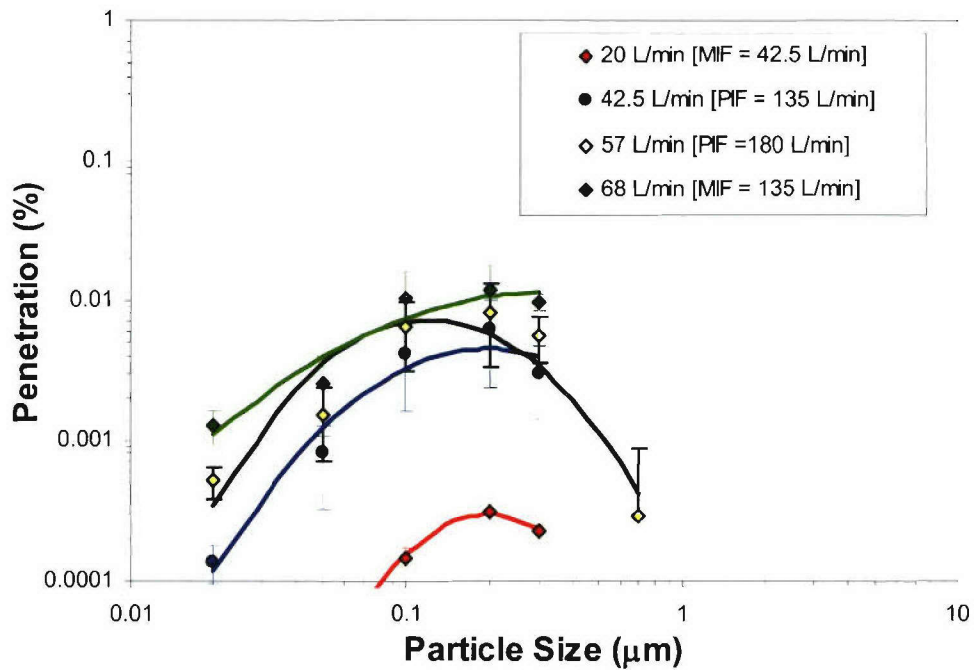
Figure 8. Effect of Particle Size and Cyclic Flow Rate on Measured Penetration through SEA HE-T P100 Cartridge
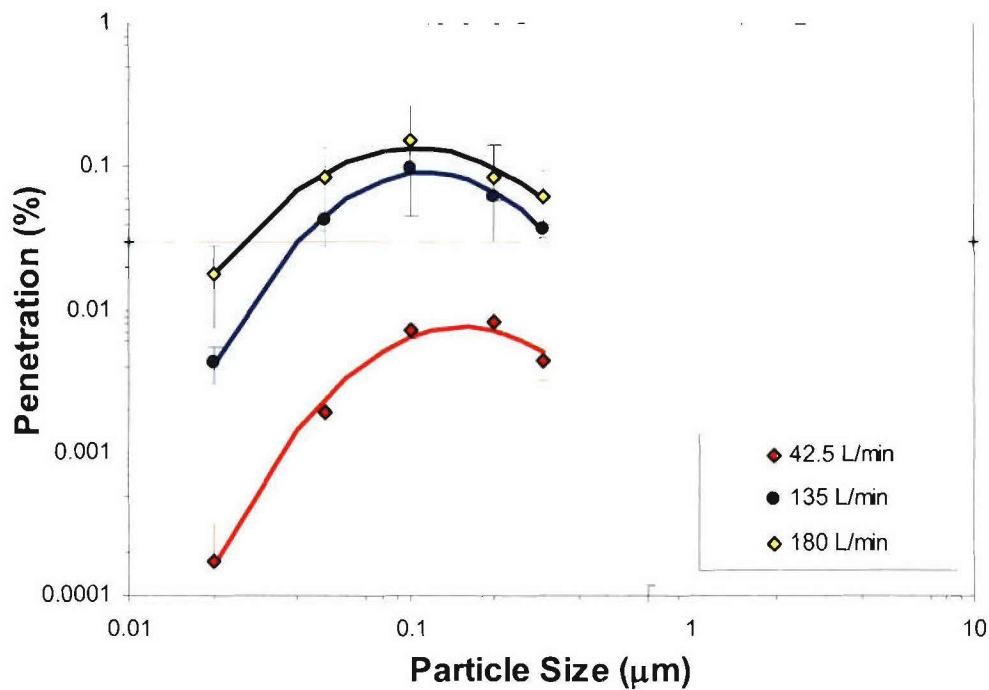
Figure 9. Effect of Particle Size and Constant Flow Rate on Measured Penetration through Survivair® 1050 P100 Cartridge
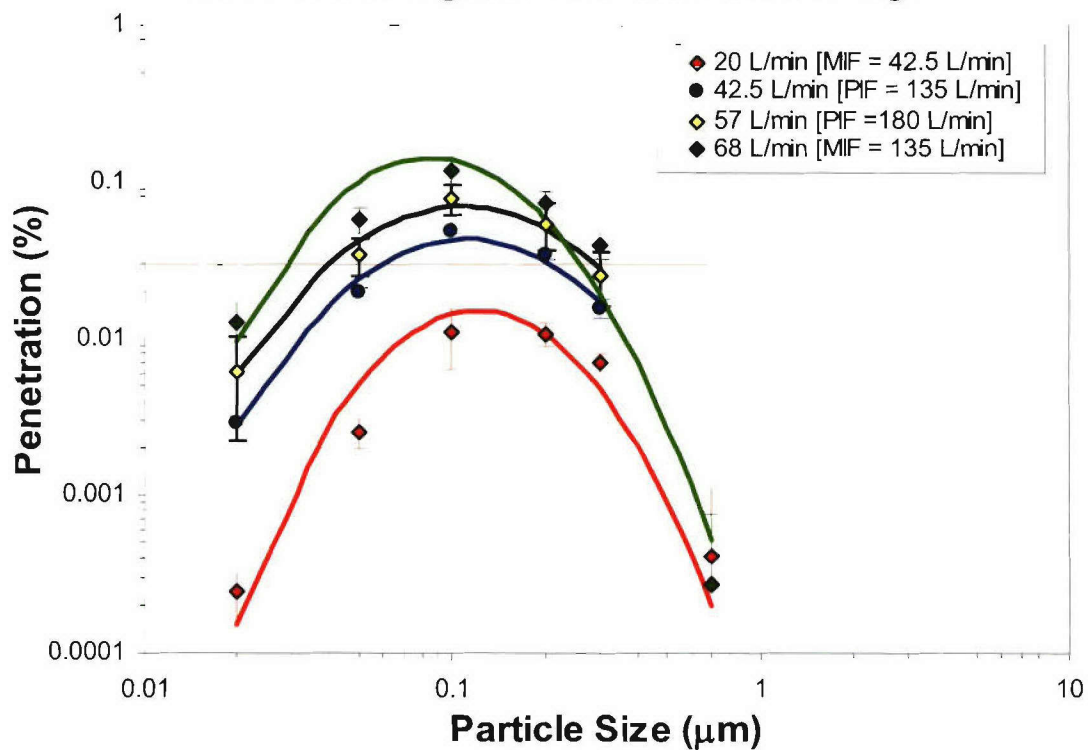
Figure 10. Effect of Particle Size and Cyclic Flow Rate on Measured Penetration through Survivair® 1050 P100 Cartridge

The SEA HE-T filter met the requirement for a P100 filter across all particle sizes at all flow conditions tested. Penetrations in excess of 0.03 percent were measured for the Survivair® filter. This is potentially due to differences in surface areas between the two filters. The SEA filter has approximately double the surface area and, thus, the filtration velocity would be half that of the Survivair filter at an equivalent flow rate. The measured penetrations of 0.1 μm particles (approximately the MPPS) under constant flow conditions are plotted as a function of filtration velocity in Figure 11. Note that the measured penetrations are similar at equivalent face velocities. Based on Figure 11, the filters exceed 0.03 percent penetration when the face velocity exceeds approximately 3.3 cm/sec.
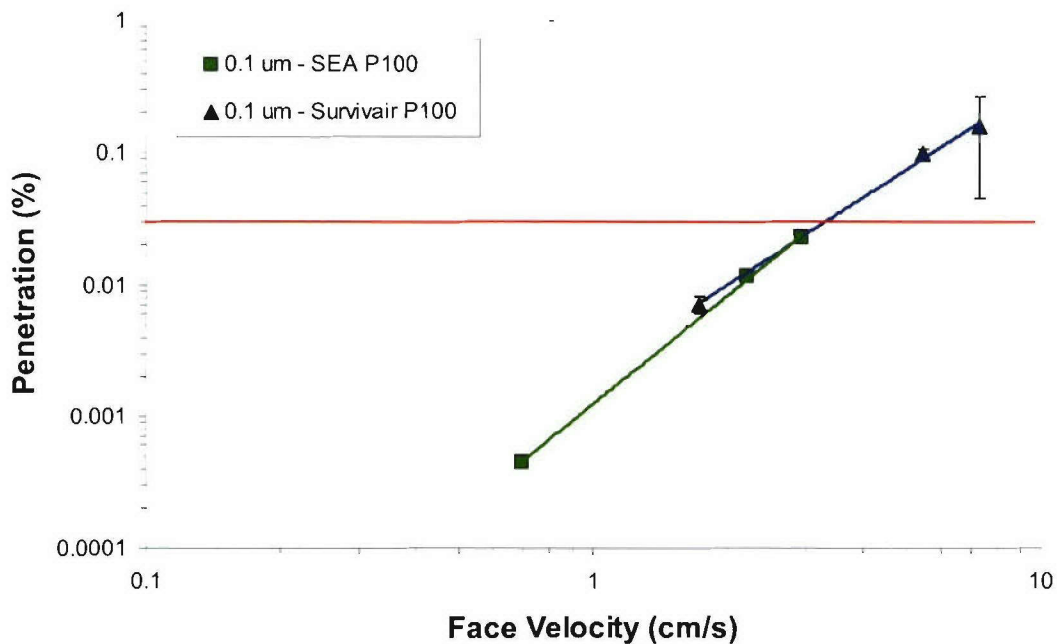
Figure 11. Penetration of 0.1 μm Particles as Function of Face Velocity for SEA and Survivair® P100 Cartridge Filters

The effects of particle size and flow condition on measured penetrations through the North 7506 and MSA Flexi-Filter N95 cartridges are shown in Figures 12 through 15. Both filters efficiently removed particles greater than 1 μm as penetrations were less than 0.1 percent regardless of flow condition. As observed for the P100 cartridges, the penetration of submicron particles tended to increase with increased flow rate. For both N95 cartridge filters, the MPPS was approximately 0.05 μm and generally independent of flow rate. This MPPS was smaller as

compared to that observed for the P100 filters. This could be due to higher filtration velocities as compared to the P100 cartridges that contained pleated media. The estimated surface areas and corresponding face velocities at the three constant flow rates are compared in Table 7. Recall, the MPPS is expected to decrease as the face velocity increases. The smaller MPPS could also be attributed to differences in the media type (i.e., electrostatic property, fiber diameter, solidity, thickness). However, evaluation of these properties was beyond the scope of this effort. Penetrations of 0.02 and 0.05 μm particles through the North cartridge exceeded 10 percent at the highest flow conditions. Based on its small size and low surface area, it is not suitable for use under the high flow conditions evaluated in this study.
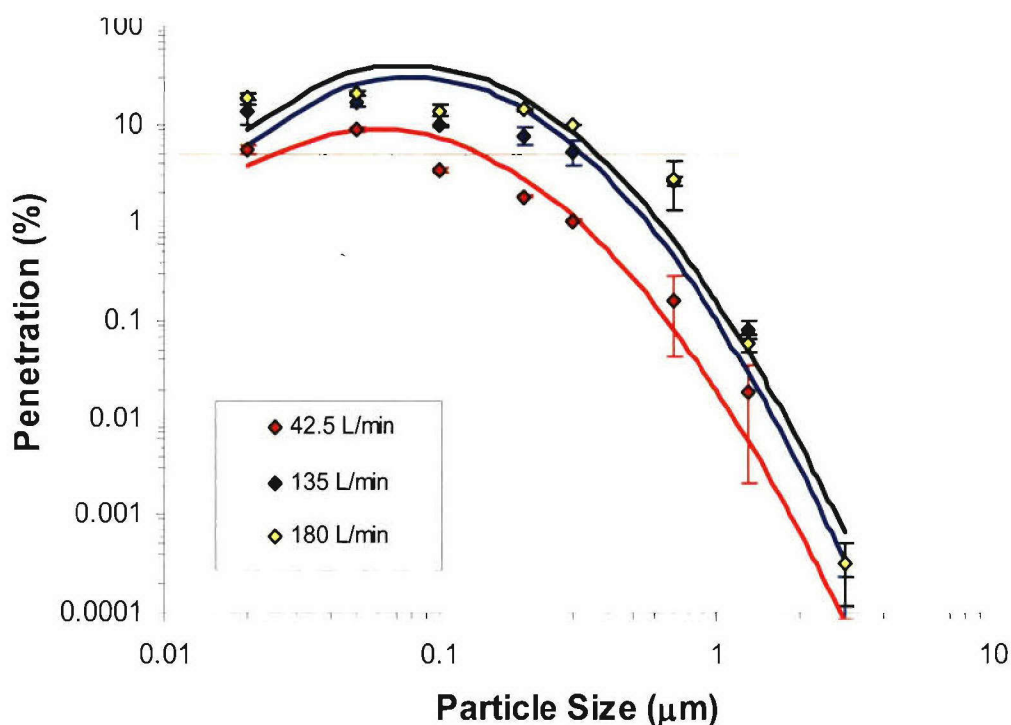
Figure 12. Effect of Particle Size and Constant Flow Rate on Measured Penetration through North 7506 N95 Cartridge
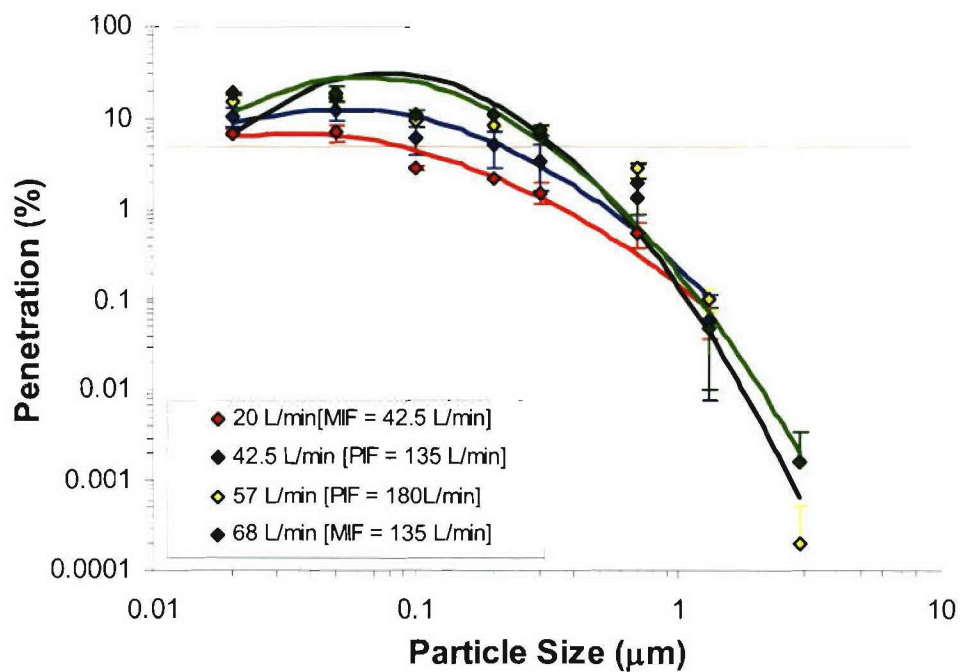
Figure 13. Effect of Particle Size and Cyclic Flow Rate on Measured Penetration through North 7506 N95 Cartridge
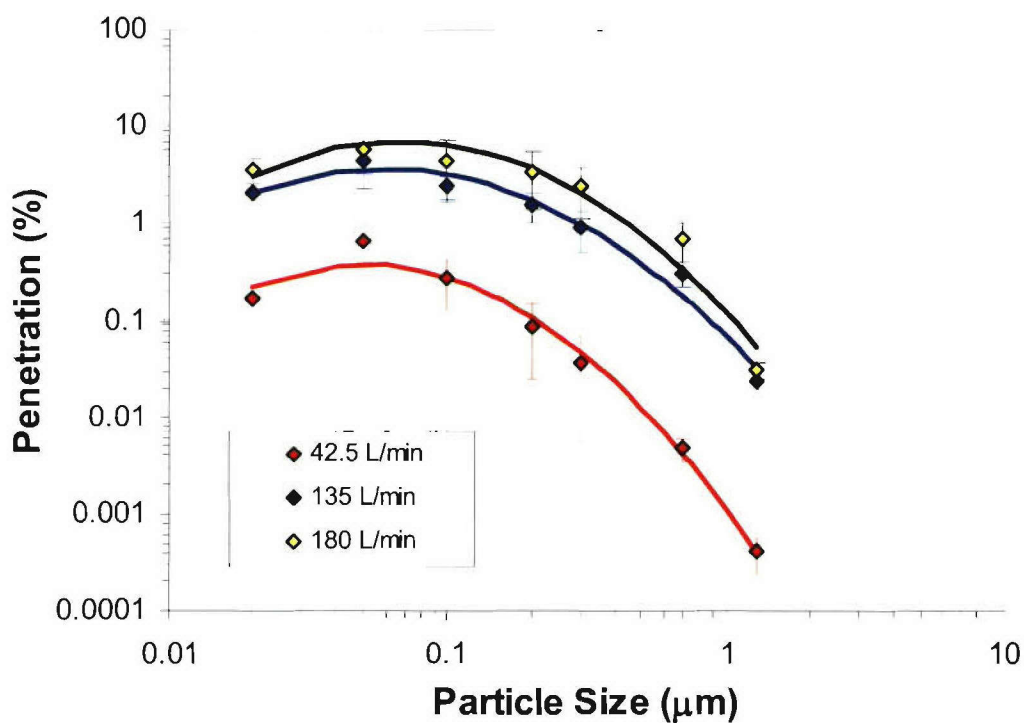
Figure 14. Effect of Particle Size and Constant Flow Rate on Measured Penetration through MSA Flexi-Filter N95 Cartridge
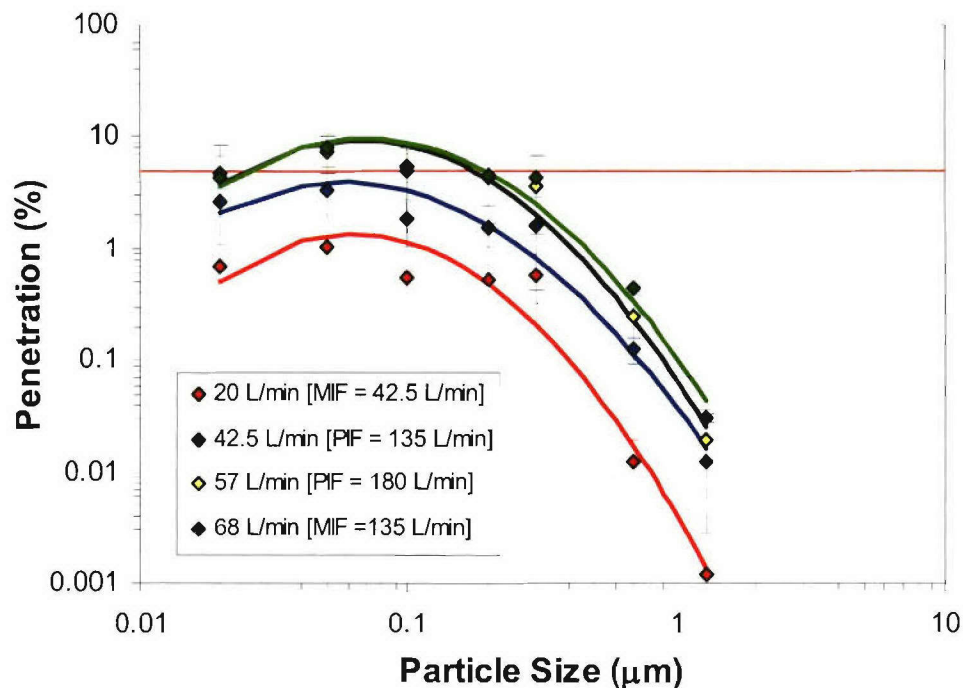
Figure 15. Effect of Particle Size and Cyclic Flow Rate on Measured Penetration through MSA Flexi-Filter N95 Cartridge

Table 7. Comparison of Face Velocities for P100 and N95 Cartridges

Filter	Estimated Surface Area (cm²)	Flow Rate (L/min)		
		42.5	135	180
		Face Velocity (cm/s)		
SEA P100	1,000	0.7	2.2	2.9
Survivair P100	400	1.7	5.5	7.3
MSA N95	100	7.1	23	30
North N95	50	14	45	60

As discussed above, the penetration through both the P100 and N95 cartridges tended to increase with increased flow rate. However, the magnitude of this increase was dependent on filter type and particle size. For example, Figure 16 compares the ratios of penetrations at 180 and 135 L/min for each cartridge. For the P100, the largest increases were seen with the 0.02 μm particles. It should be noted that both P100 filters effectively filtered the 0.02 μm particles even at the highest flow rates as penetrations were less than the 0.03 percent requirement. In contrast, increases in penetration across the particle sizes shown was fairly uniform for the N95 filter but the highest increases in penetration were observed for the 0.3 μm particles.
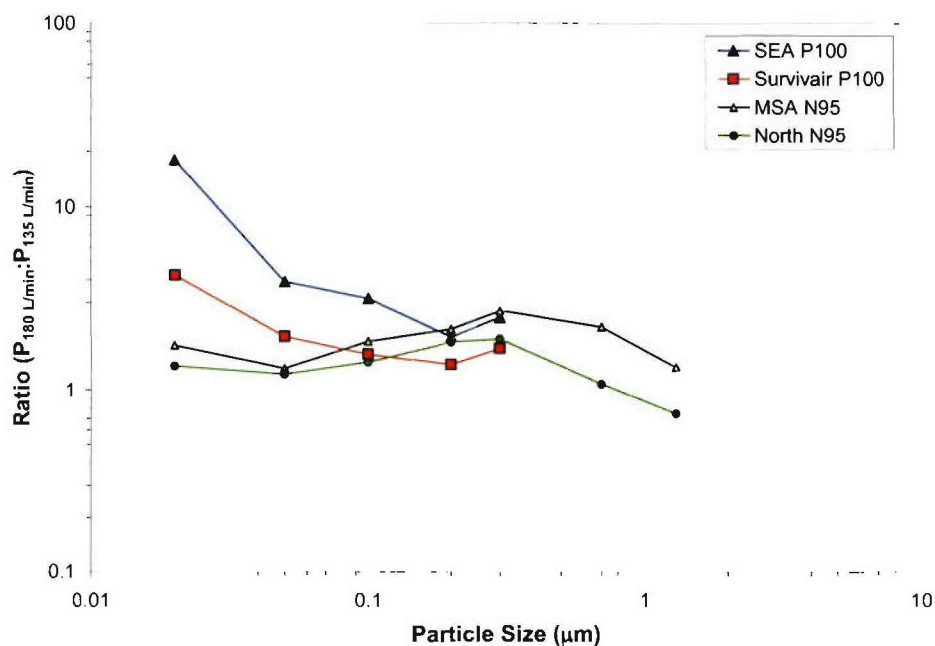
Figure 16. Comparison of Ratios of Penetrations Measured through P100 and N95 Cartridges at 180 and 135 L/min

3.5.1.2 Filtering Facepieces. The effects of particle size and flow condition on measured penetration through the 3M™ P100 filtering facepiece are shown in Figures 17 and 18. Regressions were not provided due to the extremely poor fit to the data. The MPPS was 0.02 to 0.05 μm. As seen with the cartridges, the 3M filter was very efficient against the 1.3 and 2.9 μm challenges as penetrations were less than 0.001 percent. The penetration of submicron particles was highly dependent on flow conditions. Similar trends were observed for the constant and cyclic flow conditions. Penetrations of 0.02 to 0.01 μm particles increased by more than an order of magnitude between the lowest and highest flow rates.
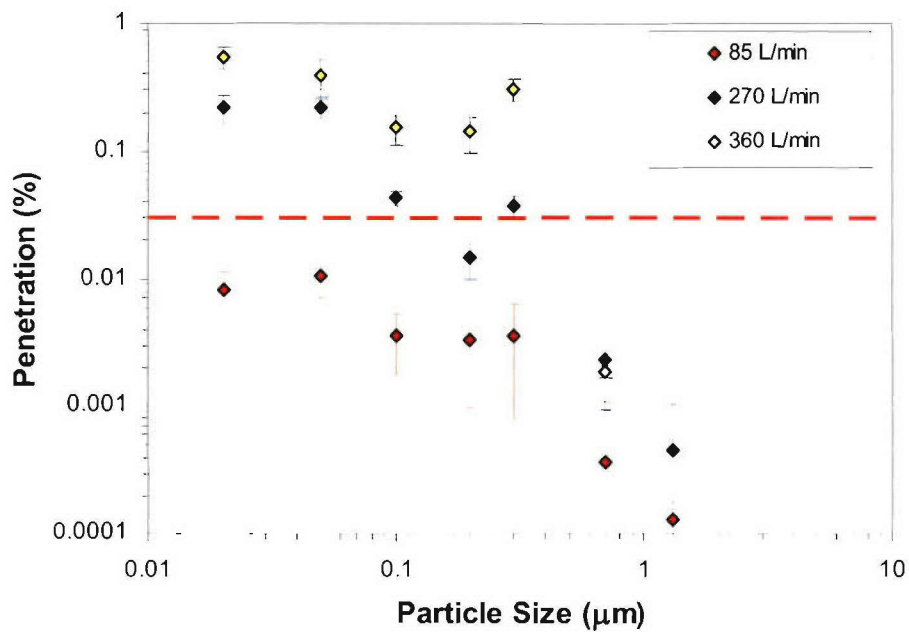
Figure 17. Effect of Particle Size and Flow Rate on Measured Penetration through 3M™ P100 Filtering Facepiece at Constant Flow
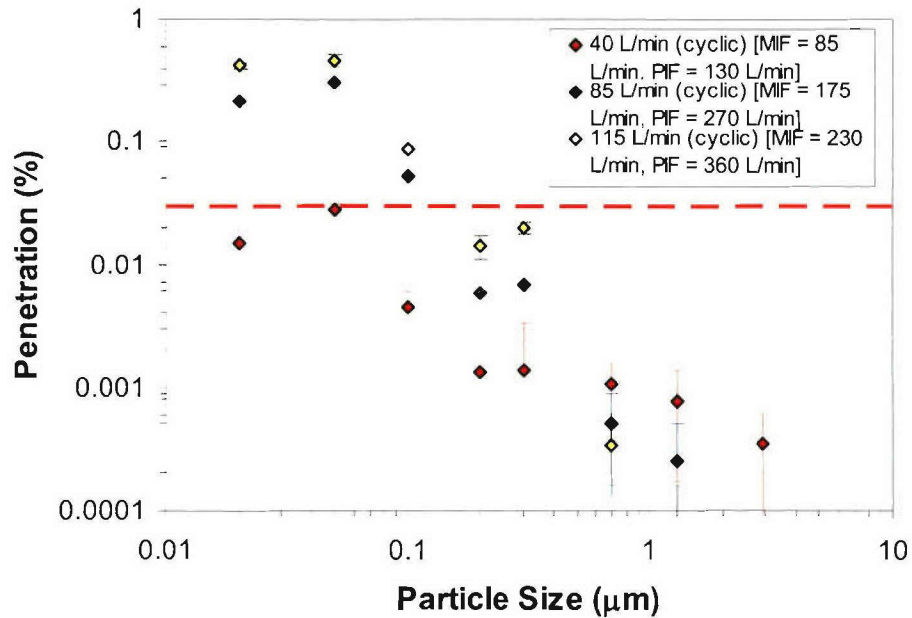
Figure 18. Effect of Particle Size and Flow Rate on Measured Penetration through 3M™ P100 Filtering Facepiece at Cyclic Flow

The effects of particle size and flow condition on measured penetration through the Moldex® P100 filtering facepiece are shown in Figures 19 and 20. For the constant flow testing the penetrations increased more than an order-of-magnitude as the flow increased from 85 to 270 L/min. Penetrations did not increase significantly when tested at 360 L/min. The MPPS at 85 L/min was 0.05 µm and penetrations clearly declined as particle size increased or decreased. In fact, the penetrations measured between 0.05 and 0.3 µm particles varied by more than an order of magnitude. In comparison, the penetrations measured over the same particle size range at 270 and 360 L/min varied by less than a factor of two.
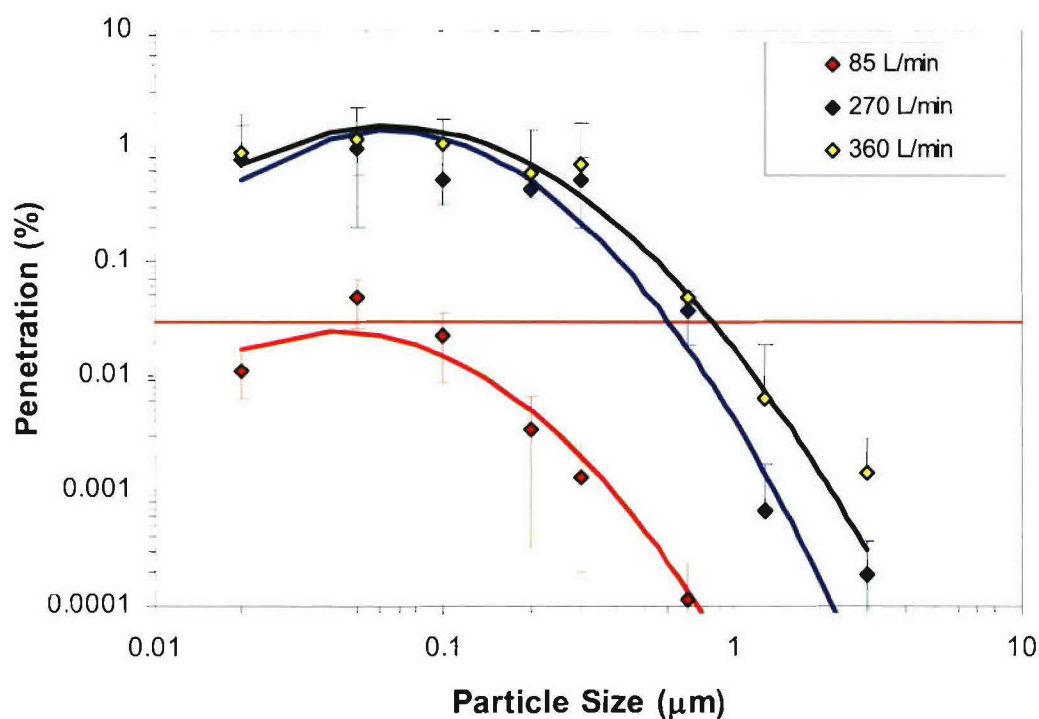
Figure 19. Effect of Particle Size and Flow Rate on Measured Penetration through Moldex P100 Filtering Facepiece at Constant Flow
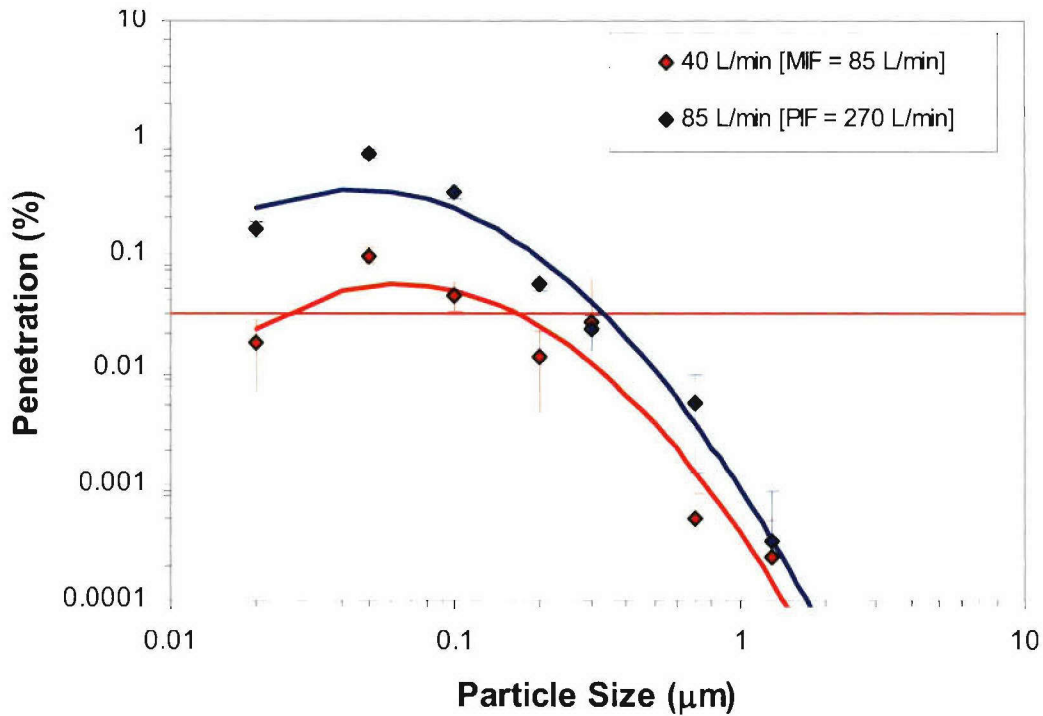
Figure 20. Effect of Particle Size and Flow Rate on Measured Penetration through Moldex P100 Filtering Facepiece at Cyclic Flow

The effects of particle size and flow conditions on measured penetrations through the Gerson® and MSA N95 filtering facepieces are shown in Figures 21 through 24. Penetrations of 1.3 and 2.9 μm particles were less than 1 percent under all flow conditions. Penetration of submicron particles increased significantly between 85 and 270 L/min constant flow. The penetrations for each particle size at 270 and 360 L/min were similar. Penetrations of particles between 0.02 and 0.3 μm were greater than 5 percent at the highest flow conditions tested.
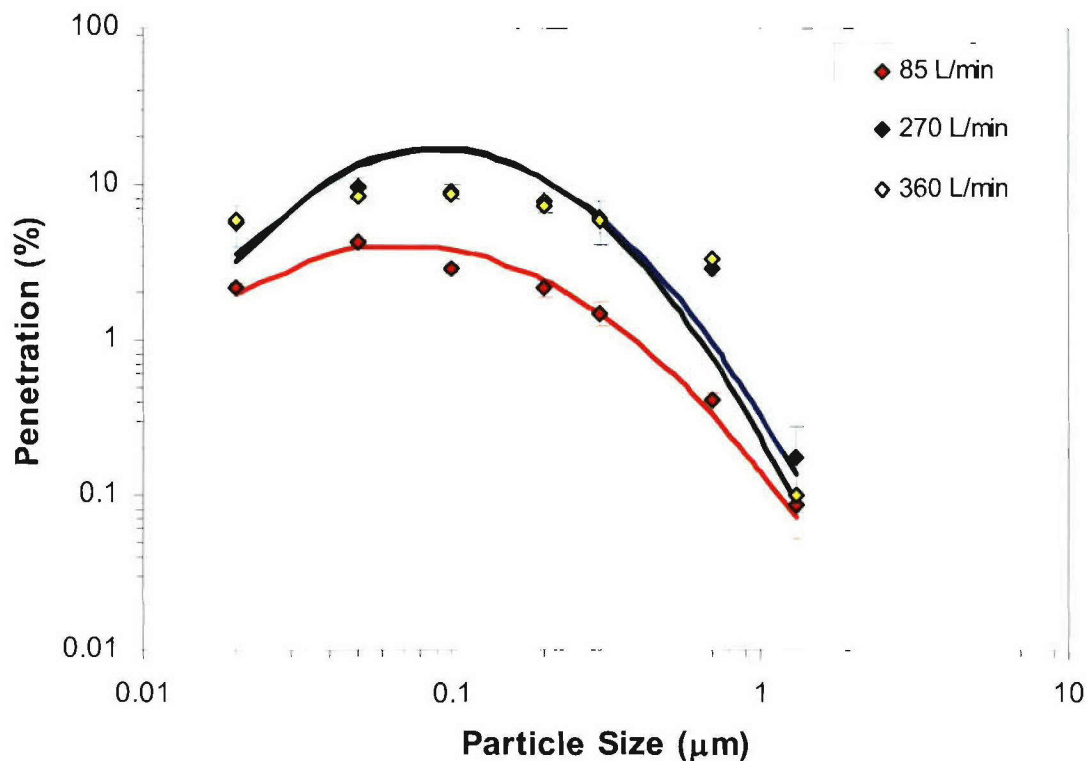
Figure 21. Effect of Particle Size and Flow Rate on Measured Penetration through Gerson® N95 Filtering Facepiece at Constant Flow
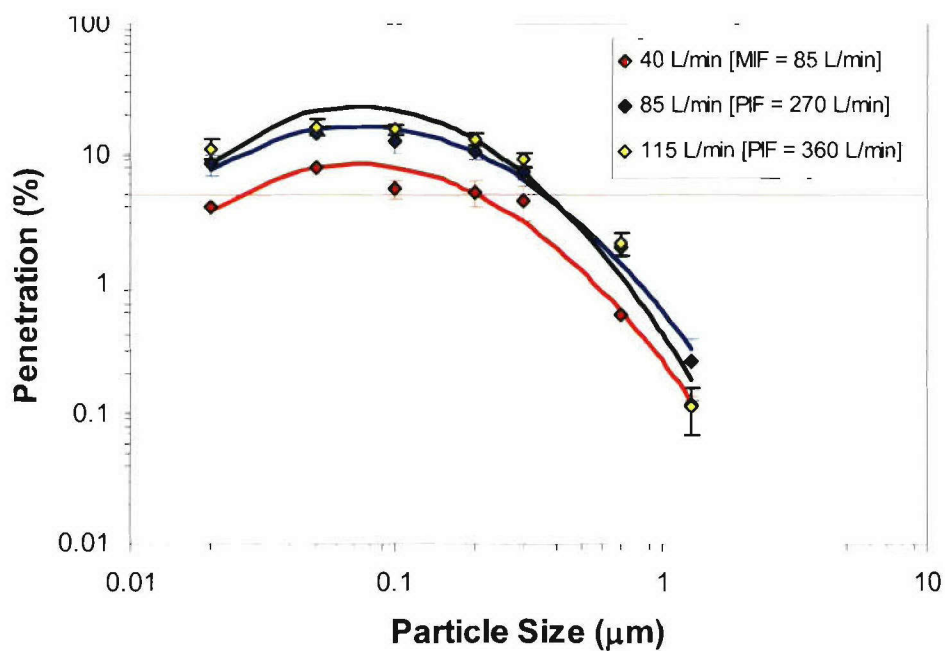
Figure 22. Effect of Particle Size and Flow Rate on Measured Penetration through Gerson® N95 Filtering Facepiece at Cyclic Flow

39
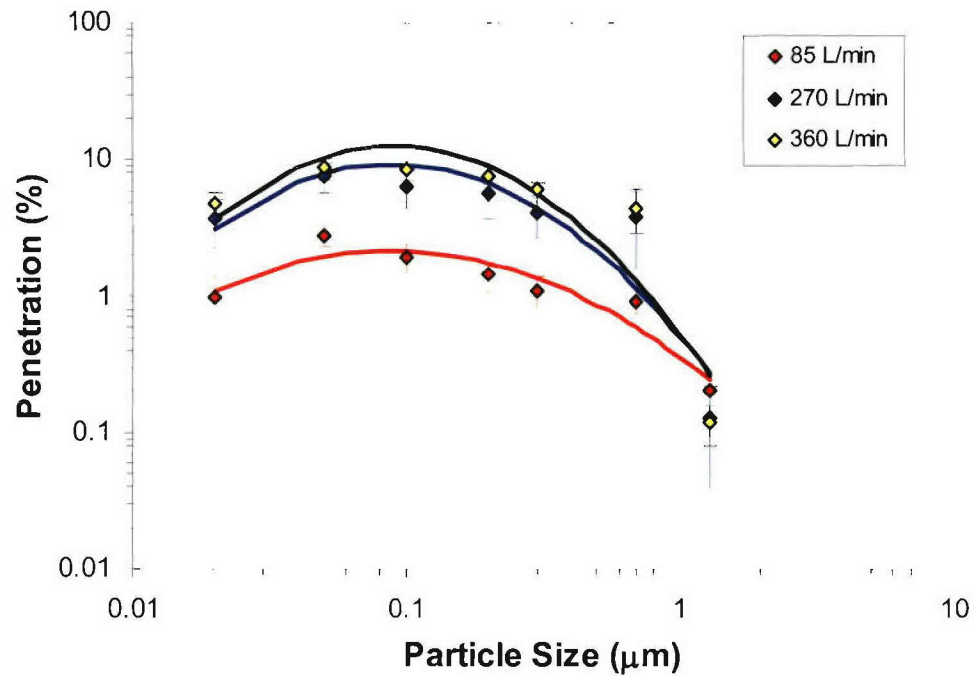
Figure 23. Effect of Particle Size and Flow Rate on Measured Penetration through MSA N95 Filtering Facepiece at Constant Flow
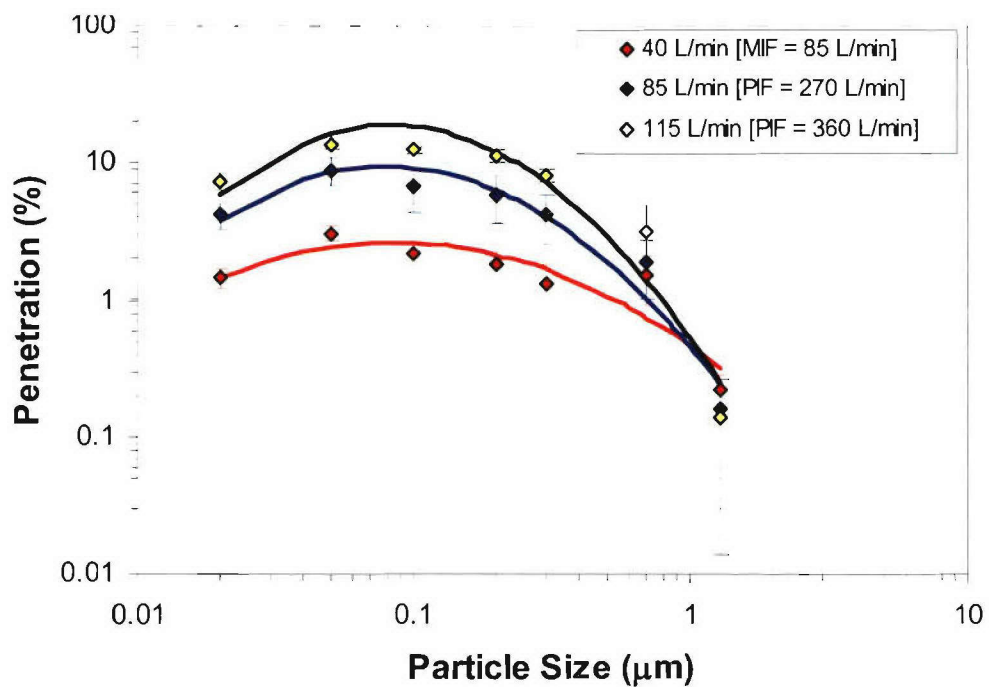
Figure 24. Effect of Particle Size and Flow Rate on Measured Penetration through MSA N95 Filtering Facepiece at Cyclic Flow

40

3.5.2 Constant/Cyclic Flow Comparisons

An important aspect of this task was to compare penetrations measured under constant and cyclic flow conditions. NIOSH certification testing of particulate filters is performed at a constant flow rate of 85 L/min (42 CFR 84, 1995) to demonstrate that filters meet a minimum requirement under controlled laboratory conditions. However, measurements of physiological parameters of workers show peak inhalation flow rates in excess of 300 L/min for short durations during high work load activities (Caretti et al., 2004; Kaufman and Hastings, 2005). As described in Section 2.1, few studies have been completed to correlate performance measured under constant and cyclic flow. Thus, there is concern that current certification test flow conditions may underestimate performance under actual use conditions.

The cyclic and constant flow conditions for this task were selected to allow comparisons based on cyclic flow: (1) minute volume, (2) MIF, and (3) PIF. Recall, the MIF is the average flow rate over the inhalation portion of the breathing cycle and the PIF is the maximum flow rate obtained. The flow conditions used to make these comparisons where noted in Table 3. For example, the 85 L/min constant flow matches a cyclic flow minute volume (2.3 L tidal volume, 37 breaths/min) and a MIF (1.6 L tidal volume, 25 breaths/min).

Figure 25 compares the penetrations measured under 85 L/min cyclic (based on minute volume) and constant flows. Although not explicitly shown, the data points correspond to the measured penetrations over the range of particle sizes tested (i.e., 0.02 to 2.9 µm). The black line is the 1-to-1 line and represents perfect agreement between the penetrations measured under the different flow conditions. The red and blue solid lines represent the best fit regressions of the cartridge and filtering facepiece data, respectively. The dashed lines represent 95 percent confidence intervals. The regression lines are both above the 1-to-1 line by a factor of 5 to 10 indicating higher penetrations were measured under cyclic flow for a given minute volume or constant flow of 85 L/$_{min}$. The regressions for the cartridges and filtering facepieces were nearly identical indicating that the trend is not dependent on filter type (i.e., cartridge versus filtering facepiece). Higher penetrations under cyclic flow were expected and are in agreement with the literature (Brosseau et al., 1990). For the sinusoidal flow used in this task (2.3 L and 37 breaths/min), over 95 percent of the inhalation volume passes through the filter at a rate in excess

41

of the minute volume. The peak flow reaches 270 L/min. As discussed above, penetration tends to increase with increased flow rate.
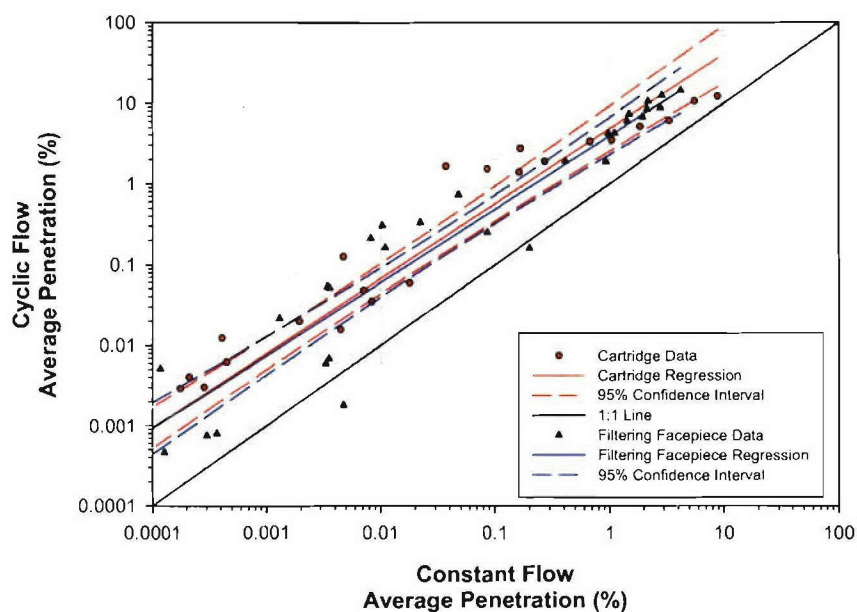
Figure 25. Comparison of Measured Penetrations under Cyclic and Constant Flow Conditions with Minute Volumes of 85 L/min

Figure 26 and 27 compare the measured penetrations under constant flow with those measured under cyclic flow with an equivalent MIF or PIF for the cartridges and filtering facepieces, respectively. The trends were nearly identical for both filter types. The MIF data points tend to lie above the 1-to-1 line indicating the penetrations measured under constant flow equivalent to the MIF were lower (40 percent lower on average) than the corresponding cyclic flow penetration. The converse was observed for the PIF comparison indicating that testing at a constant flow equivalent to the PIF provides a conservative estimate of filter performance under cyclic flow. The regression line for the PIF comparison nears the 1-to-1 line at the higher penetrations (>1%) where the data is for the N95 filters. Thus, it may be more important to consider the PIF when testing N95 filters, especially at the high volumetric flow rates that can be experienced during heavy work loads. As stated earlier, the N95 cartridges and both types of filtering facepieces are not well-suited for the high flow rates due their lower surface area as compared to the P100 cartridge filters evaluated in this study. A similar plot containing only P100 cartridge data is provided in Figure 28. Good agreement (within a factor of two) is observed between the constant flow penetrations and those measured at a cyclic flow with an

equivalent MIF. A method to estimate the cyclic flow penetration based on measured constant flow is provided in Appendix F. Good agreement is shown between the predicted and measured cyclic flow penetrations from this study.
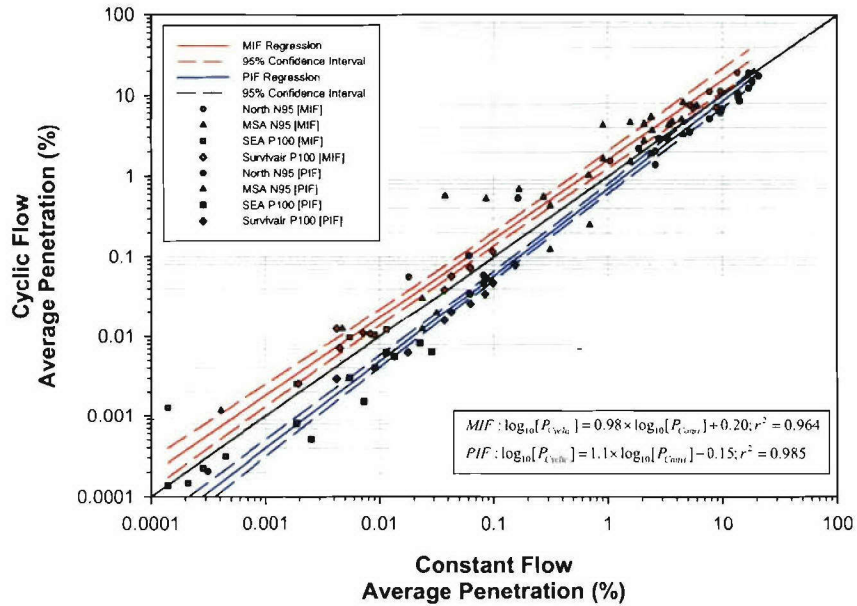
Figure 26. Comparison of Penetrations Measured under Constant and Cyclic Flow Conditions for Cartridge Filters
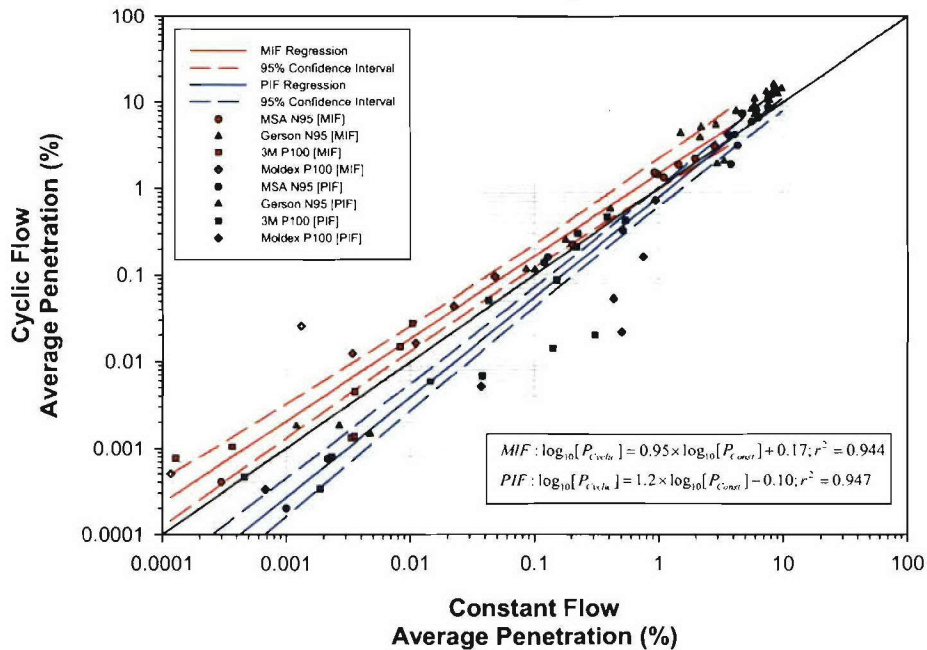
Figure 27. Comparison of Penetrations Measured under Constant and Cyclic Flow Conditions for Filtering Facepieces
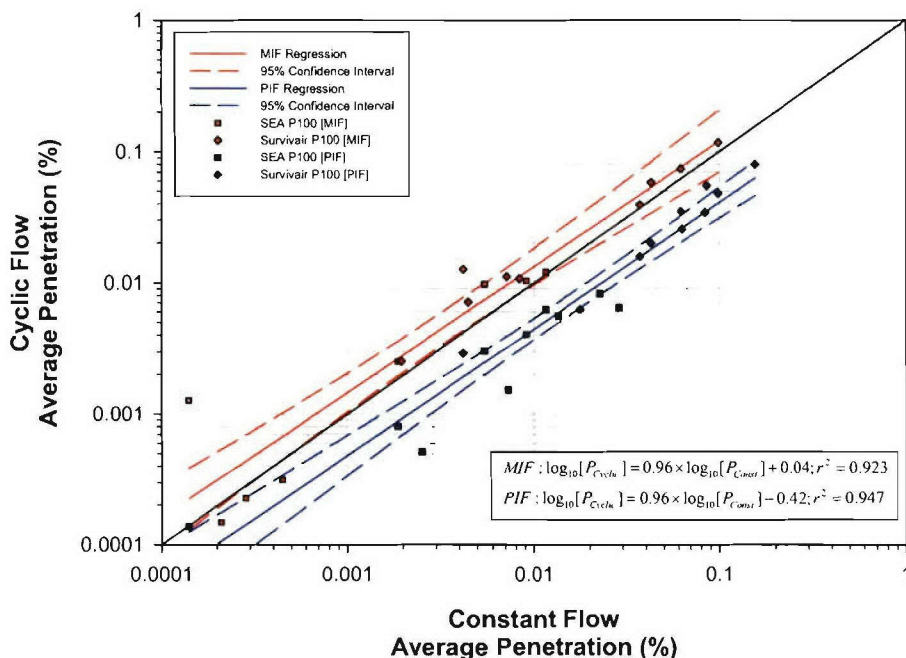
Figure 28. Comparison of Penetrations Measured under Constant and Cyclic Flow Conditions for P100 Cartridge Filters

3.6 Inert Aerosol Testing Summary

Filter efficiency testing was completed to assess the effect of particle size and flow condition on measured penetration. The following trends were observed:

- Penetration of submicron particles tended to increase with increased volumetric flow rate. The magnitude of increase was dependent on the filter type and particle size.

- The MPPS for P100 cartridges was generally between 0.1 to 0.2 μm and shifted toward the lower end of this range with increased flow.

- The MPPS for the N95 cartridges was generally 0.05 to 0.1 μm for all flow conditions.

- The MPPS for both P100 and N95 filtering facepieces was 0.05 to 0.1 μm.

- All filters efficiently removed the 0.7, 1.3, and 2.9 μm particles. Penetrations through P100 and N95 filters were less than 0.03 and 5 percent respectively, at all flow conditions and, thus, met the NIOSH requirement.

- Penetrations of submicron particles were in excess of the NIOSH requirements under the high flow conditions for all filters except the SEA HE-T P100 cartridge. The

Assigned Protection Factor (APF) of the mask and workplace breathing rates must be taken into account to determine if the increase in penetration is significant.

The following trends were observed regarding the comparison of penetrations measured under constant and cyclic flow conditions:
- Higher penetrations were measured under cyclic flow conditions as compared to a constant flow with an equivalent minute volume.
- Testing at a constant flow equivalent to the cyclic flow PIF provided a conservative estimate of filter performance under cyclic conditions.
- For the P100 cartridges, penetrations measured under constant flow and cyclic flow with an equivalent MIF were within a factor of two.

4.0 BIOAEROSOL FILTRATION EFFICIENCY TESTING

NIOSH-approved N, R, and P series particulate respirator filters have been shown to be effective against inert test aerosols in the most penetrating size range. However, it has not been well established that these filters provide comparable protection against biological aerosols especially with regard to high breather flow rates. This section describes the test methods and matrices that were used to characterize the performance of NIOSH-approved N95 and P100 filters using bacterial and viral aerosols under high breathing flows. The flow conditions and filter types were the same as described in Section 3.0 to allow direct comparison to the inert aerosol results. The two primary objectives were to: (1) assess respirator performance against bioaerosols, both bacterial and viral, under high flow conditions and (2) compare the measured aerosol penetrations to those of the inert aerosols.

4.1 Test Parameters

The filters tested included two N95 filtering facepieces, two P100 filtering facepieces, two N95 cartridges, and two P100 cartridges. They were the same brands and models as described in Table 2 of Section 3.1 and once again the exhalation valves were not sealed. The environmental conditions during testing were maintained at ambient temperature (25 ± 3°C) and

45

relative humidity (40 ± 10%). The filters were not preconditioned prior to testing (i.e., tested as-received). Tests were performed at two cyclic and two constant flow rates. The cyclic flow conditions had minute volumes of 85 and 135 L/min. Refer to Table 4 for the tidal volumes and breathing rates. The constant flow rates were 85 and 270 L/min. The 85 L/min was selected as it is the NIOSH certification flow rate. The 270 L/min provided an equivalent PIF and MIF to the cyclic flow conditions. Again, cartridges were tested at half the flow rate.

The biological aerosols consisted of bacterial Bg spores and viral MS2 phage. Both were generated using two different methods referred to as "wet" and "dry". Wet denotes dispersion of organisms in an effort such that the primary organism is achieved from a liquid suspension using a nebulizer. Dry denotes generation from a powder with a special carrier material or as agglomerates. Preparation and aerosol generation methods are described in Section 4.3. Bg spores were selected as the test aerosol due to their robustness. Thus, they have a high probability of remaining viable during the test. Bg spores are also a simulant commonly used for anthrax spores. Bg spores are rod-shaped with an approximate diameter of 0.7 to 0.8 μm and a length of 1.5 to 1.8 μm (Johnson et al., 1994). The aerodynamic diameter is typically 0.8 to 1.0 μm when suspended in water and aerosolized using a collison nebulizer (McCullough et al., 1997; Hanley and Foarde, 2003; Hofacre and Forney, 1996).

MS2 was selected as a representative viral aerosol as its viability after aerosolization has been demonstrated in a previous study (Hofacre et al., 1996). Viruses range in size from 0.02 to 0.3 μm and are generally found airborne as part of a droplet nuclei or attached to inert particles (Hinds, 1999). MS2 phage is icosahedron-shaped measuring approximately 20 nm in diameter. It is a bacteriophage that replicates inside host *E. coli* cells. Bacteriophages are non-pathogenic to humans and thus are safe to use for testing with limited engineering controls. As described earlier, Hofacre et al. (1996) aerosolized MS2 phage using a three-jet Collison nebulizer and measured the particle size distribution using a high-sensitivity laser aerosol spectrometer (HS-LAS, Particle Measuring Systems, Boulder, CO). The MS2 was present over a wide range of particle sizes likely as aggregates. The number distribution mode was approximately 0.1 μm and the mass distribution mode was 0.3 to 0.4 μm.

The bioaerosol challenge concentration was dependent on the target particle size and generation method. During characterization, suitable operating parameters were determined to permit measurement of aerosol penetrations of at least 0.03 percent, the NIOSH P100

requirement. Estimates of the minimum measurable penetration were made based on the challenge concentration, downstream sampling duration, and minimum detection limit of the aerosol sensing instrument. The minimum measurable penetration was generally 0.003, an order-of-magnitude lower than the NIOSH P100 requirement.

4.2 Test Matrix

The test matrices completed with the bioaerosol challenges are provided in Tables 8 and 9 for cyclic and constant flows, respectively. Three replicates were completed for each cell in the test matrix with the exception of the MS2 "dry" testing where only two replicates were performed due to the high efficiency of the filters. Each test included measurement of the aerosol penetration using both a bioassay method for viable organisms and an aerosol sensing instrument to measure total particle penetration.

Table 8. Test Matrix Completed to Assess Filter Performance under Cyclic Flow Conditions Using a Bioaerosol Challenge

Minute Volume (L/min)	Challenge Aerosol	Filtering Facepiece				Cartridges			
		MSA N95	Gerson N95	3M P100	Moldex P100	North N95	MSA N95	SEA P100	Survivair P100
85[a]	Bg "wet"	3	3	3	3	3	3	3	3
	Bg "dry"	3	3	3	3	3	3	3	3
	MS2 "wet"	3	3	3	3	3	3	3	3
	MS2 "dry"	2	2	2	2	2	2	2	2
135[a]	Bg "wet"	3	3	3	3	3	3	3	3
	Bg "dry"	3	3	3	3	3	3	3	3
	MS2 "wet"	3	3	3	3	3	3	3	3
	MS2 "dry"	2	2	2	2	2	2	2	2

(a) Cartridges were tested at half the minute volume.

Table 9. Test Matrix Completed to Assess Filter Performance under Constant Flow Using a Bioaerosol Challenge

Flow Rate (L/min)	Challenge Aerosol	Filtering Facepiece				Cartridges			
		MSA N95	Gerson N95	3M P100	Moldex P100	North N95	MSA N95	SEA P100	Survivair P100
85[a]	Bg "wet"	3	3	3	3	3	3	3	3
	Bg "dry"	3	3	3	3	3	3	3	3
	MS2 "wet"	3	3	3	3	3	3	3	3
	MS2 "dry"	2	2	2	2	2	2	2	2
270[a]	Bg "wet"	3	3	3	3	3	3	3	3
	Bg "dry"	3	3	3	3	3	3	3	3
	MS2 "wet"	3	3	3	3	3	3	3	3
	MS2 "dry"	2	2	2	2	2	2	2	2

(a) Cartrdiges were tested at half the flow rate.

4.3 Technical Approach

4.3.1 Test System

The test system used for biological testing was very similar to that used at ECBC for the inert testing with the large particle challenges (i.e., 0.7 to 2.9 μm). The test system, illustrated in Figure 29 for generating with a nebulizer, included an aerosol generator, exposure chamber with filter holder, aerosol classifier/sampler, and breathing machine. The aerosol generation and sampling systems varied depending on the biological aerosol being generated and are described in Sections 4.3.2 and 4.3.3.
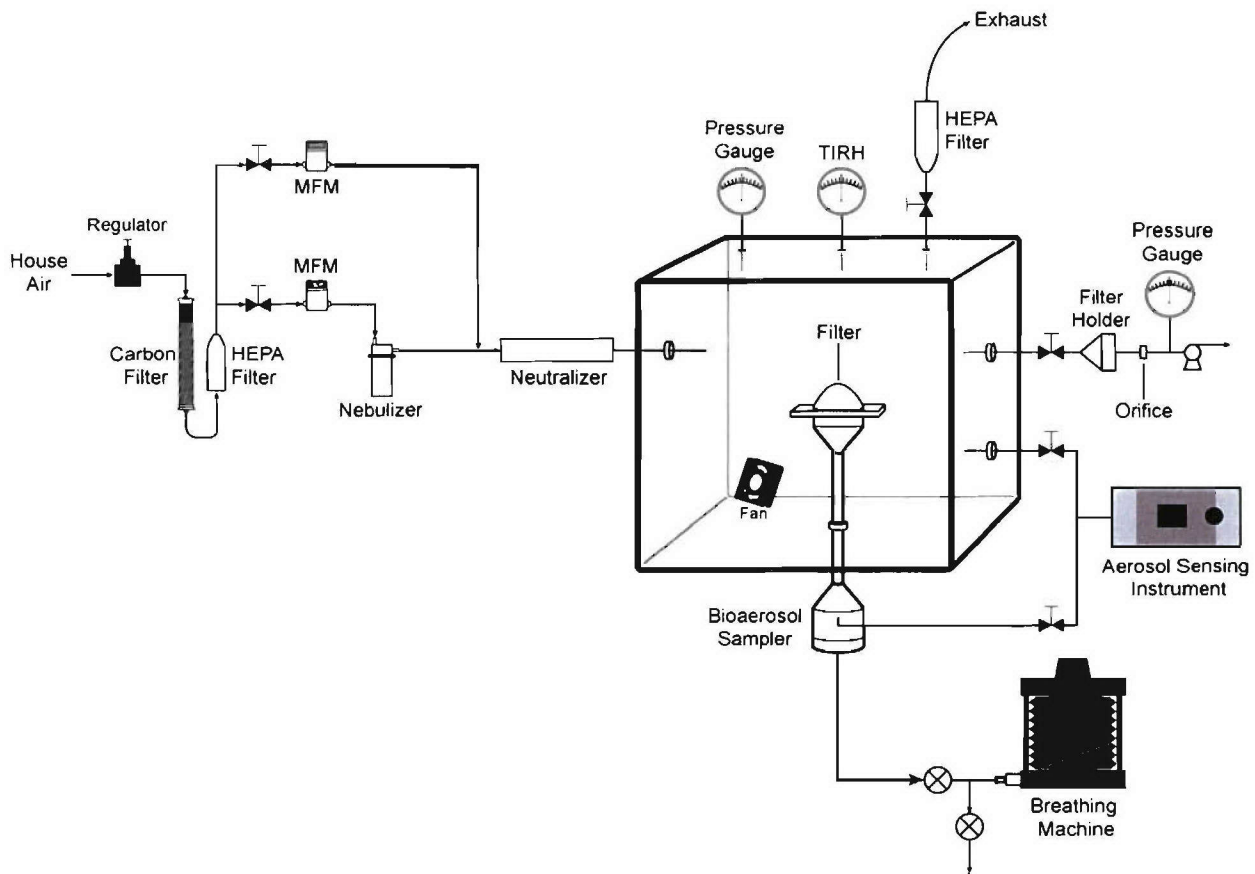
Figure 29. Schematic of Test System Used to Measure Bioaerosol Penetration

The aerosol generation systems delivered a continuous flow of aerosol laden air to the chamber to ensure a fresh, stable challenge aerosol was maintained. The challenge laden air exiting the generator was mixed with HEPA filtered dilution air. When generating from a liquid

48

solution, this mixing promoted the drying of the aerosol. The aerosol was then passed through a charge neutralizer (Model 3012, TSI, Shoreview, MN) and introduced into the test chamber where it was dispersed by small mixing fans. Excess challenge was vented through a HEPA filter and exhausted into the hood. The HEPA filters also allowed additional dilution air to be pulled into the chamber upon demand. The mask filter (filtering facepiece or cartridge) was mounted onto a holder and sealed inside the chamber. The holder was connected to the breathing machine (cyclic flow) or vacuum pump (constant flow) by flexible tubing. Similar to the approach used at ECBC for the inert testing, the downstream aerosol was sampled from a small chamber equipped with a stainless steel sample probe. The downstream chamber was also fitted with a port for sampling with the aerosol sensing instruments.

4.3.2 Bioerosol Generation Methods

Biological aerosols were generated using two different methods: (1) from an aqueous solution and (2) from a dry powder. This section describes both of these aerosol generation methods. For details regarding the preparation of the Bg spores and MS2 phage, refer to Appendix G.

4.3.2.1 Wet. The aerosol generation system for the wet technique consisted of a nebulizer, dryer, and charge neutralizer. The Bg spores or MS2 were suspended in filtered, deionized water and aerosolized using a 24-jet Collison nebulizer. Typical suspension concentrations were 1×10^8 colony forming units (cfu)/ml for the Bg spores and 1×10^{11} plaque forming units (pfu)/ml for MS2 phage. The aerosol was diluted with filtered house air and then pass through a Kr-85 charge neutralizer (Model 3012, TSI, Shoreview, MN) prior to delivery to the test chamber. Typical viable challenge concentrations were 1×10^5 cfu or pfu/L air. The charge neutralizer had to be removed from the test system when challenged with MS2 "wet" to obtain the target concentration.

4.3.2.2 Dry. The preparation of the dry powders is described in Appendix G. The dry powders were aerosolized using the Vilnius Aerosol Generator (VAG, CH Technologies, Westwood, NJ) shown in Figure 30. The VAG consists of three primary components:

(1) disperser, (2) aerosol monitor, and (3) output controller. The dry powder is placed on a membrane in the aerosolization chamber. Compressed air is used to vibrate the membrane to aerosolize the powder and also activate a rotary turbovane which deaglommerates the particles. The aerosolization chamber and turbovane are shown in Figure 31. The Microdust 880 (Casella, Bedford, UK) is used to continuously monitor the aerosol output. The controller processes the signal from the Microdust 880 and adjusts the frequency of vibration to maintain a steady aerosol output. Typical viable aerosol concentrations were generally 1×10^4 to 1×10^5 cfu or pfu/L air.

Figure 30. Vilnius Aerosol Generator
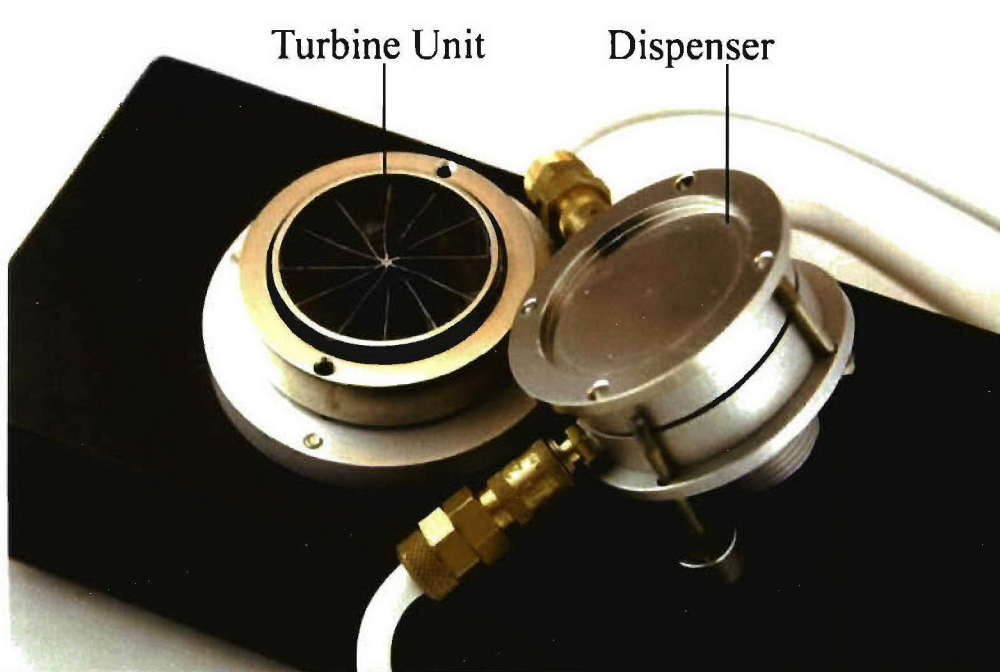
Figure 31. Aerosolization Chamber and Rotary Vane of Vilnius Aerosol Generator

4.3.3 Aerosol Sampling and Classification

Samples to assess penetration of viable organisms were collected on 47-mm filters as described in Section 4.3.3.1. In addition, two types of light scattering instruments, described in Section 4.3.3.2 were used to measure total-particle efficiencies.

4.3.3.1 Viable Samples. Viable samples were collected on 47-mm filters for subsequent bioassay. Bg spores were collected on mixed cellulose ester filters and the MS2 phage was collected on water soluble gelatin filters. The mixed cellulose ester filters were not used with the MS2 due to poor collection efficiency at the smaller particle size. The challenge sample was collected through a sampling probe that extended away from the chamber wall. The 47-mm filter was housed in a 47 mm filter holder and a sample pump was used to pull 4 L/min through the filter. A critical orifice was used to control the flow rate. The filters were analyzed as described in Appendix G to determine the number of colony forming units (cfu) or plaque forming units (pfu) per liter of air sampled.

4.3.3.2 Optical Particle Counters. The Aerosizer® (Amherst Proscess Instruments, Hadley, MA) classifies particles based on their aerodynamic behavior. The instrument measures the time-of-flight as particles are accelerated through the sensing zone of the instrument. The time-of-flight is proportional to particle size and density. The density of the aerosol material is used to determine the particle size distribution either on a number, surface, or volume (mass) basis. The Aerosizer® can classify particles ranging from 0.5 to 200 µm. Data reducing software that accompanies the instrument permits user selected size ranges to be analyzed. Thus, polydisperse aerosols could be analyzed within a selected size range. The sample flow rate is 1.5 L/min.

The laser aerosol spectrometer (LAS-X, Particle Measuring Systems, Boulder, CO) is a laser aerosol spectrometer capable of classifying particles between 0.1 and 3.0 µm in diameter into 16 size discrete bins. The LAS provides a measure of the particle size based on the light scattering properties of the aerosol. Particles are focused into the sensing region by the pneumatic system such that particles pass through one at a time. The light from the He-Ne laser is scattered by the particle, which is then collected by receiving optics. The signal intensity produced is proportional to the particle size and the number of signals is a measure of the number of particles counted. Thus, the LAS gives a number distribution of the aerosol and size specific channels of interest which can be selected for data analysis. The sample flow rate is approximately 100 cm^3/min.

4.3.3.3. Cascade Impactor. A cascade impactor (Model 266 Marple Impactor, Sierra Instruments, Carmel Valley, CA) was used to characterize the aerodynamic particle size distribution of the viable biological aerosols. The impactor was operated at 2.4 L/min. Particles of sufficient size and inertia cross the flow streamline and are impacted on slides and collected. Smaller particles are able to remain in the flow streamlines and pass on to the next stage. Each stage has an associated diameter cut-point equivalent to particle size (diameter). A calculation of the loaded mass of the impactor slide and the volumetric flow rate, in conjunction with volume-density relationship, reveals the number of particles with a given size bin. Characteristics of the impactor are listed in Table 10 with ranges of aerodynamic particle diameters highlighted. The number of viable particles collected on each stage was determined by bioassay.

Table 10. Particle Size Range Six-Stage Cascade Impactor

Impactor Stage	Aerodynamic Diameter Range (μm)
Backup filter	$d \leq 0.29$
Stage 1R	$0.29 < d \leq 0.78$
Stage 6	$0.78 < d \leq 1.5$
Stage 5	$1.5 < d \leq 3.2$
Stage 4	$3.2 < d \leq 6.8$
Stage 3	$6.8 < d \leq 12$
Stage 2	$12 < d \leq 19$
Stage 1	$d > 19$

4.3.4 System Characterization

Prior to efficiency testing, shakedown testing was performed to establish proper operating conditions. This included comparison of the Battelle and ECBC test systems, characterization of the aerosol generators, measurement of bioaerosol particle size distributions, and characterization of the viable particle samplers. The shakedown testing is described in Appendix H.

4.3.5 Test Procedure

The mask filter was mounted to the test fixture and the exposure chamber sealed. The breathing machine and bioaerosol generation system were started and allowed to operate for approximately 10 minutes to reach a steady state challenge concentration. The mask filter and downstream bioaerosol sampler were bypassed during system startup. After approximately 10 minutes, sampling with the viable particle samplers began by directing the flow through the mask filter. The upstream and downstream 47-mm filters were collected simultaneously. Sample duration depended on the expected aerosol concentration and was typically 2 minutes for the challenge aerosol and 10 minutes for the downstream. Two sets of 47 mm filters were collected in sequence. The average measured concentrations were used to determine the penetration.

Sampling with the HS-LAS or Aerosizer® was performed simultaneously with the viable particle samplers. First, the challenge was sampled for approximately two minutes. The sampling line was then switched to downstream of the filter and adequate time was given for the

instrument response to stabilize. The downstream sample duration ranged from five to fifteen minutes to provide sufficient time to count a statistically significant number of particles. A second sample of the challenge was then recorded. If the two challenge samples (before and after downstream sampling) were not within 20 percent of each other, the test was repeated. After sampling was complete, the aerosol generation system was stopped and the chamber flushed with clean air. The viable particle samplers were removed from the test system for analysis.

4.4 Calculation of Aerosol Penetration

The aerosol penetration was defined in Section 3.4 for the inert aerosols. Efficiencies were measured based on both total and viable particle concentrations. For the total particle analyzers, the size specific channels of interest were selected for the analysis. The challenge concentration was the average of the measurements made before and after the downstream sample. The aerosol number concentration used was determined by summing the number of particles in the selected size range and dividing by the volume of air sampled (product of sampling flow rate and sampling duration). The viable particle concentration was determined from the bioassay of the 47-mm filters. Two upstream and two downstream samples were collected during each test. The number of particles, after correcting for dilution factors during bioassay, was divided by the volume of air sampled to obtain the number concentration. The average values were used to calculate the penetration.

As described in Section 4.1, the challenge concentration was maintained at a level to measure penetrations of at least 0.03 percent. Minimum detection limits were established for both the Bg spore and MS2 phage enumeration methods. The limits were 2 cfu or pfu/L air sampled. The typical challenge concentration for the Bg spore testing was 1×10^5 cfu/L resulting in a minimum measurable penetration of 0.002 percent. Likewise, depending on flow condition, the challenge concentration of MS2 phage ranged between 1×10^4 and 1×10^5 leading to minimum penetrations of 0.02 to 0.002 percent. The actual minimum penetration varied from trial to trial depending on the measured challenge concentration.

4.5 Bioaerosol Results

This section summarizes the results of testing with biological aerosols. Section 4.5.1 discusses the measured Bg spore particle size distributions and the measured penetrations. A similar discussion follows in Section 4.5.2 for the MS2 phage. Section 4.5.3 compares the penetrations measured using the biological aerosols to those measured with the inert aerosols.

4.5.1 Bg Spore Results

4.5.1.1. Particle Size Distribution. The aerosol size distributions of the Bg spores generated using the "wet" and "dry" methods were characterized using the cascade impactor and Aerosizer. The results are summarized in Table 11 and are compared graphically in Figures 32 through 34 as measured by the impactor and Aerosizer. Note that the lower limit for the Aerosizer is 0.5 μm. Both instruments indicated that aerosolization from the dry powder led to a slightly larger median diameter and broader distribution. The particle size distributions were consistent with the literature which indicated an aerodynamic diameter ranging from 0.8 to 1.0 μm (McCullough et al., 1997; Hanley and Foarde, 2003; Hofacre and Forney, 1996).

Table 11. Comparison of "Wet" and "Dry" Bg Size Distributions

Generation Method	Aerosizer		Impactor	
	NMD (μm)	$\sigma_g^{(a)}$	AMMD (μm)	σ_g
Bg "wet"	1.1	1.1	0.7	2.5
Bg "dry"	1.3	1.6	0.9	2.7

(a) σ_g = Geometric standard deviation.
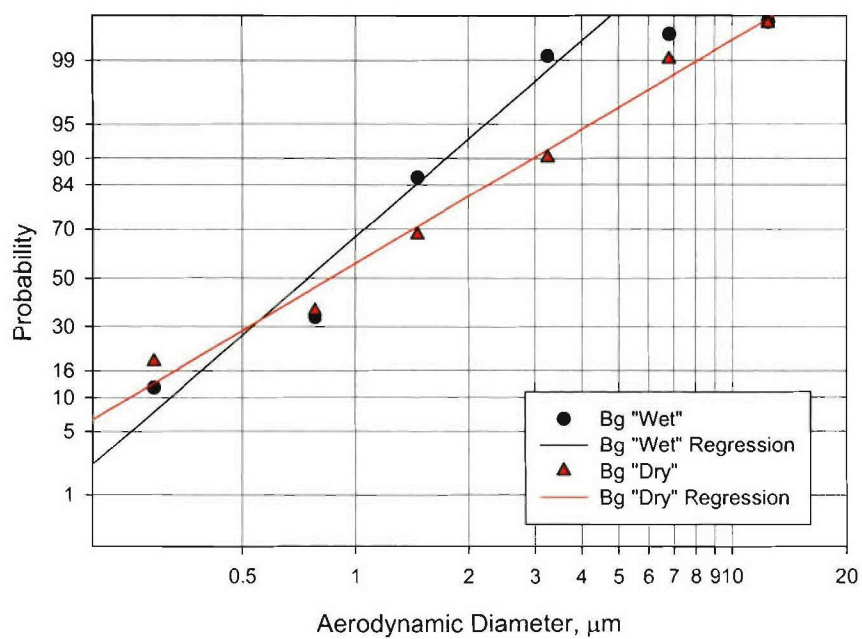
Figure 32. Size Distribution of "Wet" and "Dry" Bg Spores Measured Using the Cascade Impactor
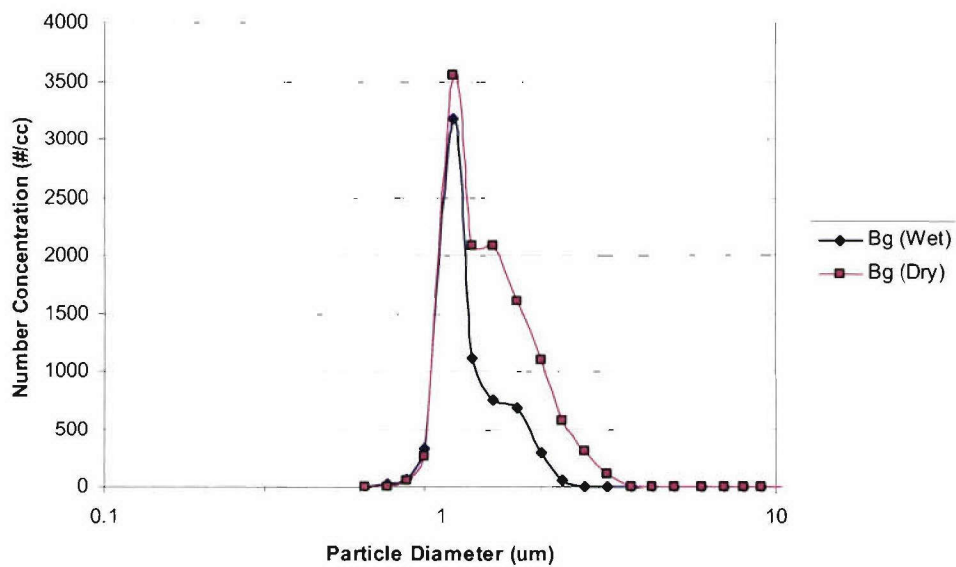
Figure 33. Size Distribution of Bg Spores Measured Using the Aerosizer
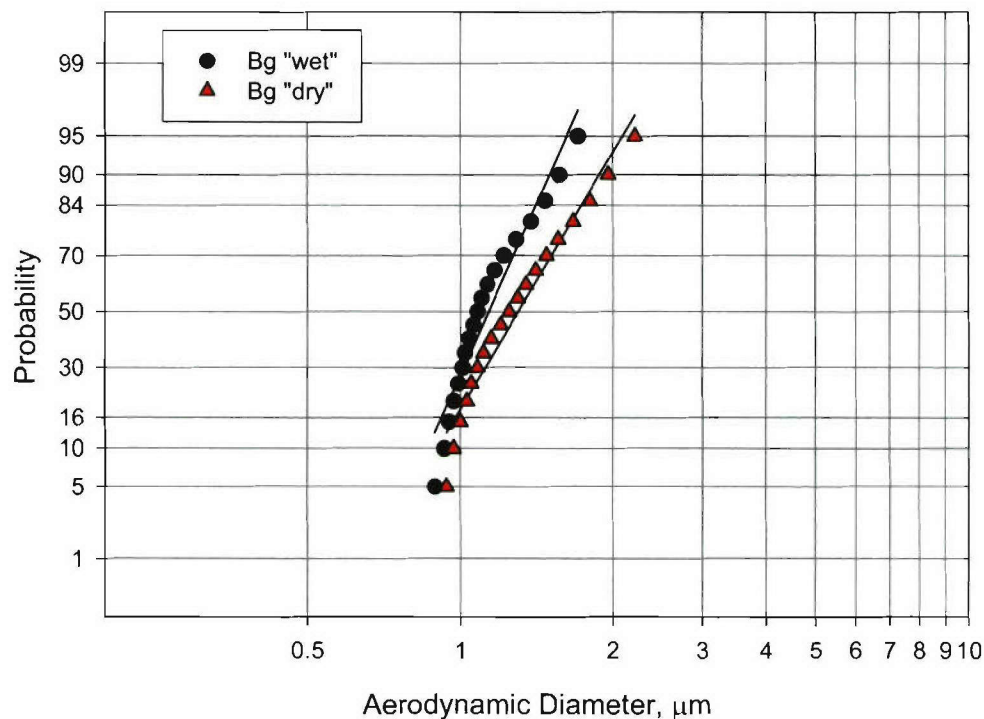
Figure 34. Size Distribution of Bg Spores Measured Using the Aerosizer (Cumulative Number Distribution)

4.5.1.2 Bioassay Penetration Results. The penetrations measured using the Bg spore aerosol challenge and bioassay method are summarized in Tables 12 and 13 for the "wet" and "dry" generation techniques. The penetrations generally represent the average of at least three trials. Average penetrations with at least one trial below the minimum detection limit (~0.002%) are noted and standard deviations are not provided. The results from the individual trials are summarized in Appendix I. Both the P100 cartridges and filtering facepieces were very efficient against the Bg spore challenge as all penetrations were less than the 0.03 percent requirement, generally by at least an order-of-magnitude. The N95 filters were less efficient as compared to the P100 filters but still had penetrations generally less than 0.5 percent. As shown in Figures 35 and 36, the penetrations increased with increased flow rate with exception of the MSA Affinity Plus® filtering facepiece and the "wet" Bg challenge. The cause of this anomaly was not identified and repeated tests provided similar results. This trend was not observed for the Bg "dry" aerosol.

Table 12. Comparison of Penetration Measured Using Bioassay Method and Bg Spore "Wet" Aerosol Challenge under Constant and Cyclic Flow Conditions

Filter Type	Filter	Flow Rate[a] (L/min)			
		Constant		Cyclic	
		85	270	85	135
		Average Penetration (%)			
Cartridge	MSA N95	0.002[b]	0.005±0.001	0.003[b]	0.034±0.041
	North N95	0.005	0.009[b]	0.006±0.004	0.014±0.007
	Survivair® P100	0.003[b]	0.004[b]	0.001[b]	0.006[b]
	SEA P100	0.004[b]	0.004[b]	0.002[b]	0.002[b]
Filtering Facepiece	MSA N95	0.13±0.12	0.13±0.10	0.35±0.18	0.047±0.024
	Gerson® N95	0.036±0.23	0.40±0.18	0.21±0.08	0.26±0.07
	3M® P100	0.003[b]	0.010[b]	0.005[b]	0.005[b]
	Moldex P100	0.023[b]	0.012[b]	0.006±0.002	0.009±0.002

(a) Cartridge testing performed at half the flow rate
(b) At least one trial resulted in penetration below detectable limit

Table 13. Comparison of Penetration Measured Using Bioassay Method and Bg Spore "Dry" Aerosol Challenge under Constant and Cyclic Flow Conditions

Filter Type	Filter	Flow Rate[a] (L/min)			
		Constant		Cyclic	
		85	270	85	135
		Average Penetration (%)			
Cartridge	MSA N95	0.005[b]	0.014±0.004	0.013±0.002	0.030±0.011
	North N95	0.006±0.005	0.074±0.075	0.055±0.047	0.032±0.001
	Survivair® P100	0.003[b]	0.030[b]	0.002[b]	0.003[b]
	SEA P100	0.001[b]	0.003[b]	0.003[b]	0.002[b]
Filtering Facepiece	MSA N95	0.035±0.030	0.042±0.016	0.13±0.048	0.64±0.59
	Gerson® N95	0.028±0.007	0.20±0.064	0.20±0.14	2.4±2.5
	3M® P100	0.008[b]	0.03[b]	0.001[b]	0.003[b]
	Moldex P100	0.017±0.015	0.004[b]	0.003[b]	0.003[b]

(a) Cartridge testing performed at half flow rate
(b) At least one trial resulted in penetration below detectable limit
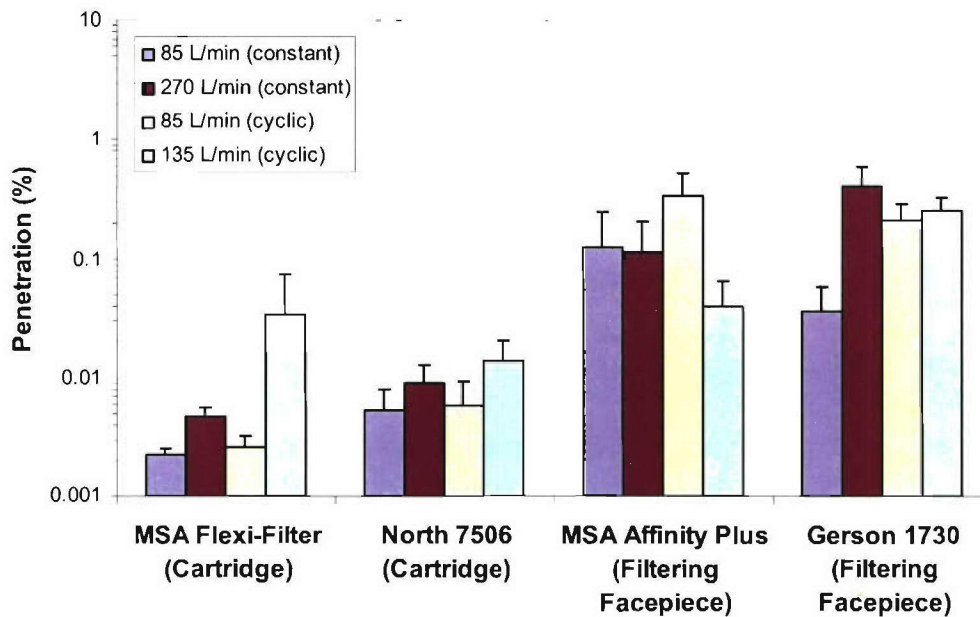
Figure 35. Comparison of Measured Bg "Wet" Penetrations through N95 Filters
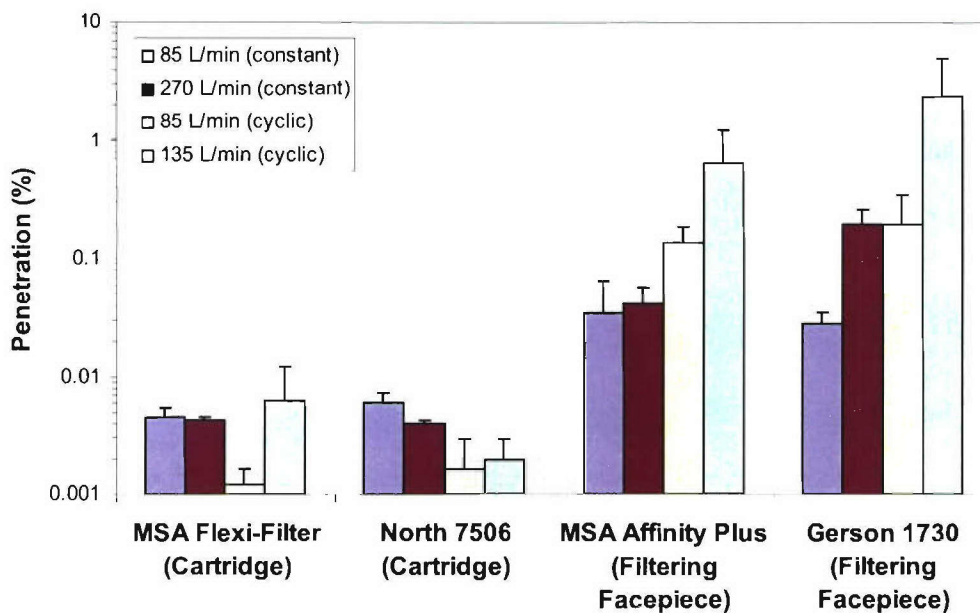
Figure 36. Comparison of Measured Bg "Dry" Penetrations through N95 Filters

The penetrations measured using the "wet" and "dry" Bg challenges with the bioassay method are compared in Figures 37 and 38 for the cartridges and filtering facepieces, respectively. The black diagonal line is the 1-to-1 line and represents perfect agreement. The

error bars represent one standard deviation about the mean. In general, the penetrations measured with each challenge for each filter were within a factor of four. From a practical perspective, the differences in the penetrations were not significant.
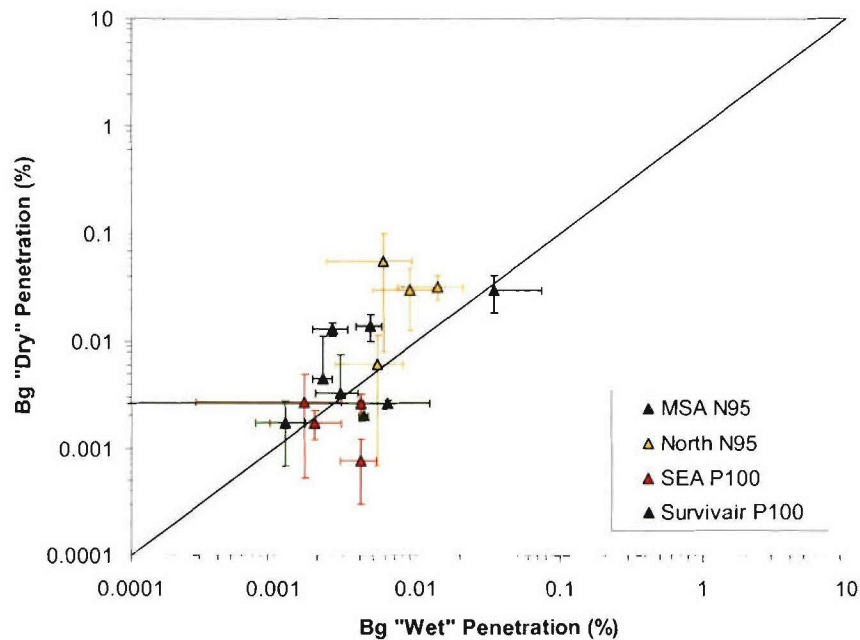
Figure 37. Comparison of Bg "Wet" and "Dry" Penetrations through Cartridge Filters
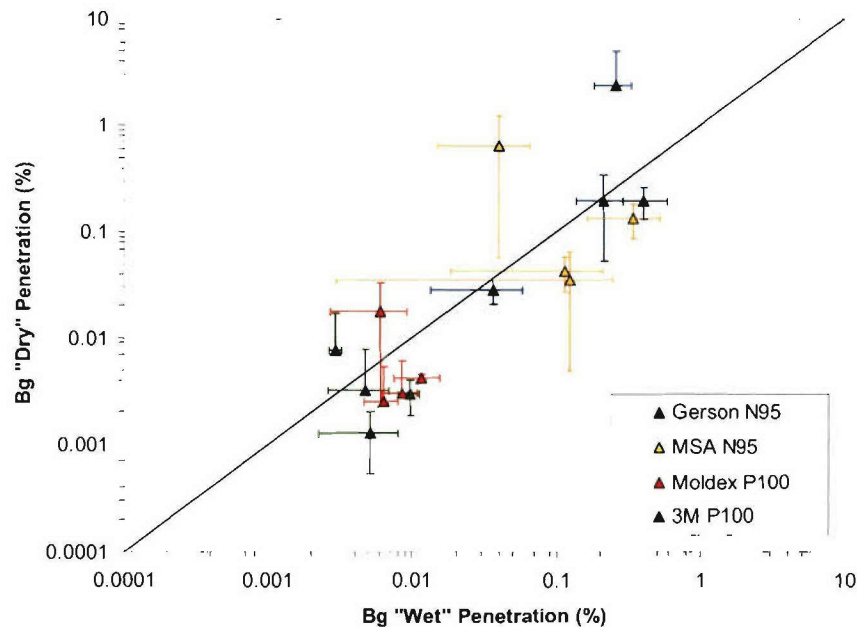
Figure 38. Comparison of Bg "Wet" and "Dry" Penetrations through Filtering Facepieces

Figure 39 compares the penetrations measured using the bioassay method with that using the LAS-X. Again, the black diagonal line represents the 1-to-1 line. During each trial, the penetration was measured using both techniques creating paired data. For the LAS-X, the penetration was calculated based on size specific channels ranging from 0.65 to 1.25 μm (Channels 9, 10, and 11). The results from each trial are plotted in Figure 39. Higher penetrations tended to be measured using the LAS as compared to the bioassay method as evidenced by the majority of the data points lying below the 1-to-1 line. This is likely because the LAS measured total particle penetration while the bioassay method measured only the viable particle penetration. These results demonstrate that using an optical light scattering instrument such as the LAS to measure bacterial aerosol penetration provides a conservative estimate of filter performance. This conclusion is consistent with the literature (Brosseau et al., 1994) and is notable since the LAS-X method is much less labor intensive compared to the bioassay method.
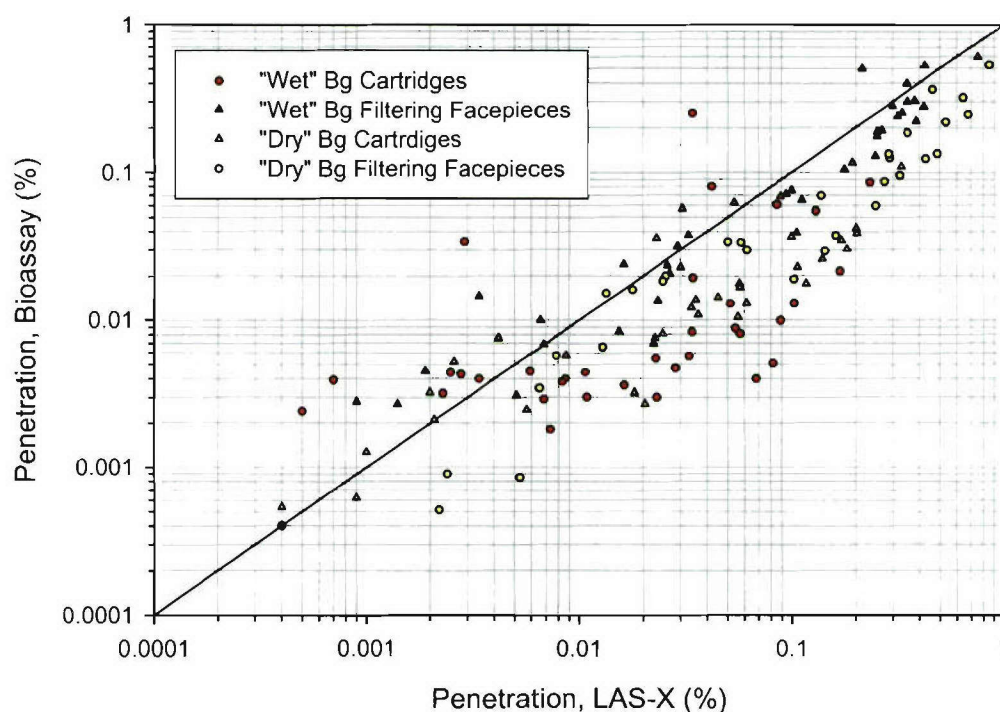
Figure 39. Comparison of Bg Spore Penetrations Measured Using the Bioassay Method and LAS-X

4.5.2 MS2 Phage Results

4.5.2.1. Particle Size Distribution. The aerosol size distributions of the MS2 phage generated using the "wet" and "dry" aerosolization methods were characterized using the cascade impactor, LAS, and Aerosizer. The results are summarized in Table 14 and are compared graphically in Figures 40 through 42. Note that the lower limit for the Aerosizer is 0.5 μm and the LAS is 0.1 μm.

Table 14. Comparison of "Wet" and "Dry" MS2 Aerosol Size Distributions

Generation Method	LAS/Aerosizer		Impactor	
	NMD (μm)	σ_g	AMMD (μm)	σ_g
MS2 "wet"	0.2[a]	1.4	0.5	1.3
MS2 "dry"	2.3[b]	1.3	2.5	2.0

(a) Size distribution measured using LAS-X only.
(b) Size distribution measured using Aerosizer only.
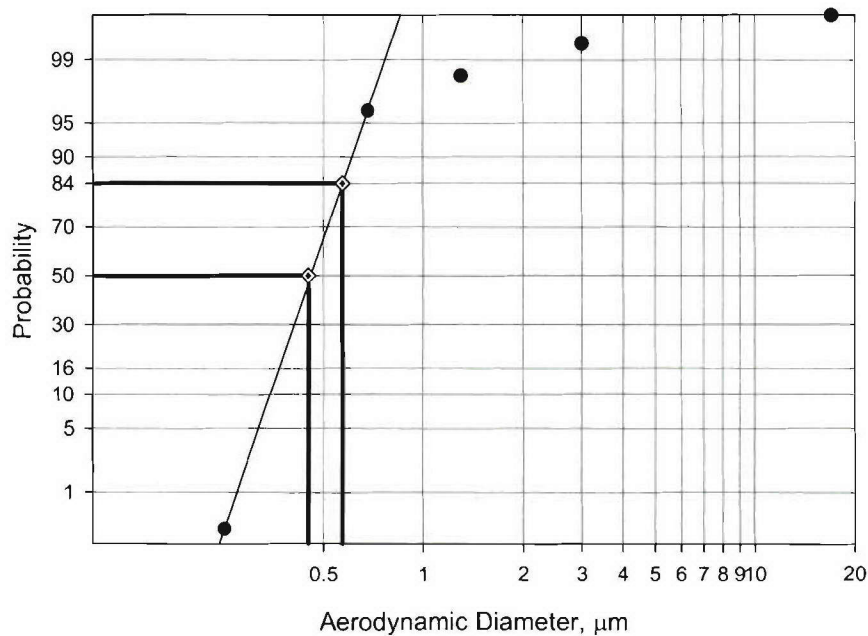
Figure 40. Size Distribution of MS2 "Wet" Measured Using the Sierra Impactor
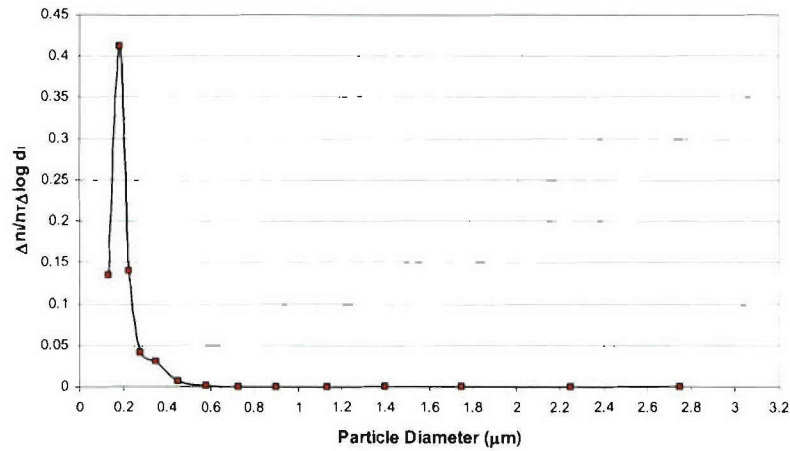
Figure 41. Size Distribution of MS2 "Wet" Measured Using the LAS-X
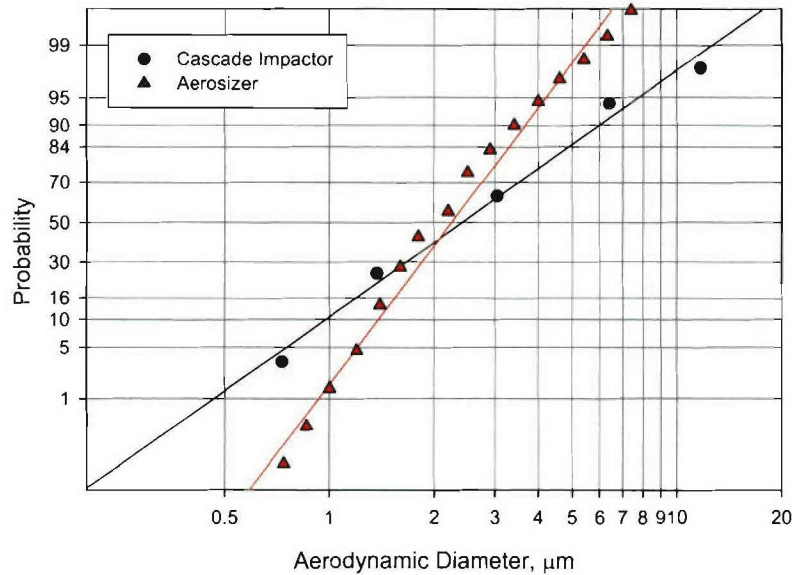
Figure 42. Size Distribution of MS2 "Dry" Measured Using the Sierra Impactor and Aerosizer

4.5.2.2 MS2 Penetration Results. The penetrations measured using the MS2 phage aerosol challenge and bioassay method are summarized in Tables 15 and 16 for the "wet" and "dry" aerosol generation techniques. The results from the individual trials are summarized in Appendix I. The P100 and N95 filters both met their respective penetration requirements (i.e., maximum 0.03 and 5 percent penetration) at all flow conditions tested. This is significant because the MS2 "wet" aerosol is near the MPPS for both types of filters. As shown in Figure 43, mean penetration of the "wet" MS2 aerosol tended to increase with increased flow rate. All

filters were highly efficient at removing the MS2 "dry" aerosol challenge as expected since it had a count median diameter above 1 μm. Flow rate did not have as significant an effect on MS2 "dry" aerosol penetrations as with the smaller MS2 "wet" as shown in Figure 44. The P100 filters are not included in Figures 43 and 44 as the measured penetrations were generally below detectable limits. Assuming that inertial impaction is the primary mechanism for collection of the MS2 "dry" aerosol, penetration would not be expected to change significantly with increased flow.

Table 15. Comparison of Penetration Measured Using Bioassay Method and MS2 "Wet" Aerosol Challenge under Constant and Cyclic Flow Conditions

Filter Type	Filter	Flow Rate[a] (L/min)			
		Constant		Cyclic	
		85	270	85	135
		Average Penetration (%)			
Cartridge	MSA N95	0.55±0.75	1.3±1.2	1.1±1.0	0.54±0.36
	North N95	0.30±0.10	1.9±1.1	1.7±2.0	2.5±1.7
	Survivair® P100	0.022±0.015	0.018[b]	0.012[b]	0.030[b]
	SEA P100	0.002[b]	0.009[b]	0.007[b]	0.015[b]
Filtering Facepiece	MSA N95	0.51±0.37	1.7±1.8	0.93±0.60	1.1±0.61
	Gerson® N95	0.51±0.30	1.8±0.55	0.48±0.07	0.89±0.43
	3M® P100	0.001[b]	0.014[b]	0.002[b]	0.003[b]
	Moldex P100	0.005±0.003	0.050±0.007	0.001[b]	0.010±0.006

(a) Cartridge testing performed at half the flow rate
(b) At least one trial resulted in penetration below detectable limit

Table 16. Comparison of Penetration Measured Using Bioassay Method and MS2 "Dry" Aerosol Challenge under Constant and Cyclic Flow Conditions

Filter Type	Filter	Flow Rate[a] (L/min)			
		Constant		Cyclic	
		85	270	85	135
		Average Penetration (%)			
Cartridge	MSA N95	0.009[b]	0.007±0.004	0.003[b]	0.025±0.005
	North N95	0.001[b]	0.022±0.001	0.005±0.002	0.012±0.009
	Survivair® P100	0.002[b]	0.002[b]	0.005[b]	0.012[b]
	SEA P100	0.001[b]	0.002[b]	0.001[b]	0.004[b]
Filtering Facepiece	MSA N95	0.007	0.009±0.004	0.022±0.009	0.082±0.030
	Gerson® N95	0.22±0.27	0.52±0.69	0.60	0.075±0.034
	3M® P100	0.002[b]	0.004[b]	0.009[b]	0.003[b]
	Moldex P100	0.004[b]	0.004[b]	0.014[b]	0.004[b]

(a) Cartridge testing performed at half flow rate
(b) At least one trial resulted in penetration below detectable limit
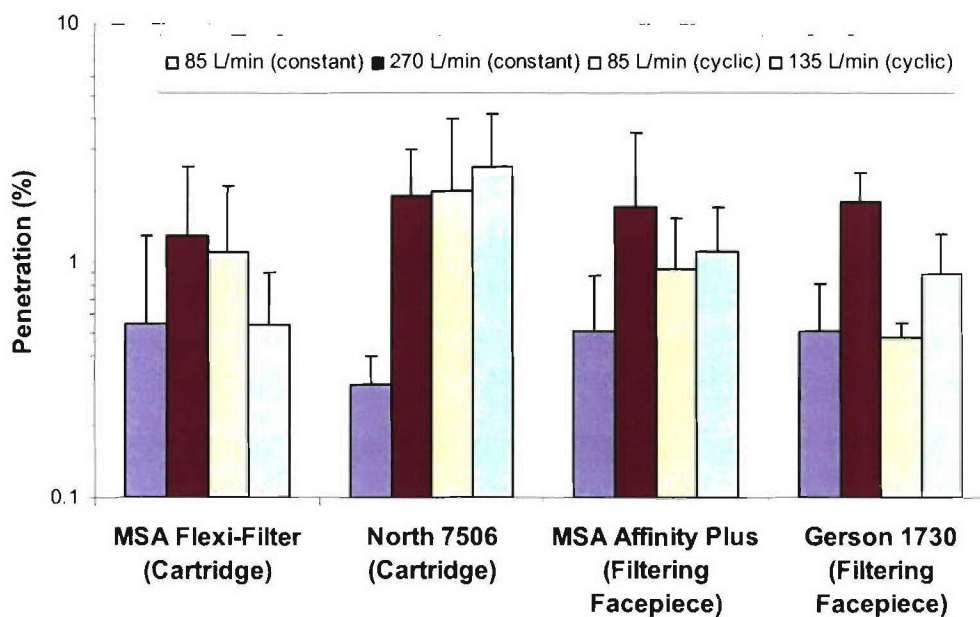
**Figure 43. Comparison of Measured MS2 "Wet" Penetrations through N95 Filters**
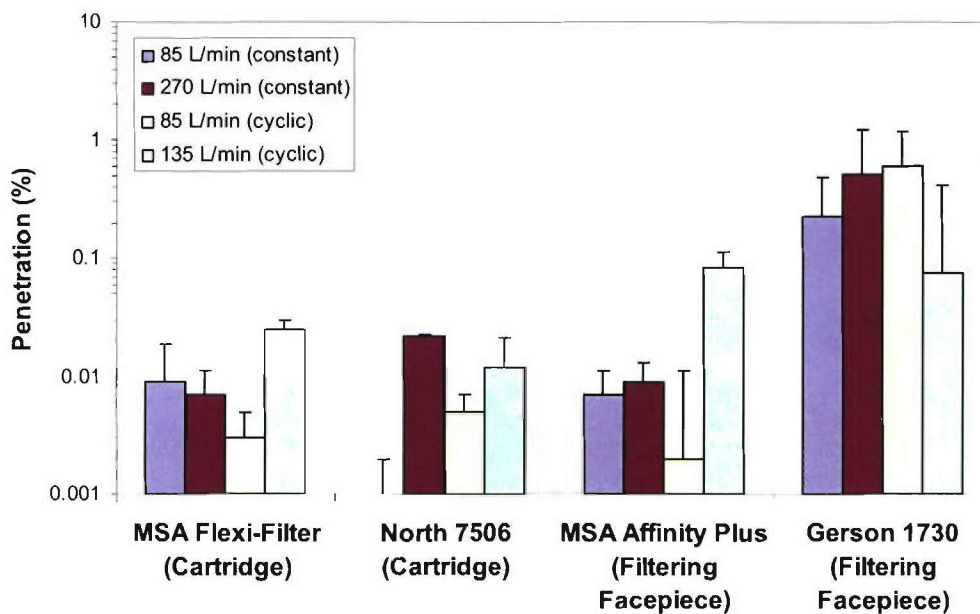
Figure 44. Comparison of Measured MS2 "Dry" Penetrations through N95 Filters

Figure 45 compares the penetrations measured using the bioassay method with that using the LAS-X for the MS2 "wet" aerosol challenge. The "dry" aerosol results are not

included as the majority of the penetrations measured using the bioassay method were below detectable limts. For the LAS-X, the penetration was calculated based on size specific channels ranging from 0.13 to 0.25 μm (Channels 2, 3, and 4). As observed for the Bg spores, higher penetrations tended to be measured using the LAS as compared to the bioassay method.
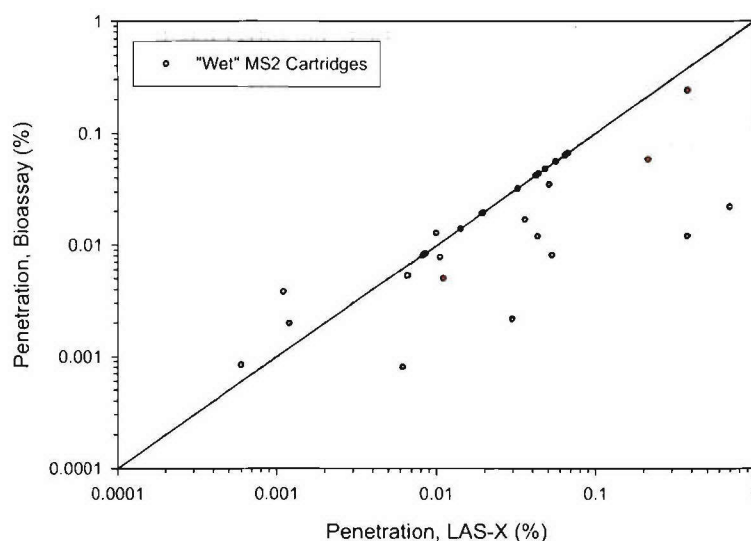
Figure 45. Comparison of MS2 Phage Penetrations Measured Using the Bioassay Method and LAS-X

4.5.3 Inert Comparisons

This section compares the penetrations measured using the biological aerosols with those measured using the inert aerosols as described in Section 3.0. The Bg spore comparisons are provided in Section 4.5.4.1 and the MS2 comparisons follow in Section 4.5.4.2. The comparisons were performed only on the N95 filters as they generally had measurable penetrations. The biological penetrations through the P100 filters were generally below detectable limits.

4.5.3.1 Bg Spores. Figure 46 compares the "wet" and "dry" aerosol penetrations through the North 7506 cartridge with the 0.7 and 1.3 μm PSL. As shown, similar penetrations were measured with the 1.3 μm PSL as with the Bg acrosols. The penetration of 0.7 μm PSL was typically an order-of-magnitude higher. Figure 47 also demonstrates the agreement with a

micron sized particle. The red and blue horizontal lines represent the average penetrations measured using the Bg challenge at 42.5 and 135 L/min constant flow, respectively. The intersection of these lines with the inert results is an indication of the inert particle size that provides an equivalent penetration. For example, measured bioaerosol and inert penetrations intersect at a particle size of approximately 1.7 μm for the North 7506 cartridge at a 135 L/min flow rate. This intersection is designated by the blue circle. The Bg spores had an AMMD of approximately 1.2 μm as measured by the Aerosizer. Similar trends were observed for the other N95 filters in Figures 48 through 50. In most cases, the 1.3 μm PSL provided the best agreement as inert and Bg penetrations were generally within a factor of five.
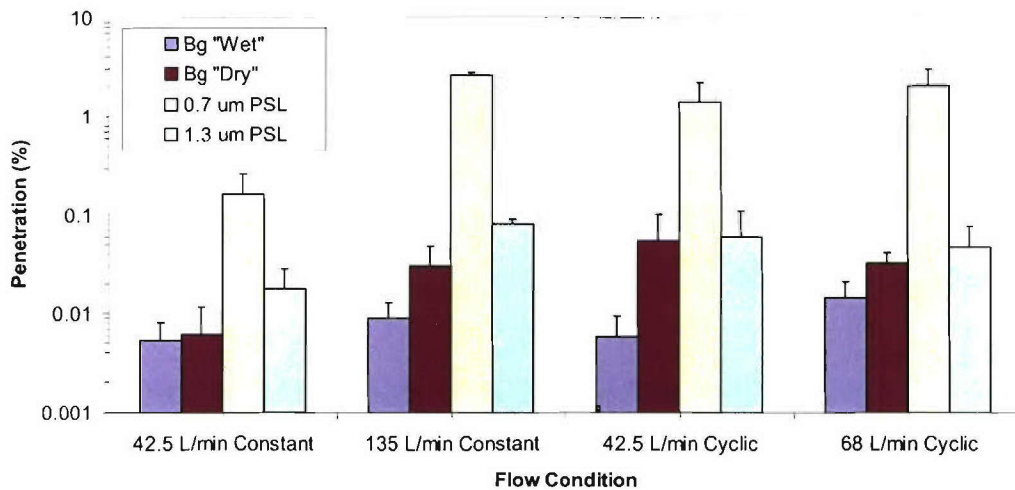
Figure 46. Comparison of Bg Spore and Inert Penetrations through the North N95 7506 Cartridge
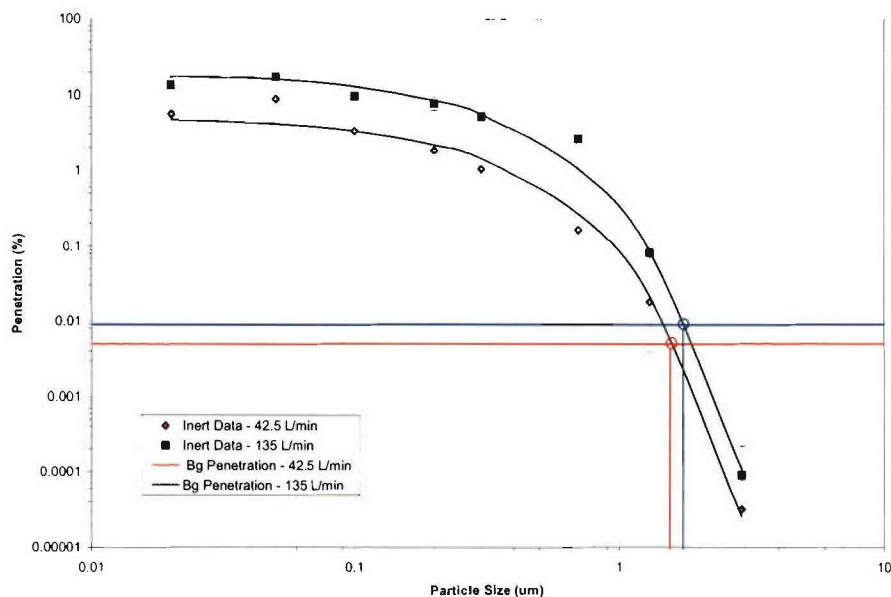
Figure 47. Comparison of Measured Inert and Bg Bioaerosol Penetrations through the North 7506 Cartridge at Constant Flows of 42.5 and 135 L/min
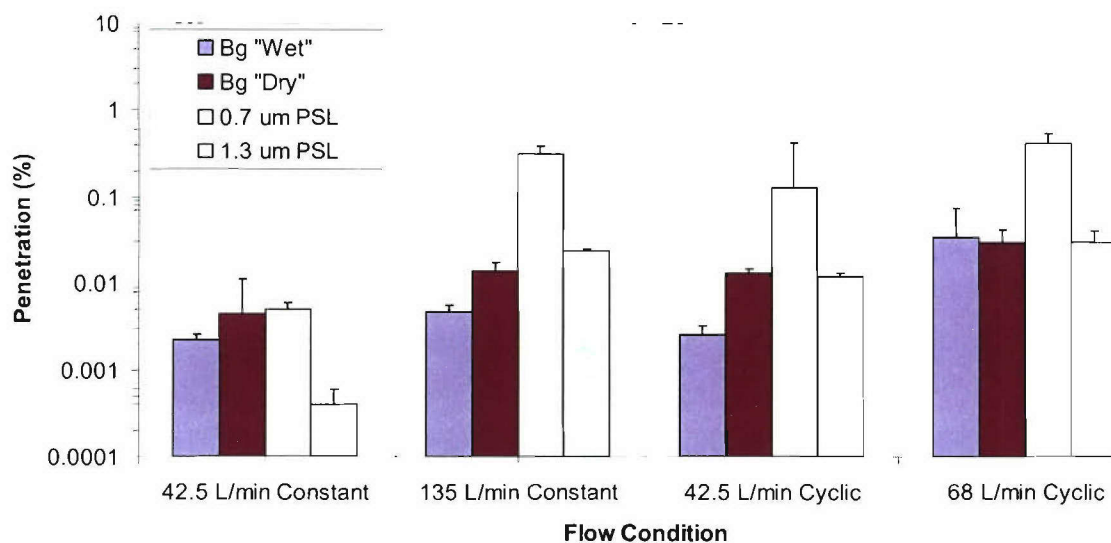
Figure 48. Comparison of Bg Spore and Inert Penetrations through the MSA N95 Flexi-Filter Cartridge
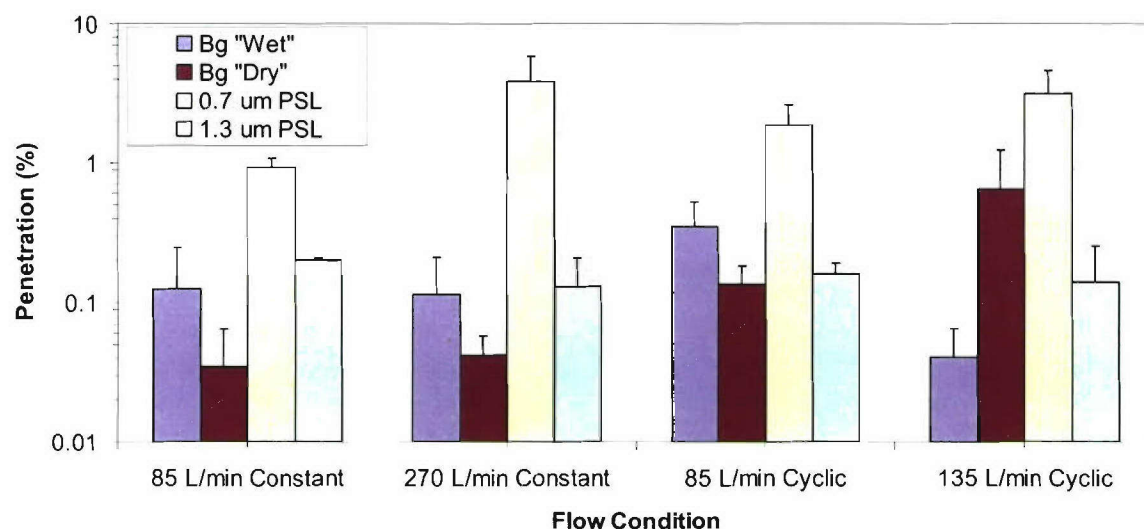
Figure 49. Comparison of Bg Spore and Inert Penetrations through the MSA N95 Affinity Plus Filtering Facepiece
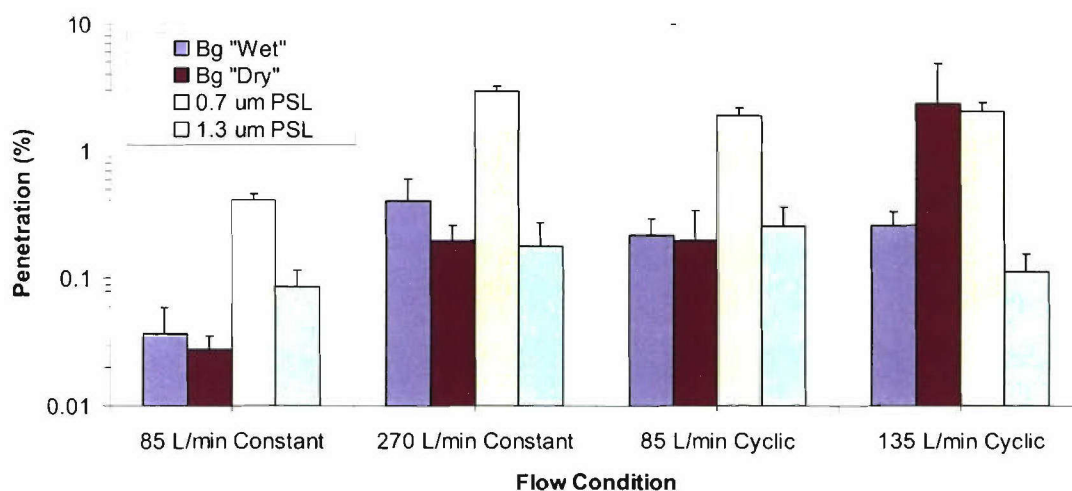
Figure 50. Comparison of Bg Spore and Inert Penetrations through the Gerson N95 1730 Filtering Facepiece

4.5.3.2 MS2 Phage. Similar comparisons are provided in Figures 51 through 54 for the MS2 phage aerosol and 0.1, 0.3, and 0.7 μm PSL penetrations through the N95 filters. The comparisons are not as well-defined for the MS2 phage. For the N95 cartridges, penetrations of 0.1 and 0.3 μm PSL were generally higher than that of the MS2 "wet" aerosol and, thus, would provide a conservative estimate of filter performance. Due to its smaller size, the MS2 "wet"

aerosol penetration tended to be slightly higher than the 0.7 μm PSL. For the N95 filtering facepieces, the MS2 "wet" aerosol penetrations tended to be lower than those measured with the 0.1, 0.3, and 0.7 μm PSL. The penetration of the MS2 "dry" aerosol was typically below detectable limits. This was consistent with the penetrations measured for an inert aerosol of similar size (i.e., 2.9 μm PSL).
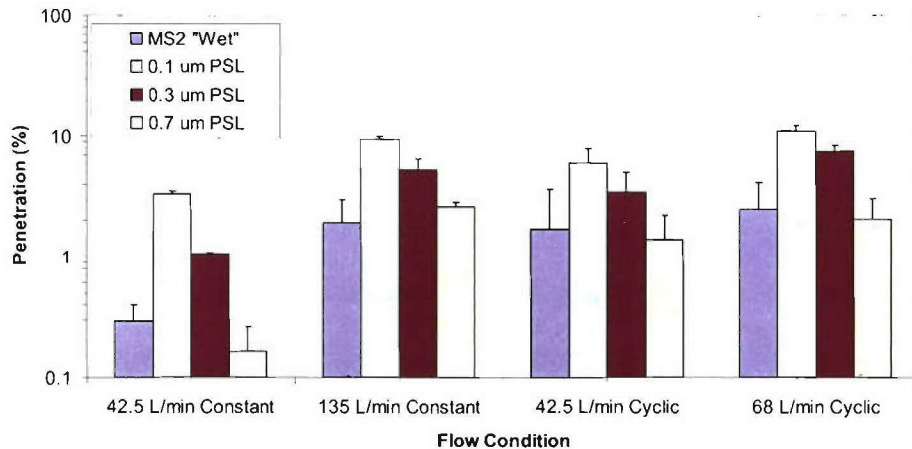
Figure 51. Comparison of MS2 "Wet" and Inert Penetrations through the North N95 7506 Cartridge
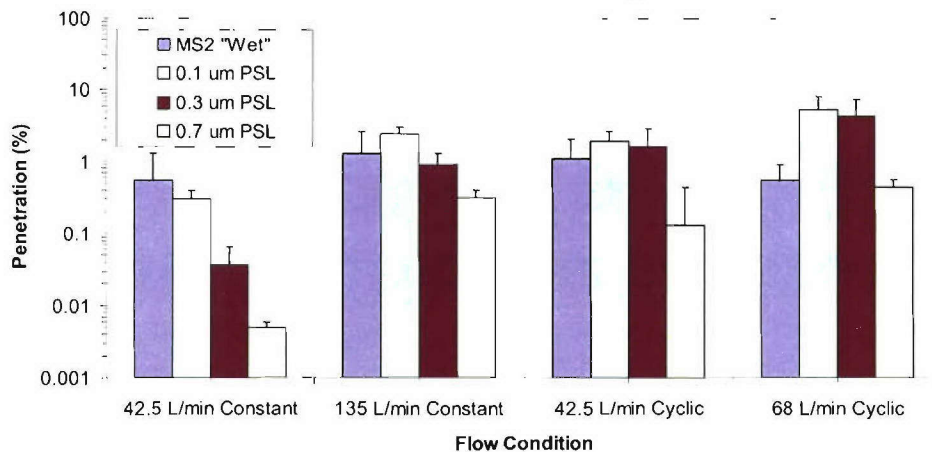
Figure 52. Comparison of MS2 "Wet" and Inert Penetrations through the MSA N95 Flexi-Filter Cartridge
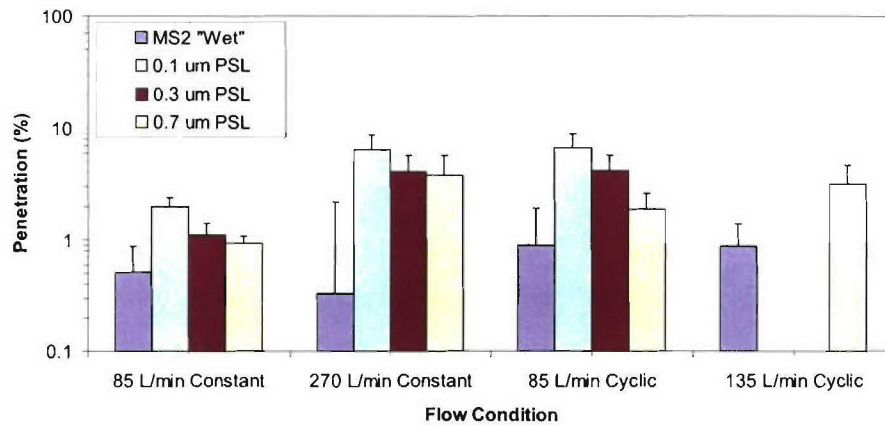
Figure 53. Comparison of MS2 "Wet" and Inert Penetrations through the MSA N95 Affinity Plus Filtering Facepiece
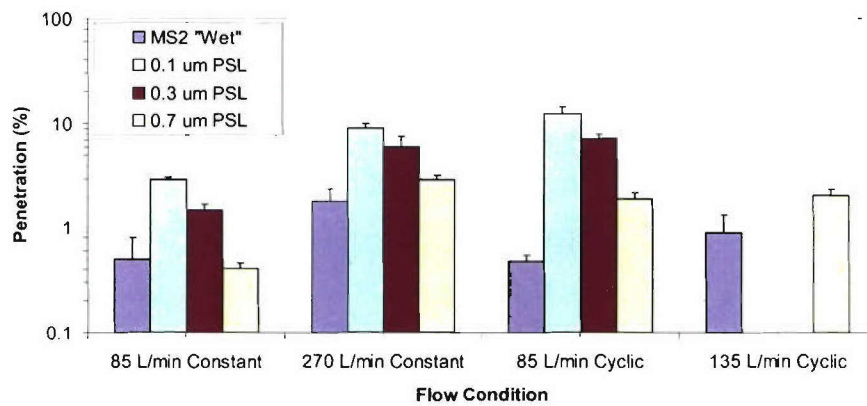
Figure 54. Comparison of MS2 "Wet" and Inert Penetrations through the Gerson N95 1730 Filtering Facepiece

4.6 Summary

The performance of NIOSH-approved N95 and P100 respirator filters has been assessed against bioaerosol challenges under high volumetric flow conditions. Mean penetrations were below the penetration requirements for the respective filter types (i.e., penetration less than 5 percent for N95 and less than 0.03 percent for P100 filters) under all flow conditions tested. Penetrations of Bg spores through the P100 filters were typically below detectable limits and, thus, had penetrations at least an order-of-magnitude below the P100 requirement. The N95 filters also were very efficient at removing the bacterial aerosol challenges as average penetrations were less than 0.5 percent. There were not significant differences in the

penetrations measured using the "wet" and "dry" Bg spore aerosolization methods. The most penetrating of the biological aerosols tested was the "wet" MS2 phage as the particle size was closest to the MPPS. Average penetrations through the N95 and P100 filters were less than 2 and 0.03 percent, respectively, under all flow conditions. An inert aerosol of similar aerodynamic diameter was shown to provide a reasonable estimate of performance against biological aerosols as measured penetrations were generally within a factor of five. The Bg spore "wet" and "dry" aerosol penetrations agreed favorably with the 1.3 μm PSL results. In magnitude, the MS2 "wet" penetrations through the cartridges were typically between penetrations measured using the 0.3 and 0.7 μm PSL. Comparisons were not made with the MS2 "dry" as penetrations were typically below detectable limits. However, this is in agreement with the penetrations measured for the 2.9 μm PSL. The results demonstrated that testing with inert particles in the MPPS range provides a conservative estimate against the biological aerosols assessed in this study. Finally, the results demonstrated that using an optical light scattering instrument such as the LAS to measure bacterial aerosol penetration provides a conservative estimate of filter performance. This is significant due to the labor intensive nature of the bioassay method.

5.0 REAEROSOLIZATION

Reaerosolization of biological agents from previously bio-contaminated filtering facepieces is a potential concern for emergency responders and health care workers. The objective of this subtask was to assess the significance of reaerosolization of biological aerosols during simulated coughing through loaded filtering facepieces. The results were also compared to those measured using inert particles of similar size to the bioaerosols.

5.1 Test Parameters

Particle reaerosolization from two brands of N95 filtering facepieces was assessed, the MSA Affinity Plus and the Gerson 1730 and 1740. Within each brand, tests were performed on filtering facepieces with and without exhalation valves. The Gerson 1730 and 1740 models are identical with the exception that the 1740 has an exhalation valve. The exhalation valves were

not sealed during the loading or reaerosolization tests. The estimated surface areas of the filtration media for each of the filtering facepieces are summarized in Table 17. The filtering facepeices were loaded at a cyclic flow rate of 85 L/min (2.3 L tidal volume, 37 breaths/min). The filters were not preconditioned with humidified air prior to loading. The loading and reaerosolization tests were performed under ambient laboratory temperature (25 ± 5°C) and the relative humidity was measured (40 ± 10%). Fluorescent PSL (Duke Scientific, Palo Alto, CA) with nominal diameters of 0.8 and 2.2 μm were used as the inert aerosol challenge. Four biological aerosols, the same as described in Section 4.0, were used and included Bg "wet", Bg "dry", MS2 "wet", and MS2 "dry." One reaersolization flow profile was assessed that represented a cough. This profile, shown in Figure 55, was provided by ECBC and is based on measurements made during human subject testing. The peak flow rate was approximately 370 L/min which corresponded to a superficial velocity of approximately 40 cm/s assuming that the flow is evenly distributed over the entire facepiece ($\sim$170 cm^2). The cough profile was repeated three times in succession during each reaersolization test over a period of approximately 30 seconds.

Table 17. Estimated Surface Areas of N95 Filtering Facepieces

Filtering Facepiece	Surface Area (cm^2)
MSA Affinity Plus	175
MSA Affinity Plus (w/exhalation valve)	160
Gerson 1730	170
Gerson 1740 (w/exhalation valve)	150
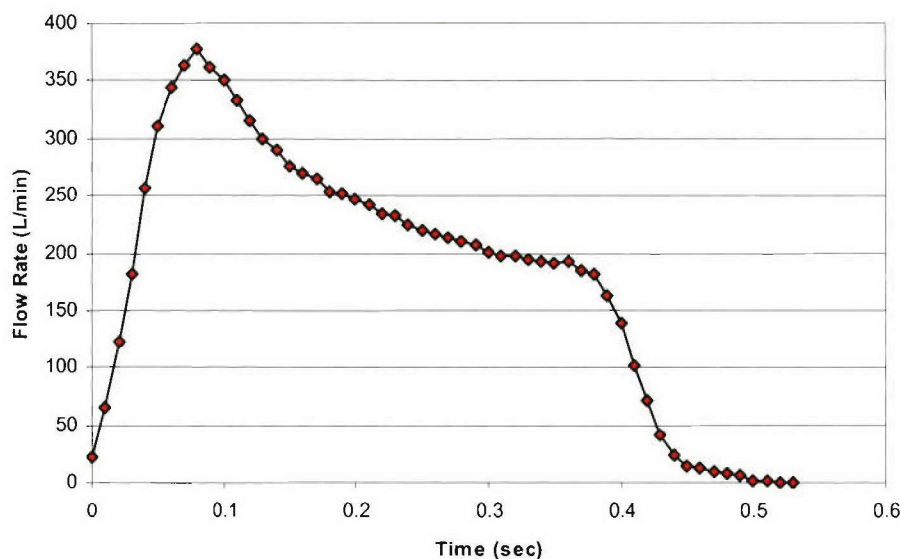
Figure 55. Cough Profile for Reaersolization Testing

The target loading level was 1×10^4 particles/cm^2 based on modeling by Stuempfle et al. (2004) who estimated the respirable concentration-time profile in ventilated enclosures (buildings) immediately following an intentional bio-agent release. The model was used to estimate resuspension of respirable pathogens by human activity after delayed entry into a contaminated area. This represents a "worst case" scenario for users of filtering facepiece respirators. Based on the model results and assuming a breathing rate of 40 L/min, an 8-hour exposure, and a filter surface area of approximately 200 cm^2, a loading of 1×10^4 particles/cm^2 represents a threat-based level. A limited set of tests were performed with the 0.8 μm inert aerosol to assess the effect of higher particle loading. Tests were performed at loading levels of 1×10^5 and 1×10^6 particles/cm^2 with the MSA Affinity Plus. The loading of 1×10^5 particles/cm^2 is consistent with Qian et al. (1997a).

5.2 Test Matrix

The test matrix completed to assess the extent of reaerosolization from the N95 filtering facepieces is provided in Table 18. Factors investigated included filter type, particle size, particle type, and loading level. The inert aerosols selected for testing were fluorescent PSL with nominal diameters of 0.8 and 2.2 μm. The 0.8 μm PSL had a similar diameter as the Bg spores and the 2.2 μm PSL had a similar diameter as the MS2 phage aerosolized as a dry powder.

74

Table 18. Test Matrix Completed to Assess Reaerosolization

Loading Flow (L/min)	Aerosol	Target Load = 1 x 10^4				1 x 10^5	1 x 10^6
		Gerson 1730 No Ex. Valve	Gerson 1740 Ex. Valve	MSA Affinity Plus No Ex. Valve	MSA Affinity Plus Ex. Valve	MSA Affinity Plus No Ex. Valve	MSA Affinity Plus No Ex. Valve
85 Cyclic	Bg "wet"	3	2	2	3	0	0
	Bg "dry"	1	1	0	0	0	0
	MS2 "wet"	3	1	3	3	0	0
	MS2 "dry"	3	3	0	0	0	0
	0.8 µm PSL	3	2	2	3	3	3
	2.2 µm PSL	3	3	0	0	0	0

5.3 Test Method

5.3.1 Test System Description

The test system used to load the filtering facepieces with the inert or biological particles was the same as described in Section 4.3.1. The bioaerosol generation system was as described in Section 4.3.2. The inert aerosol challenge was generated from aqueous suspension using a 6-jet Collison nebulizer. The flow from the nebulizer was diluted with filtered, house air and passed through a Kr-85 charge neutralizer (Model 3012, TSI, Shoreview, MN). Samples of the challenge aerosol were collected on 47-mm filters to quantify the challenge concentration. The inert particles were collected on membrane filters (Type HA, Millipore, Bedford, MA) with a rated pore size of 0.45 µm. Membrane filters were used such that the particles would be collected on the surface of the filter and not embedded within the fibers. This was important as a counting method using a fluorescent microscope was used to quantify the number of particles collected. The bioaerosol samples were collected on either mixed cellulose ester or water-soluble filters for subsequent bioassay.

A separate test system, illustrated in Figure 56, was used to measure the percent reaersolization. It consisted of the breathing machine, filtering facepeice holder, reaerosolization chamber, and aerosol sampling/classification system. The breathing machine used to simulate the cough was connected to the filter holder using 2.5-cm OD flexible tubing. The inlet air to the breathing machine was HEPA filtered such that the exhaled air was particulate free. The holder for the filtering facepiece consisted of a flat plate with a 7.5 cm hole centrally located to permit

airflow. This plate was welded onto a cone that allowed the flow from the breathing machine to expand and distribute over the entire area of the filter. The filter holder sealed to the top of the reaerosolization chamber. The chamber was cylindrical with a 0.7 m diameter and 0.6 m height. The bottom of the chamber tapered down to the 47-mm collection filter. The internal volume of the chamber was approximately 300 L. A vacuum pump was used to pull a continuous, constant flow through the chamber and collection filter. Make-up air was drawn through the HEPA filters located at the top of the chamber as needed.
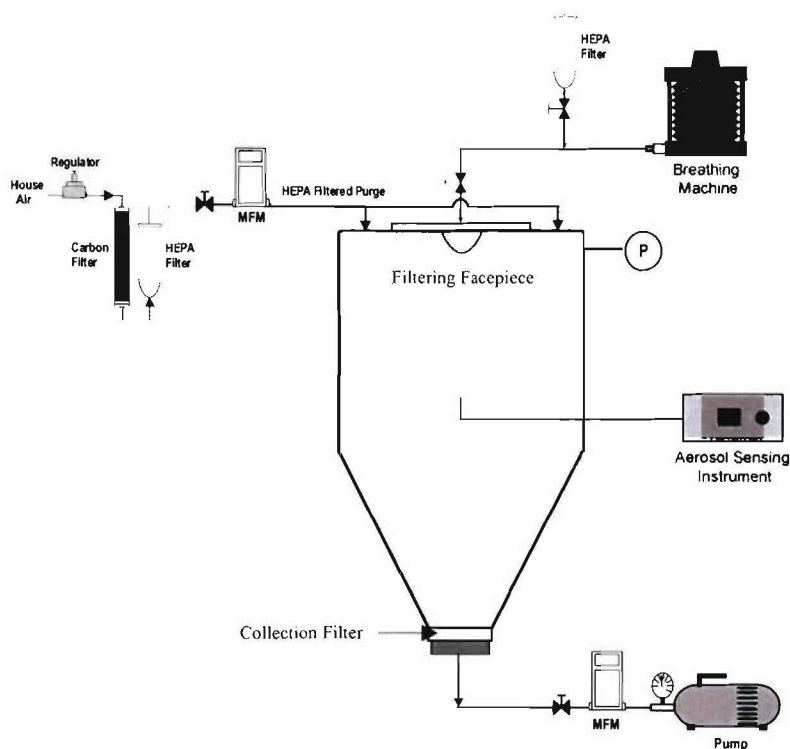
Figure 56. Schematic of Reaerosolization Test System

5.3.2 Test Procedure

The filtering facepeice was sealed to the holder and placed in the exposure chamber described in Section 4.3.1 for loading. The breathing machine was started and pulled 85 L/min (2.3-L tidal volume, 37 breaths/min) through the filtering facepeice. The aerosol generation system was started to begin loading the filtering facepiece. For both inert and biological aerosol, samples were also collected on 47-mm reference filters. The required loading duration was

76

estimated based on the challenge concentration, flow rate, and filter surface area. It was assumed that the filtering facepieces were 100 percent efficient against all challenge aerosols. At the desired loading level, the aerosol generation system and breathing machine were stopped and the chamber flushed with HEPA filtered air.

The filtering facepeice and holder were removed from the exposure chamber and sealed to the reaerosolization chamber shown in Figure 56. The sample pump was started to flush the chamber with HEPA filtered air and sampling began with a pre-cough collection filter. Sample duration was sufficient to exchange the air within the chamber three times (typically 15 to 25 minutes depending on sample flow rate). The sample pump was then stopped and the 47-mm collection filter replaced. The sample pump was started again and the breathing machine was used to simulate the cough. The cough profile was repeated three times. A valve was used such that the inhaled air between coughs was HEPA filtered room air. The chamber was again sampled for sufficient time to exchange the chamber volume three times. The sample pump was stopped and the filter removed from the system for analysis. Polonium-210 static eliminators were used to minimize particle loss during transport to laboratory for analysis.

5.3.3 Analytical Methods

Filtering facepiece loadings ($\#/cm^2$) were estimated based on the loading of a 47-mm reference filter loaded simultaneously. The loading on the reference filter was transformed to the loading on the filtering facepiece by taking into account the relative collection flow rates, durations, and surface areas (refer to Section 5.3.5). The methods used to quantify the loading on the reference filters are described in Sections 5.3.2.1 and 5.3.2.2 for the inert and biological aerosols, respectively.

5.3.3.1 Inert Aerosols. The number concentrations of inert aerosols collected on the membrane filters were quantified using a fluorescent microscope (Model SZX12, Olympus, Melville, NY) to count the particles collected on selected regions of the filter. The area of the field-of-view was known based on the magnification and allowed the number of particles/cm^2 to be determined. The method assumed that particles were evenly distributed over the surface of the filter as only a percentage of the surface area was analyzed. The selected areas ranged from

the center to the edge to identify any potential bias in the radial direction. As shown in Figure 57, five areas were analyzed for the loading filters and 20 areas were analyzed for the collection filters. More areas were analyzed for the collection filter due to the expected lower loading levels. Magnification for analysis of the loading filters was 45x resulting in a field of view that was 1 mm in diameter. Less magnification (12x) was used for the collection filter to increase the viewing area to 5 mm and maximize potential to locate particles. This permitted approximately 25 percent of the collection filter to be analyzed.
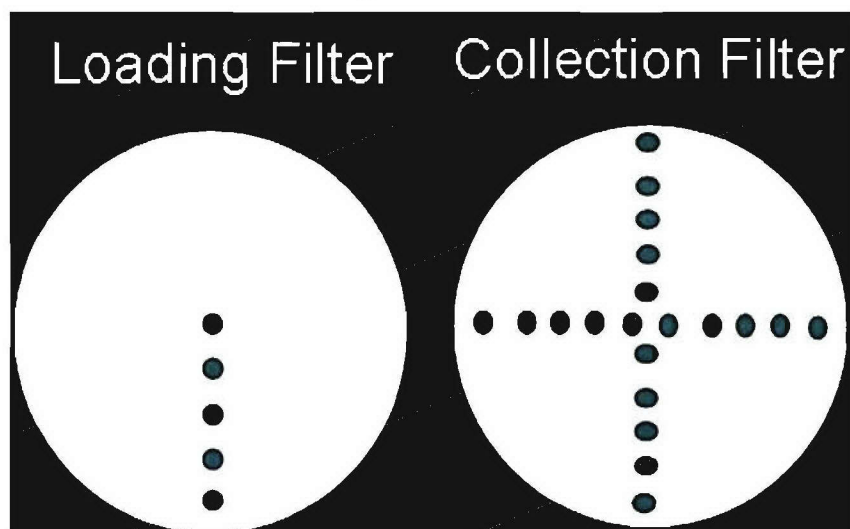
Figure 57. Analysis Patterns on 47-mm Collection Filters Used with Fluorescent Microscope to Quantify Loadings of Inert Particles

5.3.3.2. Biological Aerosols. The biological samples were collected on 47-mm filters for subsequent bioassay using the methods that were described in Section 4.3.3.1.

5.3.4 System Characterization

Shakedown tests were initially conducted to characterize the test system and establish the proper operating conditions. Significant effort went into the design of the test chamber and several iterations were explored. The initial test chamber was cylindrical with an internal volume of only 10 L. The advantage of the relatively small chamber was the short time required to flush the chamber when sampling at 40 L/min. However, the small chamber provided too much resistance for the breathing machine during the cough such that the 360 L/min peak flow could not be reached. Efforts to reduce pressure within the chamber were unsuccessful. It was

not feasible to increase the sample flow rate enough to adsorb the high peak flow. The highest flow rate that could be pulled through the membrane filter was 40 L/min. Using multiple collection filters or increasing the surface area would have been disadvantageous from the analytical perspective (i.e., low numbers of particles spread across a larger surface area). Thus, the chamber was scaled up to the final volume of 300 L/min. The cough profile was verified by measuring the flow rate using a rapid response mass flow meter (Model 4000, TSI) that is capable of measuring and data logging the flow rate at 10 ms intervals. The measured cough profile is compared with the target profile in Figure 58 and demonstrates the 360 L/min peak flow was obtained.
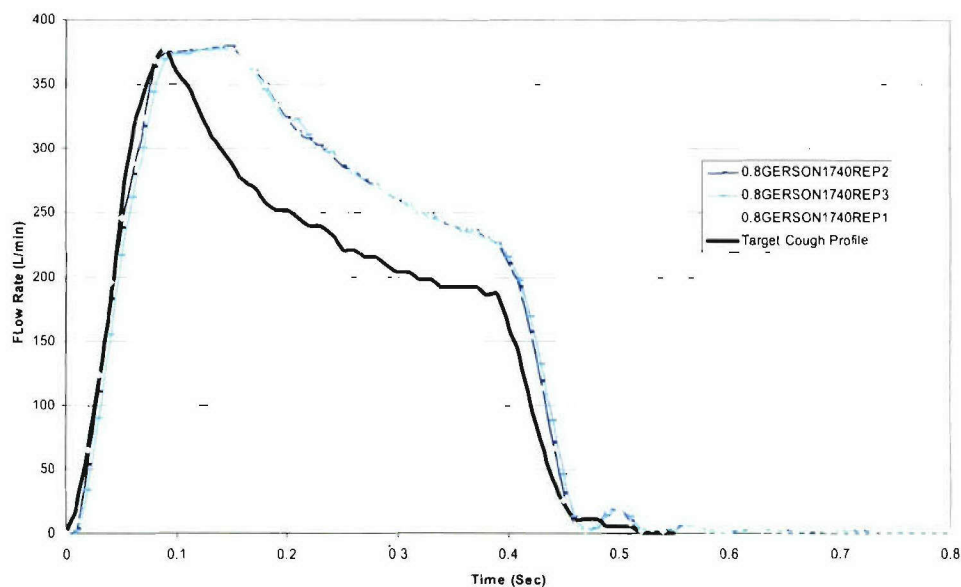
**Figure 58. Comparison of Target and Measured Cough Profile Used
for Reaerosolization Testing**

The larger chamber was disadvantageous from a sample collection perspective as longer sample durations were required and there was more surface area for particles to adhere. The chamber was designed to create an airflow pattern directed downward toward the collection filter to reduce particle loss to the chamber walls, dead spots, or circulating air flow. In addition, the system was oriented such that gravity would enhance particle collection due to settling. A series of shakedown tests using the 0.8 μm PSL challenge were performed to assess the sampling approach. Initially three 47-mm filters were collected during each reaerosolization test: (1) a pre-cough filter to determine if particles were shed during the attachment of the loaded filter to the system, (2) a post-cough filter to collect particles displaced by the cough, and (3) a post-test filter

79

to verify the chamber was flushed. Particles were consistently collected on the pre-cough filter. The counts were not attributed to contamination within the test system as the post-test filters were generally found to have zero counts indicating minimal carryover between tests. Thus, the particles collected on the pre-cough filter were attributed to the physical process of connecting the loaded filter to the chamber.

Following the shakedown testing, only the pre- and post- cough samples were collected. The particle counts on the pre- and post-cough 47-mm filters are compared in Figure 59 for each of the trials completed with the 0.8 μm PSL. The trials are shown in the order of completion. The post-cough filters had higher counts in 15 of the 18 trials. The highest pre-cough counts were observed in trials 2 and 6 and both had higher counts than the post-cough filter from the previous test. Thus, the high counts were attributed to the process of connecting the filter to the test system. Unfortunately, no samples were collected between the pre- and post-cough filters to demonstrate the chamber had been completely flushed before the cough. However, even if the pre-cough filter is treated as a system background, the results demonstrate that particles were reaerosolized from the filtering facepieces as particle counts were generally higher post-cough. This trend was consistent throughout all challenge aerosols. The average particle counts pre- and post- cough are compared for each of the inert and biological challenges in Figure 60.
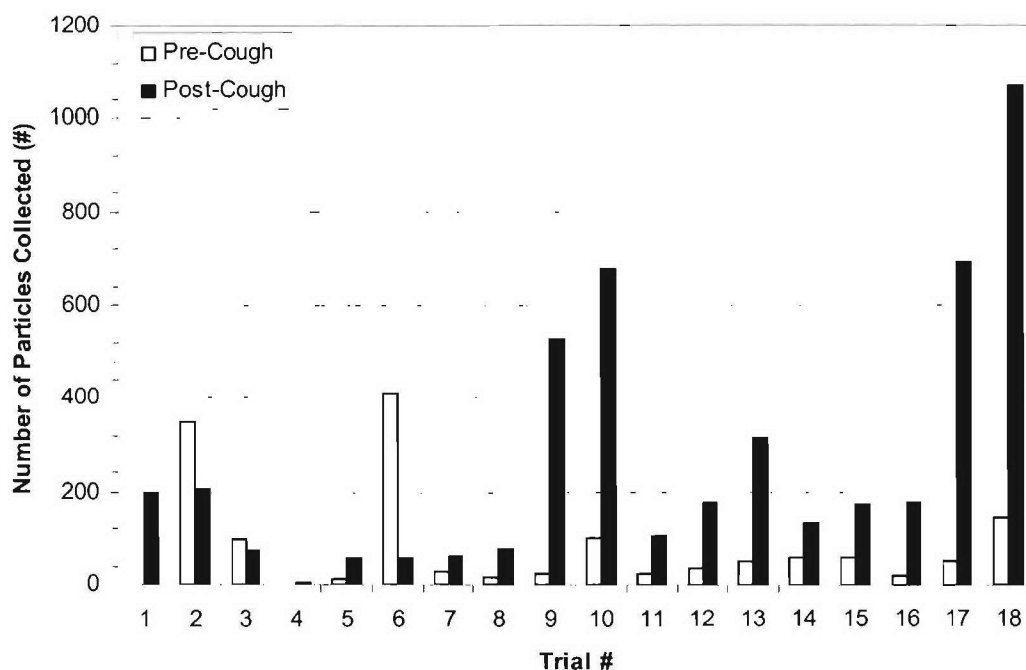
Figure 59. Comparison of Number of Particles Collected on Pre- and Post-Cough Filters for Tests Performed with the 0.8 μm PSL
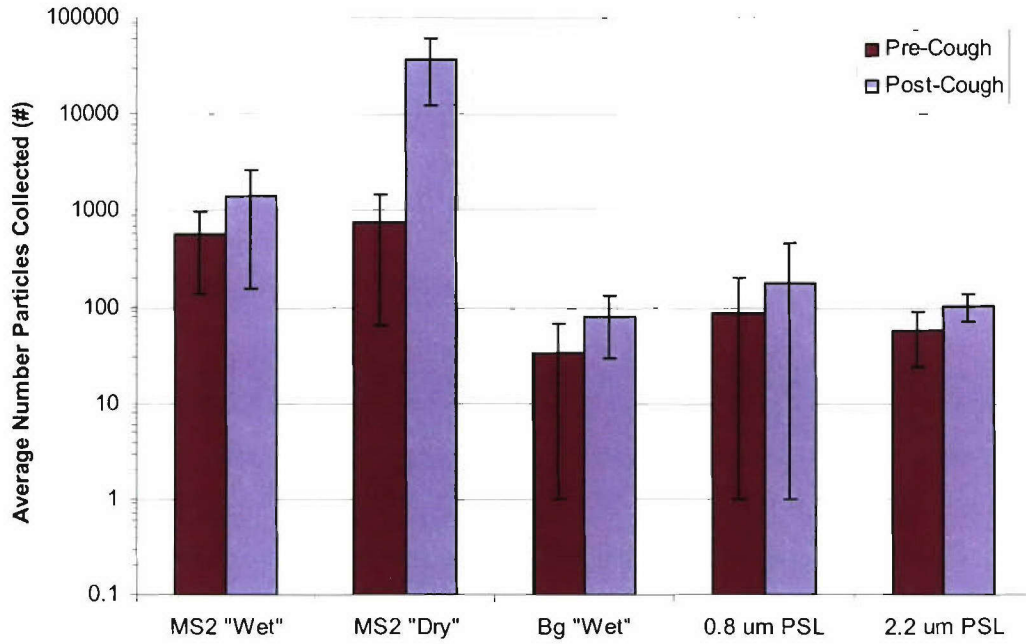
Figure 60. Comparison of Number of Particles Collected on Pre- and Post-Cough Filters for Tests Performed with the Biological and Inert Aerosols

5.3.5 Calculation of Reaerosolization

The challenge aerosol concentration (C_{Chal}) was derived from the results of the reference filter analysis using the following relationship:

$$C_{Chal}(\# / L) = \frac{P_R \times A_R}{Q_R \times t_L}$$

where P_R is the loading density determined for the reference filter ($\#/cm^2$), A_R is the area of the reference filter (cm^2), Q_R is the flow rate through the reference filter (L/min), and t_L is the loading duration (min). The number of particles loaded (P_{FF}) onto the filtering facepiece was then determined using the following equation:

81

$$P_{FF}(\#) = C_{Chal} \times Q_{FF} \times t_L$$

where Q_{FF} is the flow rate through the filtering facepiece (L/min). It was assumed that the filters were 100 percent efficient for all challenge aerosols.

The number of particles reaerosolized (P_C) was based on the bioassay or fluorescence analysis of the collection filter. The percent of particles reaerosolized (f_R) was then the ratio of the number of particles reaerosolized (P_C) to the number of particles loaded on the filtering facepiece (P_{FF}):

$$f_R(\%) = \frac{P_C}{P_{FF}} x100$$

5.4 Results

Table 19 summarizes the results of the reaerosolization testing with both the inert and biological aerosols. Results from individual trials are summarized in Appendix J. The target loading level was 1×10^4 particles/cm^2 for all challenge aerosols with the exception of the higher loading tests performed with the 0.8 μm PSL. The average measured loadings for each challenge type are also summarized in Table 19. Note that tests with the 2.2 μm PSL and Bg "wet" aerosols had loading levels approximately an order-of-magnitude less than the target due to lower than expected challenge concentrations. In all cases, the percent reaerosolization was less than one percent of the number of particles loaded onto the filtering facepiece. The inert aerosol results are further discussed in Section 5.4.1 and the biological results in Section 5.4.2.

Table 19. Summary of Reaerosolization Results

Filter Type		Gerson 1730 (No Ex. Valve)		Gerson 1740 (Ex. Valve)		MSA Affinity Plus (No Ex. Valve)		MSA Affinity Plus (Ex. Valve)	
Challenge Aerosol	Average Loading (#/cm^2)	Reaerosolization (%)							
		Average	95% CI	Average	95% CI	Average	95% CI	Average	95% CI
0.8 μm PSL	2.2 x 10^4	0.002	0.0003	0.008	0.0005	0.0008	0.0003	0.007	0.0007
0.8 μm PSL	1.7 x 10^5	-[(a)]	-	-	-	0.0006	0.00005	-	-
0.8 μm PSL	9.4 x 10^5	-	-	-	-	0.0004	0.00001	-	-
2.2 μm PSL	2.0x10^3	0.03	0.005	0.04	0.006	-	-	-	-
Bg "wet"	1.0 x10^3	0.06	0.01	0.07	0.1	0.03	0.003	0.05	0.02
Bg "dry"	1.4x10^4	0.1		0.2	-	-	-	-	-
MS2 "wet"	3.1 x10^4	0.07	0.08	0.1	-	0.07	0.08	0.1	0.1
MS2 "dry"	4.5 x10^4	0.5	0.2	0.7	0.2	-	-	-	-

(a) No tests performed at test condition

5.4.1 Inert Aerosols

Figure 61 compares the percent reaerosolization of inert particles measured from the MSA and Gerson respirators. All reaersolizations were less than 0.1 percent. The percent reaerosolization tended to increase with increased particle size and was not significantly different between the two brands of filtering facepieces. Higher percent reaerosolizations were measured for the respirators that contained exhalation valves. The increase was more significant for the smaller particles that were not reaersolized as easily from the filter media. Reaerosolization increased by a factor of 2 for the 2.2 μm PSL and a factor of 4 to 8 for the 0.8 μm PSL. The extent of reaerosolization was expected to be lower from the filters with exhalation valves as velocity through the aerosol media was likely lower due to the flow through the valve. However, the mechanical movement of the valve and localized high velocity flow may have re-entrained particles collected on the surface of the valve or valve housing. To further investigate the higher reaerosolization, Gerson filtering facepieces with the exhalation valve covered with tape were loaded with 0.8 μm PSL. This prevented loading on the valve and housing. The tape was then removed prior to the reaerosolization test. Figure 62 compares these results with those from the

Gerson respirators with no or unprotected valves. The percent reaerosolization decreased by a factor of 2 as compared to tests with the unprotected valves.
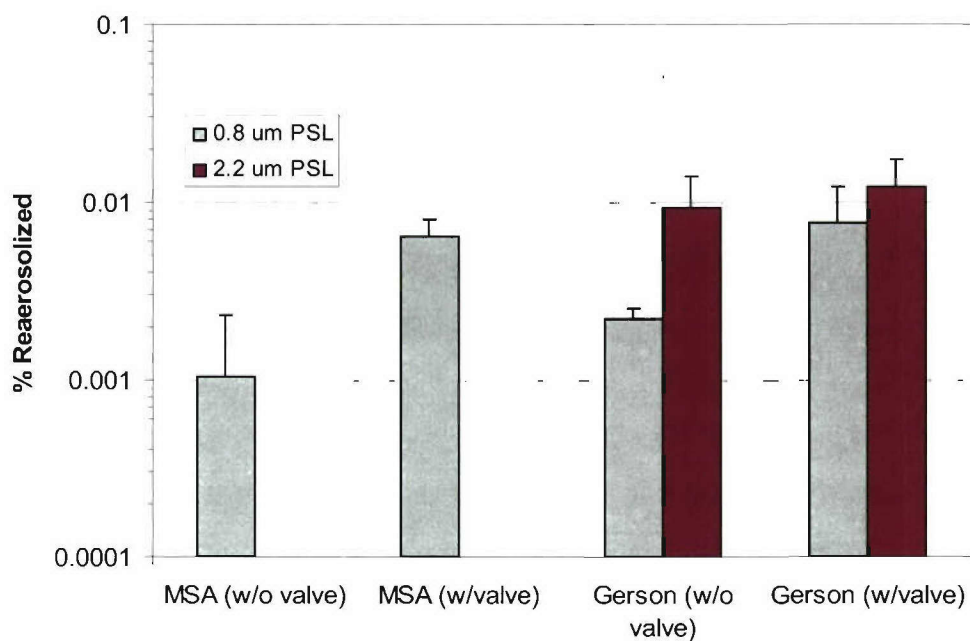
Figure 61. Comparison of Percent Reaerosolization of Inert Particles from MSA and Gerson Filtering Facepieces
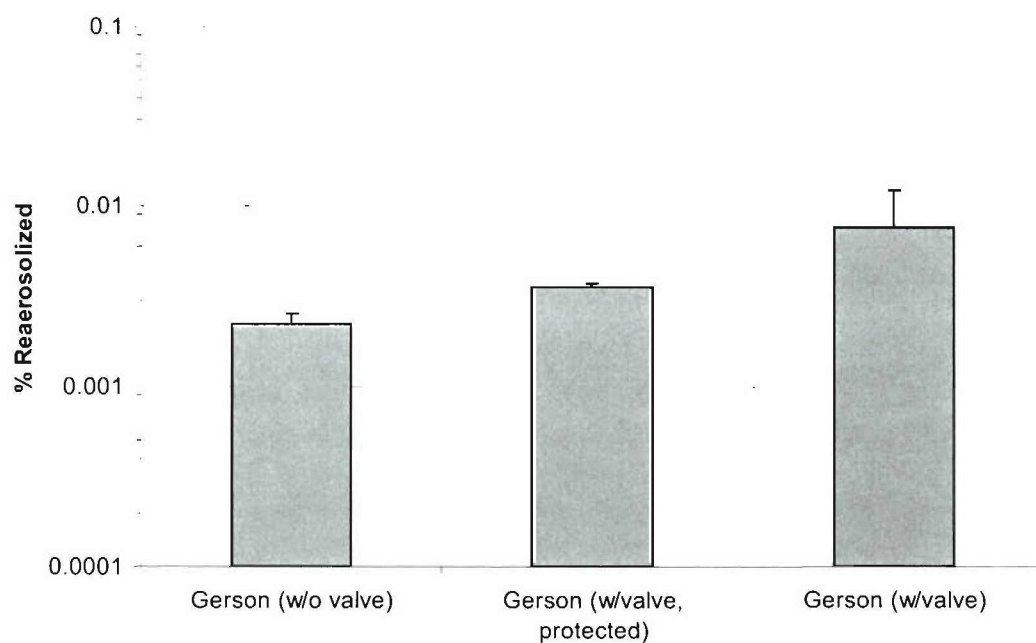
Figure 62. Comparison of Percent Reaerosolization of 0.8 μm PSL from Gerson Respirator with Exhalation Valve Protected during Loading

The effect of loading on the percent reaerosolization of 0.8 μm PSL is shown in Figure 63. Although averages were less than 0.002 percent for all loadings, the percent reaerosolization tended to decrease as the loading increased. However, more particles were reaerosolized at the higher loading levels. The average numbers of particles reaerosolized for the different loading levels were 35, 180, and 740 particles. Thus, as loading increased by an order-of-magnitude, the average number of particles reaerosolized increased only by a factor of approximately 5.
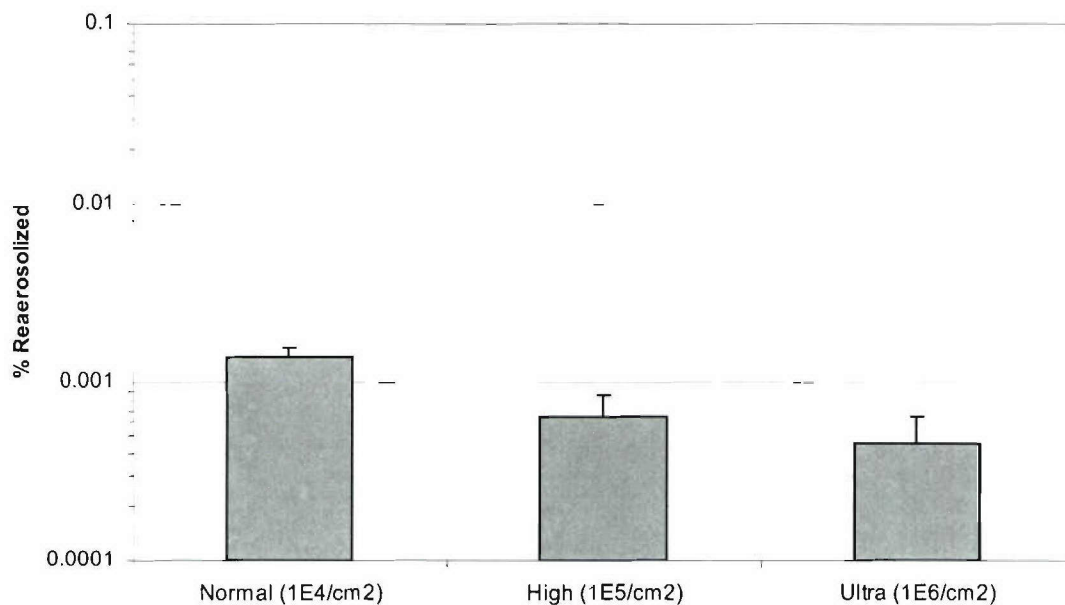
Figure 63. Comparison of Percent Reaerosolization of 0.8 μm PSL from Gerson Respirator at Loadings Ranging from 1×10^4 to 1×10^6 Particles/cm^2

5.4.2 Biological Aerosols

This section summarizes the results of the reaerosolization testing completed with the biological aerosols. The results are also compared to the inert results described above. The Bg spore results are provided in Section 5.4.2.1 and the MS2 phage results follow in Section 5.4.2.2.

5.4.2.1 Bg Spores. Figure 64 compares the measured reaersolization of the Bg "wet" and Bg "dry" aerosols to that measured for the inert 0.8 μm PSL. Recall from Section 4.0, the AMMDs for both the "wet" and "dry" Bg were approximately 1.0 μm. The mean

reaerosolization of the Bg spores tended to be higher for the respirators with exhalation valves but the effect was not as significant as observed with the 0.8 μm PSL. The percent reaerosolization of the Bg spores was generally an order-of-magnitude higher than the inert PSL.
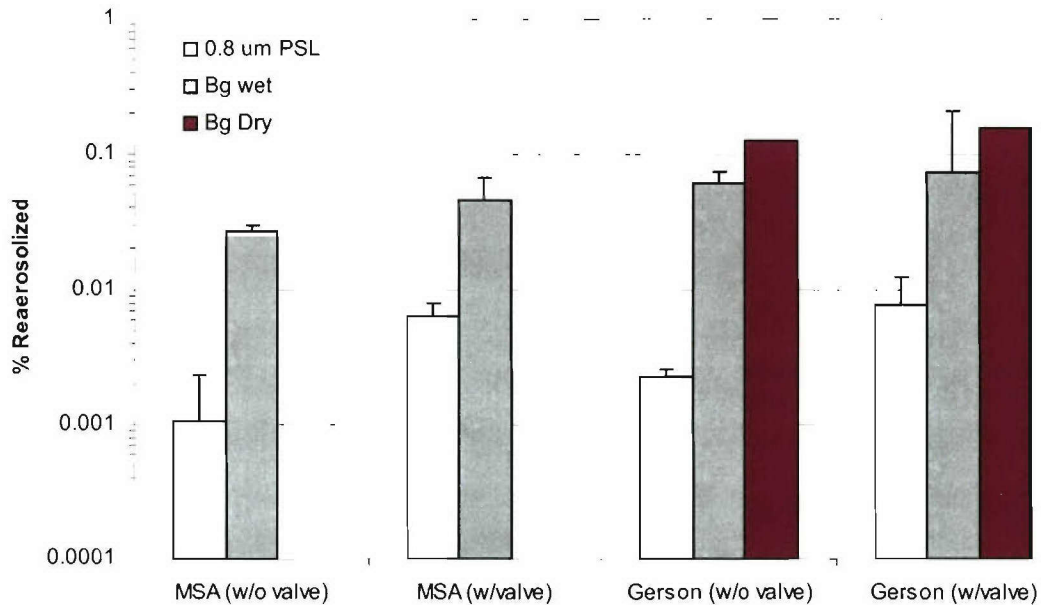
Figure 64. Comparison of Inert and Bg Spore Reaerosolization Results

5.4.2.2 MS2 Phage. Figure 65 compares the extent of reaerosolization of MS2 "wet" and "dry" aerosols with the 2.2 μm PSL. The NMD of the MS2 "dry" aerosol was 2.3 μm while the "wet" was 0.2 μm. Significant differences in reaerosolization were observed between the inert and biological aerosols. Of particular interest was the extent of reaerosolization of MS2 "wet" aerosol as it was approximately an order-of-magnitude higher than that observed for the 2.2 μm PSL. This was contrary to the inert results shown previously that indicated percent reaersolization increased with particle size. The highest reaerosolization percentages were observed for the MS2 "dry" aerosol with a mean of approximately 0.5 percent, nearly two orders-of-magnitude higher than the 2.2 μm PSL results. This difference was attributed to polydisperse size distribution of the MS2. Although both had similar NMDs, the PSL was monodisperse while the MS2 was polydisperse with significant mass between 2 and 5 μm containing viable particles. Higher percent reaerosolization is expected as the particle size approaches 5 μm as

86

was demonstrated by Qian et al. (1997a) who showed reaerosolization increased from 0.05 to 6 percent as the particle size increased from 1.5 to 5.0 μm.
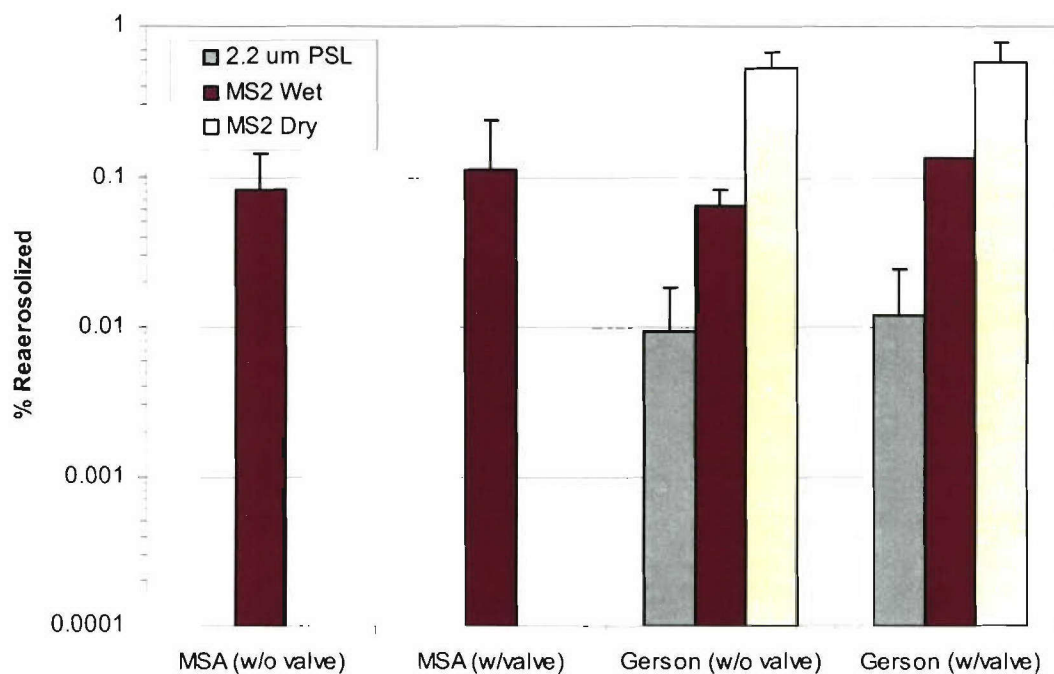
Figure 65. Comparison of Inert and MS2 Phage Reaerosolization Results

5.5 Summary and Discussion

A test method was developed to quantify the extent of reaerosolization from a filtering facepiece loaded with either an inert or biological aerosol. Tests were performed to assess the effect of particle size, particle type, and loading level. Two brands of filtering facepieces were tested, the MSA Affinity Plus and Gerson 1730. The levels and trends of reaerosolization were similar for both brands. For the inert aerosols, reaerosolization was observed to increase with increased particle size over the range tested (0.8 to 2.2 μm). This trend was consistent with that observed by Qian et al. (1997a) who attributed this to increased drag force on the larger particles. The extent of reaerosolization of 0.8 μm particles from filtering facepieces without exhalation valves was very low (less than 0.002 percent or 1 in every 50,000 particles loaded). The percent reaerosolization increased by an order of magnitude when filtering facepieces with exhalation valves were tested. This was attributed to the movement of the valve and localized high velocity air that could re-entrain particles collected on the surface of the valve or valve housing.

87

Specifically for the 0.8 μm PSL, the number of particles reaerosolized was observed to increase with increased loading over the range from 1×10^4 to 1×10^6 particles/cm^2. However, the number of particles did not increase proportionally to the increased loading. Increasing the loading by a factor of 10 only increased the number of particles reaerosolized by a factor of 5. Further work is recommended to determine if similar trends hold for larger particles.

The extent of reaerosolization of the biological aerosols was greater than that observed for the inert aerosols with a similar diameter. For example, reaerosolization of the 0.8 μm PSL was very low (~0.002%) while reaerosolization of the Bg spores was typically 0.05 to 0.1 percent. Similarly, reaerosolization of the 2.2 μm PSL was only 0.01 percent while reaerosolization of the MS2 "dry" aerosol was 0.5 percent. The higher reaerosolization for the biological aerosols was attributed to their broader size distribution. For example, the MS2 "dry" aerosol had significant mass between 2.5 and 5.0 μm that contained viable particles. As described above, the extent of reaerosolization has been shown to increase with increased particle size. Thus, it is important to consider the entire size distribution and not just the nominal particle size when selecting an inert simulant for characterizing reaerosolization.

6.0 CONCLUSIONS AND RECOMMENDATIONS

The performance of NIOSH-approved N95 and P100 filtering facepieces has been assessed against both inert and biological aerosols under high flow conditions representative of ventilation rates during heavy activity. For the inert particles, the most penetrating particle size (MPPS) was generally between 0.1 and 0.2 μm for the P100 cartridges and 0.05 and 0.10 μm for the filtering facepieces and N95 cartridges. The penetration of submicron particles tended to increase with flow rate and penetrations in excess of the NIOSH N95 and P100 requirements were measured. However, the intended use, type and size distribution of the particulate hazard, APF, and other factors must be considered to determine if this increase in penetration is significant with regard to the overall protective capability of the respirator.

As was discussed in Section 2.0, the primary factors that influence penetration are filtration velocity, particle size, and the properties of the filter media. This task strictly focused on the effect of filtration velocity and particle size. The properties of the media from the various filters were not compared to identify those that could account for differences in performance. It

is recommended to characterize the media properties including fiber diameter, solidity, and thickness. These values could then be used to model the penetrations using the single fiber theory developed by Lee and Liu (1980) and compared to the measured values contained in this report. Electret media are commonly used in N95 filters and filtering facepieces to lower inhalation resistance. Electret media may be more susceptible to the high flow conditions as the collection mechanism is less efficient. Thus, further testing to compare performance of electret and mechanical media is recommended.

In comparing penetrations measured under constant and cyclic flow conditions, the MIF and PIF were determined to be important parameters. For the P100 cartridges, similar penetrations were measured under constant and cyclic flow if the constant flow was equivalent to the MIF. However, it may be more important to consider the PIF when testing filtering facepieces or N95 cartridges, especially at the high volumetric flow rates that can be experienced during heavy work loads. These filters are not well-suited for the high volumetric flow rate applications due to their lower surface areas as compared to the P100 cartridges. Selecting a constant flow equivalent to the peak inhalation flow generally provides a conservative estimate of filter performance under cyclic flow conditions. All cyclic flow testing performed in this task used a sinusoidal flow profile. Additional testing is recommended with alternative waveforms such as a trapezoidal that may be more realistic during periods of heavy exertion (Kaufman and Hastings, 2005).

A method was developed to predict cyclic flow penetrations based on measured penetrations over a range of constant flows. The method was applied to the inert data generated in this task. Good agreement was observed between the predicted cyclic flow penetrations and those measured in this study. Similar to the recommendation above, measured cyclic flow penetrations under different types of waveforms are needed to further validate the predictive method.

The performance of NIOSH-approved N95 and P100 respirator filters has been assessed against bioaerosol challenges under high volumetric flow conditions. Mean penetrations were below the penetration requirements for the respective filter types (i.e., penetration less than 5 percent for N95 and less than 0.03 percent for P100 filters) under all flow conditions tested. Penetrations of Bg spore aerosols through the P100 filters were typically below detectable limits and, thus, had penetrations at least an order-of-magnitude below the P100 requirement. The N95

filters also were very efficient at removing the bacterial aerosol challenges as average penetrations were less than 0.5 percent. There were not significant differences in the penetrations measured using the Bg spore aerosols generated from liquid suspension and dry powder. The most penetrating of the biological aerosols tested was the "wet" MS2 phage as the particle size was closest to the MPPS. Penetrations through the N95 and P100 filters were typically less than 2 and 0.03 percent, respectively, under all flow conditions.

An inert aerosol of similar aerodynamic diameter was shown to provide a good estimate of performance against biological aerosols (i.e., measured penetrations within a factor of five). The Bg spore "wet" and "dry" penetrations agreed favorably with the 1.3 μm PSL results. In magnitude, the MS2 "wet" penetrations through the cartridges were typically between penetrations measured using the 0.3 and 0.7 μm PSL challenges. Comparisons were not made with the MS2 "dry" as penetrations were typically below detectable limits. This was consistent with the penetrations measured using a similar sized inert aerosol (i.e., 2.9 μm PSL). The results demonstrated that testing with inert particles in the MPPS range provides a conservative estimate against the biological aerosols assessed in the study. Finally, the results demonstrated that higher penetrations tended to be measured using an optical light scattering instrument such as the LAS to measure bacterial aerosol penetration as compared to the bioassay approach. Thus, it provides a worst case penetration measurement. This is significant due to the labor intensive nature of the bioassay method.

A test method was developed to quantify the extent of reaerosolization from a filtering facepiece loaded with either an inert or biological aerosol. All tests were performed with a cough profile that had a peak flow of 360 L/min. Further work is recommended to assess the effect of cough profile and increased peak flow. Tests were performed to assess the effect of particle size, particle type, and loading level. For the inert aerosols, reaerosolization was observed to increase with increased particle size over the range tested (0.8 to 2.2 μm). The extent of reaerosolization of 0.8 μm PSL particles from filtering facepieces without exhalation valves was very low (less than 0.002 percent or 1 in every 50,000 particles loaded). For the 0.8 μm PSL particles, percent reaerosolization from filters with an exhalation value increased by an order-of-magnitude. The number of particles reaersolized was shown to increase with increased loading for the 0.8 μm PSL particles. Further work is recommended to assess the

effect of loading on reaerosolization of particles larger than 1 μm since they are easier to reaerosolize.

The extent of reaerosolization of the biological aerosols was greater than that observed for the inert aerosols with a similar AMMD. For example, reaerosolization of the 0.8 μm PSL was very low (~0.002%) while reaerosolization of the Bg spores was typically 0.05 to 0.1 percent. Similarly, reaerosolization of the 2.2 μm PSL was only 0.01 percent while reaerosolization of the MS2 "dry" was 0.5 percent. The higher reaerosolization for the biological aerosols was attributed to their broader size distribution. For example, the MS2 "dry" aerosol had significant mass between 2.5 and 5.0 μm that contained viable particles. As described above, the extent of reaerosolization increases with increased particle size. Thus, it is important to consider the entire size distribution and not just the nominal particle size when selecting an inert simulant for reaerosolization experiments.

Blank

LITERATURE CITED

ASTM F 2101-01, "Standard Test Method for Evaluating the Bacterial Filtration Efficiency (BFE) of Medical Face Mask Materials, Using a Biological Aerosol of *Staphylococcus aureus*." American Society for Testing and Materials, West Conshohocken, Pennsylvania (June 2001).

Brosseau, L.M., Evans, J.S., Ellenbecker, M.J., and Feldstein, M.L., "Collection Efficiency of Respirator Filters Challenged with Monodisperse Latex Aerosols." *Am. Ind. Hyg. Assoc. J.* *50*(10): pp 544-549 (1989).

Brosseau, L.M., Chen, S.K., Vesley, D., and Vincent, J.H., "System Design and Test Method for Measuring Respirator Filter Efficiency Using Mycobacterium Aerosols." *J. Aerosol Sci. 25*(8): pp 1567-1577 (1994).

Brosseau, L.M., Ellenbecker, M.J., and Evans, J.S., "Collection of Silica and Asbestos Aerosols by Respirators at Steady and Cyclic Flow." *Am. Ind. Hyg. Assoc. J. 51*(8): pp 420-426 (1990).

Brosseau, L.M., McCullough, N, and Vesley, D., "Mycobacterial Aerosol collection Efficiency of Respirator and Surgical Mask Filters Under Varying Conditions of Flow and Humidity" *Appl. Occup. Environ. Hyg. 12*(6): pp 435-445 (1997).

Caretti, D.M., Gardner, P.D., and Coyne, K.M., "Workplace Breathing Rates: Defining Anticipated Values and Ranges for Respirator Certification Testing", U.S. Army Edgewood Chemical Biological Center Technical Report, ECBC – TR-316 (2004).

Chen, C.C., Lehtimaki, M., and Willeke, K., "Aerosol Penetration through Filtering Facepieces and Respirator Cartridges" *Am. Ind. Hyg. Assoc. J. 53*(9): pp 566-574 (1992).

Chen, S.K., Vesley, D., Brosseau, L.M., and Vincent, J.H., "Evaluation of Single-Use Masks and Respirators for Protection of Health Care Workers Against Mycobacterial Aerosols." *Am. J. Infection Control 22*(2): pp 65-74 (April 1994).

Code of Federal Regulations. Respiratory protection. Title 30, CFR, Part 11. Washington, DC: U.S. Government Printing Office, Office of the Federal Register (1972).

Code of Federal Regulations. Respiratory protection. Title 42, CFR, Part 84. Washington, DC: U.S. Government Printing Office, Office of the Federal Register (1995).

42 CFR Part 84. *Respiratory Protection; Final Rule.* Federal Register, Washington, D.C. Vol. 60, No. 110 (1995).

Department of Health and Human Services (DHHS) Publication 2003-136, "Guidance for Filtration and Air-Cleaning Systems to Protect Building Environments from Airborne Chemical, Biological, and Radiological Attacks," (April 2003).

Fardi, B., and Liu, B.Y.H., "Performance of Disposable Respirators." *Part. Part. Syst. Charact.* 8: pp 308-314 (1991).

Hanley, J.T., and Foarde, K.K., "Validation of Respirator Filter Efficacy." Report by RTI International, Research Triangle Park, N.C., RTI Contract No. DAAD 19-02-C-0097, Project No. 08621 (March 30, 2003).

Harstad, B.J. and Filler, M.E., "Evaluatin of Air Filters with Submicron Viral Aerosols and Bacterial Aerosols," Am. Ind. Hyg. Assoc. J. pp. 280-290, May-June (1969).

Hinds, W.C., *Aerosol Technology; Properties, Behavior, and Measurement of Airborne Particles.* John Wiley & Sons, New York, New York: 1999.

Hofacre, K., Schumacher, P., Hecker, R., Forney, T., "Filtration Efficiency Assessment of HEPA Filters Against a Bioaerosol Challenge." Battelle Memorial Institute Report to U.S. Army/ERDEC Armored Systems Modernization Team, Contract No. SP0900-94-D-0002, Task No. 39, Delivery Order 19 (May 15, 1996).

Hofacre, K.C. and Forney, T.L., "Test Method for Measuring Mask Protection Factors Using a Bioaerosol Challenge." Battelle Memorial Institute Final Report, February (1996)

Johnson, B., Martin, D.D., and Resnick, I.G., "Efficacy of Selected Respiratory Protective Equipment Challenged with *Bacillus subtilis* subps. *niger*" *Applied and Environmental Microbiology*, 60(6): pp 2184-2186 (1994).

Jankowska, E., Reponen, T., Willeke, K., Grinshpun, S., and Choi, K., "Collection of Fungal Spores on Air Filters and Spore Reentrainment from Filters into Air" *J. Aerosol Science*, 31(8): pp 968-978 (2000).

Kaufman, J.W. and Hastings, S.,"Respiratory Demand During Rigorous Physical Work in a Chemical Protective Ensemble," *J. of Occup. and Env. Hyg.,* 2:pp 98-110 (2005)

Martin, S.B. and Moyer, E. S., "Electrostatic Respirator Filter Media : Filter Efficiency and Most Penetrating Particle Size Effects," *Appl. Occup. Env. Hyg.* 15(8) pp. 609-617 (2000).

McCollough, N.V., Brosseau, L.M., and Vesley, D., "Collection of Three Bacterial Aerosols by Respirator and Surgical Mask Filters Under Varying Conditions of Flow and Relative Humidity." *Ann. Occup. Hyg.* 41(6): pp 677-690 (1997).

McCullough, N.V., Brosseau, L.M., Vesley, D., and Vinent. J.H., "Improved Methods for Generation, Sampling, and Recovery of Biological Aerosols in Filter Challenge Tests," *Am. Ind. Hyg. Assoc. J.* 59: pp 234-241 (1998).

Qian, Y., Willeke, K., Grinshpun, S.A., and Donnelly, J., "Performance of N95 Respirators: Reaerosolization of Bacteria and Solid Particles." *Am. Ind. Hyg. Assoc. J. 58:* pp 876-880 (1997a).

Qian, Y., Willeke, K., Ulevicious, V., and Grinshpun, S., "Particle Reentrainment from Fibrous Filters." *Aerosol Sci. and Tech. 27:* pp 394-404 (1997b).

Qian, Y., Willeke, K., Grinshpun, S.A., Donnelly, J., and Coffey, C.C., "Performance of N95 Respirators: Filtration Efficiency for Airborne Microbial and Inert Particles." *Am. Ind. Hyg. Assoc. J. 59:* pp 128-132 (1998).

Ruuskanen, J., Chen, C.-C., Carpenter, D.R., Sherman, A., and Willeke, K., "Aerosol Penetration Characteristics for Disposable Respirator Facepieces." *J. Aerosol Sci. 19*(7): pp 1445-1448 (1988).

Stafford, R.G., Ettinger, H.J., and Rowland, T.J., "Respirator Cartridge Filter Efficiency under Cyclic- and Steady-Flow Conditions." *Am. Ind. Hyg. Assoc. J.* May: pp 182-192 (1973).

Stevens, G.A. and Moyer, E.S., "Worst Case' Aerosol Testing Parameters: I. Sodium Chloride and Dioctyl Phthalate Aerosol Filter Efficiency as a Function of Particle Size and Flow Rate." *Am. Ind. Hyg. Assoc. J. 50*(5): pp 257-264 (1989).

Stuempfle, A. K, and Fischer, B.W., "Biological Aerosol Hazard Assessments of Emergency Responders in Specific Scenarios: Summary Report", OMI-762, prepared by OptiMetrics, Inc. under Contract No: DAAD13-02-F-0028 for US Army Edgewood Chemical Biological Center, Aberdeen Proving Ground, MD, 15 January 2004.

Tui man, I.L. and Steenweg, L., "The Influence of Particle Shape on the Penetration through Fibrous Filters," *J. Aerosol Science,* 29: pp S1163-S1164 (1998).

Wake, D., Bowry, A.C., Crook, B., and Brown, R.C., "Performance of Respirator Filters and Surgical Masks Against Bacterial Aerosols." *J. Aerosol Sci. 28*(7): pp 1311-1329 (1997).

Willeke, K., Qian, Y., Donnelly, J., Ginshpun, S., and Ulevicius, V., "Penetration of Airborne Microorganisms Through a Surgical Mask and a Dust/Mist Respirator." *Am. Ind. Hyg. Assoc. J. 57:* pp 348-355 (1996).

Blank

APPENDIX A

PHOTOGRAPHS OF CARTRIDGES AND FILTERING FACEPIECES

Figure A-1. SEA HE-T P100 Cartridge

Figure A-2. Survivair 1050 P100 Cartridge

Figure A-3. North 7506 N95 Cartridge

Figure A-4. MSA Flexi-Filter N95 Cartridge

Figure A-5. 3M 8293 P100 Filtering Facepiece

Figure A-6. Moldex 2360 P100 Filtering Facepiece

Figure A-7. MSA Affinity Plus N95 Filtering Facepiece

Figure A-8. Gerson 1730 N95 Filtering Facepiece

Blank

APPENDIX B

RATIONALE FOR SELECTING FLOW CONDITIONS

B.1 Introduction

The cyclic flow conditions were selected based on an analysis of data completed by the U.S. Army's Edgewood Chemical Biological Center (ECBC) to assess the relationship between workload and ventilation rate (Caretti et al., 2004). A brief review of literature regarding unencumbered ventilation is provided in Section B.2. For a complete review, refer to Caretti et al. (2004). Section B.3 presents the data compiled by ECBC illustrating the effect of breathing resistance from an APR on ventilation at different work intensities. The rationale for the selected flow conditions is provided in Section B.4.

B.2 Unencumbered Ventilation

Incremental exercise testing permits a rapid, yet thorough assessment of an individual's cardiorespiratory responses to exercise, including the level of the subject's exercise limitation. Typically, such testing spans a tolerable work rate range from low to high levels, during which, large amounts of respiratory and cardiovascular data are collected up to and including the voluntary endpoint of testing. Many published reports have documented breathing patterns adopted by healthy humans during incremental exercise [Blackie *et al.* (1991); Gallagher *et al.* (1987); Neder *et al.* (2001); Wasserman *et al.* (1987)]. In general, it has been demonstrated in subjects with various fitness levels that increasing minute volumes are due to increases in both tidal volume and breathing frequency at low exercise intensities. At high exercise intensities, increases in minute volume are accomplished mainly by increasing breathing frequency, with tidal volume showing a plateau [Gallagher *et al.* (1987)].

Normal values and ranges of ventilation at maximal exercise with respect to age, sex, and body anthropometrics have also been established using incremental testing. Blackie *et al.* (1991) exposed 231 subjects (120 women; 111 men) to a symptom-limited maximal progressive incremental cycle ergometer exercise test. All subjects underwent a medical screening and physical examination, including spirometry for those who had a history of smoking. Competitive athletes were excluded. The test subject population was dispersed in equal numbers (n =20) in ten-year age categories of 20-29 years, 30-39 years, 40-49 years, 50-59 years, 60-69 years, and 70-79 years for each sex, with the exception of men over 70 years

of age (n = 11). Measurements of minute volume ($\dot{V}E$), tidal volume (V_T), and breathing frequency (f) were obtained at the end of each subject's exercise test when maximal performance had been attained. The mean values at maximal exercise ($\dot{V}E_{max}$, $V_{T\ max}$, and f_{max}) are presented in Table B-1 for each age group for both sexes. Average $\dot{V}E_{max}$ was 97 ± 25 L·min^{-1} for all male subjects and ranged from 66 ± 12 to 114 ± 23 L·min^{-1}. For females, average $\dot{V}E_{max}$ was 69 ± 22 L·min^{-1} and ranged from 48 ± 12 to 87 ± 17 L·min^{-1}. Independent of age, $\dot{V}E_{max}$, and $V_{T\ max}$ were significantly greater (p<0.001) for males compared to females. There was no difference in f_{max} between men and women.

Table B-1. Mean Values for Ventilation at the End of Maximum Exercise
(Blackie *et al.*, 1991)

Group and Age (yr)	$V_{E, max}$ (L/min)	F_{max} (breaths/min)	$V_{T, max}$ (L)
Men 20-29	114 ± 23	42 ± 8	2.7 ± 0.4
Men 30-39	105 ± 30	40 ± 15	2.7 ± 0.6
Men 40-49	102 ± 23	36 ± 7	2.9 ± 0.6
Men 50-59	97 ± 15	36 ± 6	2.8 ± 0.3
Men 60-69	83 ± 14	33 ± 6	2.6 ± 0.4
Men 70-79	66 ± 12	30 ± 6	2.3 ± 0.4
Men Mean	97 ± 25	36 ± 9	2.7 ± 0.5
Women 20-29	87 ± 17	41 ± 7	2.2 ± 0.5
Women 30-39	88 ± 19	44 ± 8	2.0 ± 0.3
Women 40-49	74 ± 19	35 ± 8	2.1 ± 0.4
Women 50-59	60 ± 15	32 ± 8	1.9 ± 0.4
Women 60-69	56 ± 14	33 ± 9	1.7 ± 0.2
Women 70-79	48 ± 12	31 ± 7	1.6 ± 0.3
Women Mean	69 ± 22	36 ± 9	1.9 ± 0.4

Sue and Hansen (1984) reported values similar to Blackie *et. al.* (1991) for V_T (2.28 ± 0.43 L) and f (41.6 ± 9.6 min^{-1}) at maximum exercise in a population of middle-aged men (mean age = 54 years, range 34 to 74 years). Comparable values of $\dot{V}E$ have also been reported for specific age and gender groups and individual subjects at maximum efforts of incremental cycling exercise. Wasserman *et al.* (1987) measured $\dot{V}E_{max}$ values of 107 L·min^{-1} for a 55-year-old male executive, 89 L·min^{-1} for a 59 year old retired male shipyard worker, 70 L·min^{-1} for a 45-year-old female homemaker, and 90 L·min^{-1} for a 37 year old male shipyard machinist, all values that fall within age-specific data reported by Blackie *et al.* (1991).

In a study of similar design to that of Blackie *et al.* (1991), Neder *et al.* (2001) assessed breathing patterns during incremental exercise of 120 normal, healthy, sedentary individuals (60 males, 60 females) evenly distributed in age groups of 20-39 years, 40-59 years, and 60-80 years. Although these investigators were primarily interested in developing normative ventilatory data at selected submaximal ventilatory stresses, maximal $\dot{V}E$ data were reported for each age group by sex. For females, Neder *et al.* (2001) recorded average $\dot{V}E_{max}$ values of approximately 76 ± 14 L·min^{-1}, 67 ± 11 L·min^{-1}, and 50 ± 10 L·min^{-1} for the age groups of 20-39 years, 40-59 years, and 60-80 years. Maximal $\dot{V}E$ averaged 120 ± 28 L·min^{-1}, 99 ± 22 L·min^{-1}, and 77 ± 12 L·min^{-1} for the three ascending male age groups. Again, these values reflect the data reported by Blackie *et al.* (1991) for a similar subject population. Therefore, the data presented in Table A-1 serve as a reasonable representation of normal maximal ventilatory responses to exhaustive incremental exercise for a wide range of ages in both males and females.

B.3 Preliminary ECBC Data Compilation

The data in Table B-2 represent analysis of breath-by-breath ventilation data from three studies [Caretti et al. (2004); Coyne (2001); Johnson *et al.* (1999)], and provide a preliminary assessment of the impact of resistance breathing on ventilation at different work rates. The effect of breathing resistance and exercise intensity on measured breathing frequency and tidal volume are graphically illustrated in Figures B-1 and B-2. The 0.7 cm H_2O/L/s resistance condition represents a "no mask" condition. The three other resistance conditions correspond to those imposed while wearing various air-purifying respirators (APRs). For reference, the resistance of the M40 military mask is approximately 2.7 cm H_2O/L/s at 85 L/min. Both the mean tidal volume and breathing frequency tended to increase with increased work rate for each inhalation group. The breathing frequency tended to increase in higher proportions at the lower resistances. For example, the frequency increased by 65% as the exercise intensity increased from 30 to 85% at a resistance of 0.7 cm H_2O/L/s. In comparison, the mean frequency only increased by 50% at an inhalation resistance of 5.73 cm H_2O/L/s. There was not a significant difference in the tidal volumes measured for specific exercise intensities with inhalation resistances between 1.84 and

5.73 cm $H_2O/L/s$. In several cases including the 85% exercise intensity, the tidal volume tends to decrease with increased inhalation resistance.

Table B-2. Preliminary Data Compiled by ECBC to Assess Impact of Breathing Resistance and Work Intensity on Ventilation

Estimated Work Intensity (% VO_2 max)	Inhalation Resistance (cm $H_2O/L/s$)	V_E (L/min)		V_T (L)		F_R (min^{-1})		PIF (L/min)	
		$\bar{x}$	S.D.	$\bar{x}$	S.D.	$\bar{x}$	S.D.	$\bar{x}$	S.D.
30	0.7	26.1	1.4	1.0	0.2	31.5	18.0	128.3	20.0
	1.84	22.8	5.8	1.1	0.2	22.6	6.9	140.6	62.4
	3.2	21.0	7.3	1.1	0.2	19.1	4.9	128.4	26.5
	5.73	19.5	5.9	0.9	0.2	26.6	16.9	116.9	37.7
40	0.7	26.9	7.6	1.1	0.2	29.7	10.4	159.3	24.4
	1.84	30.1	7.1	1.4	0.4	22.4	3.6	179.6	96.4
	3.2	30.0	7.9	1.4	0.3	22.9	4.7	170.4	43.8
	5.73	26.9	8.2	1.2	0.3	27.2	10.9	177.5	77.8
50	0.7	31.1	10.5	1.1	0.4	41.1	22.3	182.2	33.8
	1.84	43.4	16.5	1.7	0.5	26.7	3.5	211.1	58.1
	3.2	37.1	8.6	1.5	0.4	31.1	15.1	189.3	38.8
	5.73	36.6	8.7	1.4	0.4	30.1	9.5	232.7	87.7
70	0.7	46.2	14.1	1.4	0.5	52.4	28.2	264.6	52.3
	1.84	53.4	13.1	1.9	0.6	32.4	10.6	239.1	54.4
	3.2	57.2	14.8	1.8	0.4	35.0	9.9	295.5	144.9
	5.73	51.4	15.7	1.7	0.6	36.6	11.7	349.7	94.0
85	0.7	67.4	32.1	1.7	0.5	52.0	23.8	354.8	135.8
	1.84	73.9	21.4	2.2	0.6	35.7	11.5	305.6	95.8
	3.2	75.5	23.6	2.1	0.7	38.6	9.0	349.6	117.9
	5.73	60.5	19.0	1.8	0.5	40.1	14.4	395.4	103.4
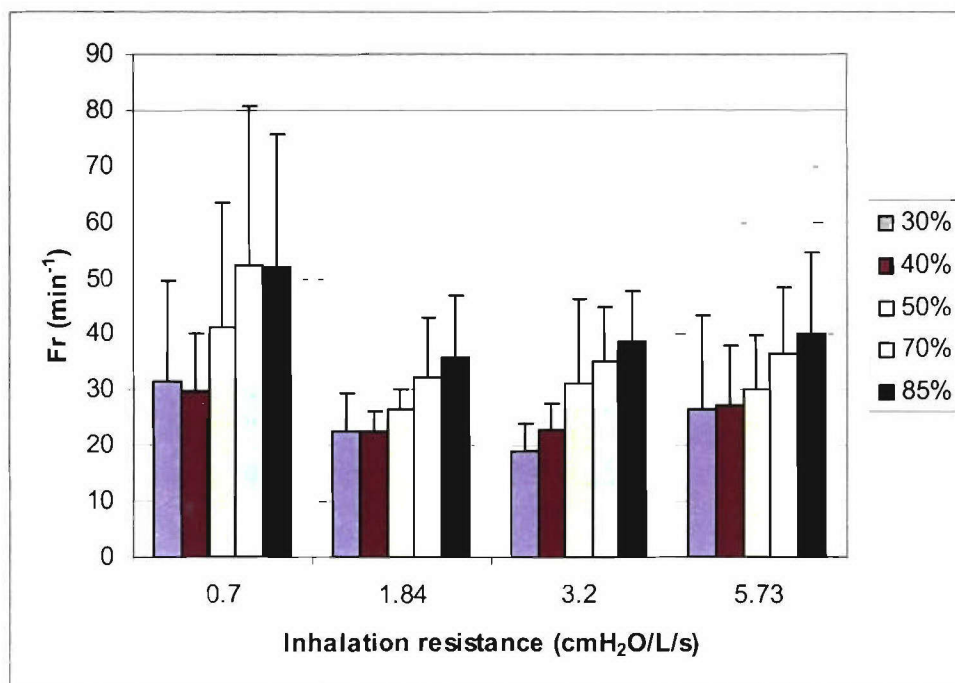
Figure B-1. Average (±SD) Breathing Frequency (Fr) at Exercise Intensities of about 30%, 40%, 50%, 70%, and 85% of Maximal Oxygen Consumption (V_{O_2} max) for Four Inhalation Resistance Conditions
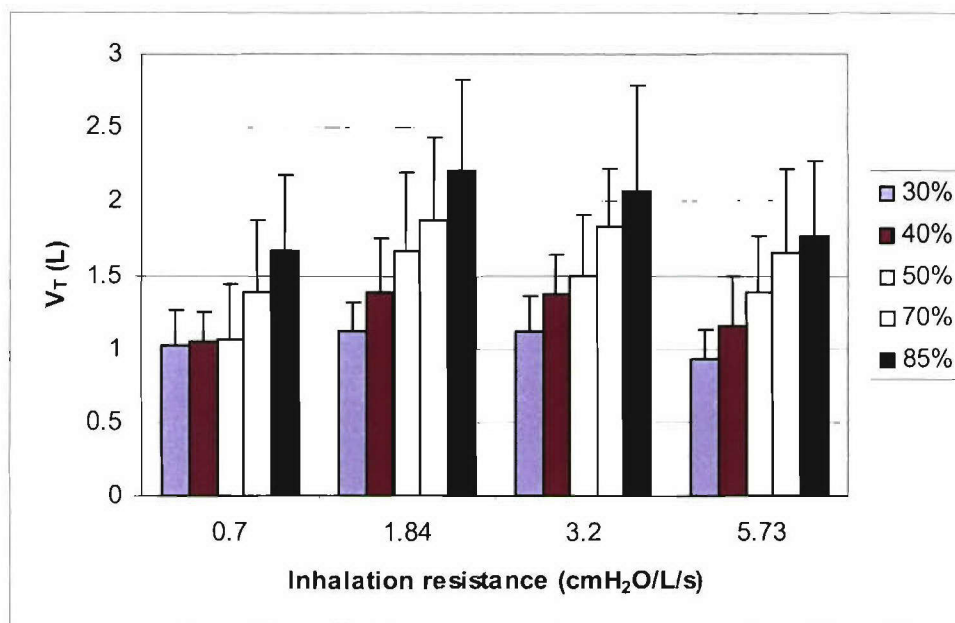
Figure B-2. Average (±SD) Tidal Volume (V_T) at Exercise Intensities of 30%, 40%, 50%, 70%, and 85% of Maximal Oxygen Consumption (V_{O_2} max) for Four Inhalation Resistance Conditions

B.4 Rationale for Selected Flow Conditions

The cyclic flow conditions, summarized in Table B-3, were selected based on the analysis described previously. The 40 L/min minute volume represents a moderate breathing condition to allow comparison with the penetrations measured at higher flows. The 85 L/minute volume corresponded to a work intensity of approximately 85 percent VO_2 max, respectively, as shown in Figures B-1 and B-2. The minute volume of 114 L/min corresponded to the average tidal volume and frequency during exhaustive incremental exercise of 20 to 29-year-old males as measured by Blackie *et al.* (1991). Adding one standard deviation to this minute volume provides the final flow condition. It is noted that the measurements made by Blackie *et al.* were unencumbered and, thus, provide a conservative estimate of breathing during maximal exercise under conditions of respirator wear.

Table B-3. Summary of Selected Cyclic Flow Conditions

Rate (breaths/min)	Tidal Volume (L)	Minute Volume (L/min)	PIF[a] (L/min)	MIF[b] (L/min)
25	1.6	40	130	85
37	2.3	85	270	175
42	2.7	115	360	230
44	3.1	135	430	275

(a) Peak inspiratory flow rate assuming ideal sinusoidal waveform
(b) Mean inspiratory flow rate assuming ideal sinusoidal waveform

B.5 Constant Flow Conditions

Three constant flows were selected for testing: 85, 270, and 360 L/min. The 85 L/min represented the constant flow rate used in NIOSH certification of N95 and P100 particulate respirator filters. The 270 and 360 L/min represented the peak inspiratory flow rates of the cyclic flows with minute volumes of 85 and 115 L/min, respectively. In addition, the 270 L/min was approximately the mean inspiratory flow of the 135 L/min cyclic flow condition.

B.6 References

Blackie, S.P., M.S. Fairbarn, N.G. McElvaney, P.G. Wilcox, N.J. Morrison, and R.L. Pardy. "Normal Values and Ranges for Ventilation and Breathing Pattern at Maximal Exercise." *Chest* 100: 136-142 (1991).

Caretti, D.M., P.D. Gardner, and K.M. Coyne, "Workplace Breathing Rates: Defining Anticipated Values and Ranges for Respirator Certification Testing," U.S. Army Edgewood Chemical Biological Center Technical Report, ECBC-TR-316, September (2004).

Coyne, K. "*Modeling the Pulmonary Effects of Respiratory Protective Masks During Physical Activity.*" University of Maryland College Park (2001).

Gallagher, C.G., E. Brown, and M. Younes. "Breathing Pattern During Maximal Exercise and During Submaximal Exercise with Hypercapnia." *J. Appl. Physiol.* 63: 238-244 (1987).

Johnson, A.T., W.H. Scott, C.G. Lausted, M.B. Benjamin, K.M. Coyne, M.S. Sahota, and M.M. Johnson. "Effect of Respirator Inspiratory Resistance Level on Constant Load Treadmill Work Performance." *Am. Ind. Hyg. Assoc. J.* 60: 474-479 (1999).

Neder, J.A., L.E. Nery, C. Peres, and B.J. Whipp. "Reference Values for Dynamic Responses to Incremental Cycle Ergometry in Males and Females Aged 20 to 80." *Am. J. Respir. Crit. Care Med.* 164: 1481-1486 (2001).

Sue, D.Y. and J.E. Hansen. "Normal Values in Adults During Exercise Testing." *Clin. Chest Med.* 5: 89-98 (1984).

Wasserman, K., J.E. Hansen, D.Y. Sue, and B.J. Whipp. "*Principals of Exercise Testing and Interpretation.*" Philadelphia: Lea & Febiger, 1987.

APPENDIX C

SHAKEDOWN TESTING OF MODEL 3160

C.1 Model 3160 Shakedown Testing

Shakedown tests were conducted to characterize the test system and establish proper operating conditions. This included assessing the effect of non-isokinetic sampling, flow calibrations, and characterization of the challenge particle size distribution.

C.2 No Filter Testing

Due to the range of flow conditions, it was not practical to sample isokinetically. However, non-isokinetic sampling is not expected to have a large effect for the small particle sizes (0.02 to 0.3 μm). To confirm this, tests were initially conducted without a test filter in the exposure chamber (i.e., Lucite® box). A penetration of 100 percent would indicate agreement between the measured upstream and downstream concentrations. Figures C-1 and C-2 compare the measured penetrations at the constant and cyclic flow conditions for the cartridge testing. Figure C-3 compares the no-filter penetrations measured at the filtering facepiece cyclic flow conditions. Data were not collected under the constant flow conditions. The data represents the means of three independent trials and the error bars represent one standard deviation. The measured penetrations were typically in the 90 to 110 percent range. From a practical perspective, the differences are not expected to have a significant impact on measured penetrations.
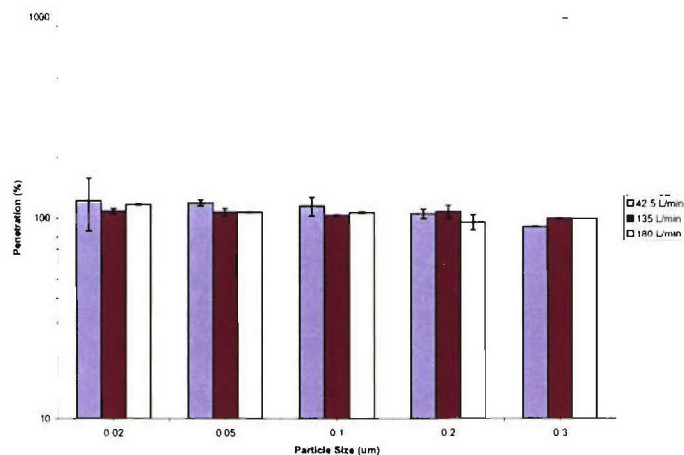
Figure C-1. Penetrations Measured Without Test Filter at Constant Flow Conditions for Cartridge Testing
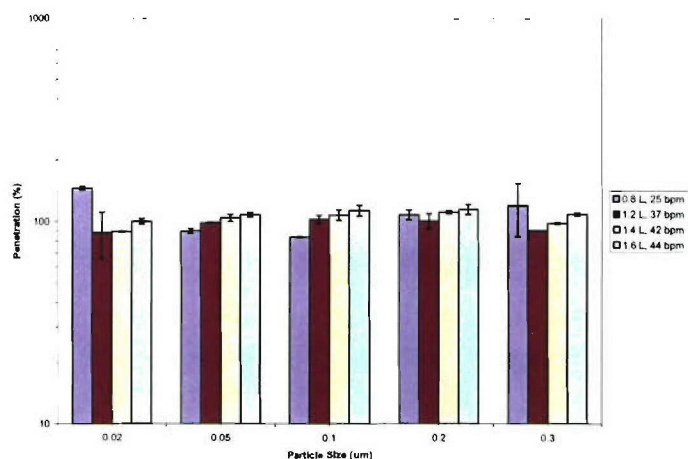
Figure C-2. Penetrations Measured Without Test Filter at Cyclic Flow Conditions for Cartridge Testing
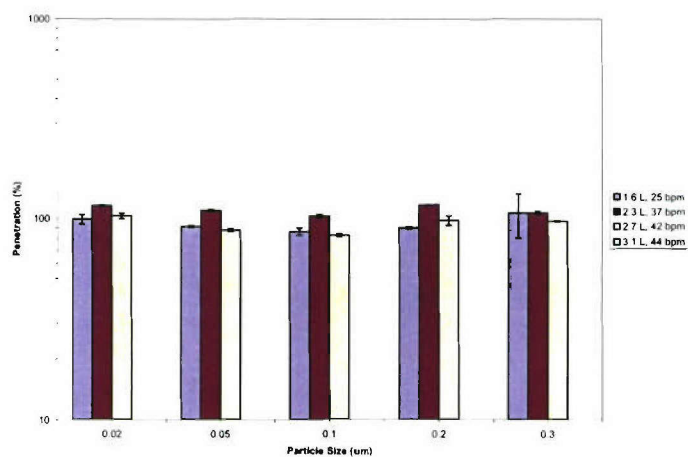
Figure C-3. Penetrations Measured Without Test Filter at Cyclic Flow Conditions for Filtering Facepiece Testing

C.3 Challenge Characterization

Shakedown tests were performed to characterize the particle size distributions of the challenge aerosols. The particle size distribution is important since the Model 3160 uses a CPC that does not classify particles into discrete size ranges. Thus, all particles are assumed to be the particle size of interest. The Model 3160 was used to sequentially generate challenge aerosols with target mean particle sizes of 0.02, 0.05, 0.1, 0.2, and 0.3 µm. An electrostatic classifier and

CPC were used to measure the particle size distributions. The measured size distributions generated by the Model 3160 at a constant flow rate of 85 L/min are shown in Figures C-4 and C-5 for the salt and oil aerosols, respectively. Recall that a salt aerosol was used for testing the N95 filters and a dioctyl phthalate (DOP) aerosol for testing the P100 filters. Distinct peaks are observed for both aerosol types at target mean particle sizes of 0.05, 0.1, and 0.2 μm. However, a significant portion of the 0.3 μm challenge is below the target particle size. In addition, the particle concentration is approximately an order of magnitude lower than the other challenges.
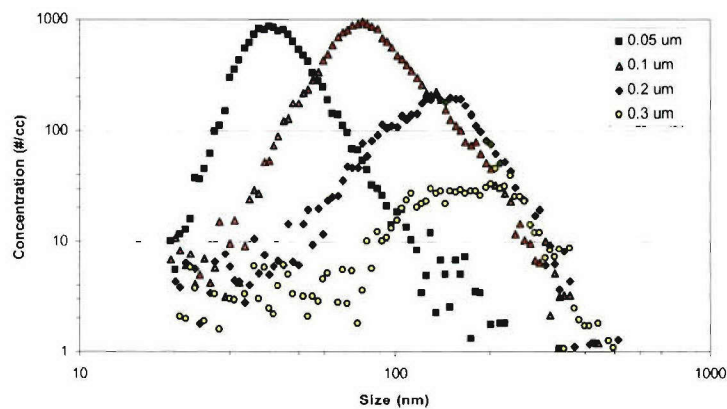
Figure C-4. Measured Particle Size Distributions of Salt Aerosol Used to Challenge N95 Filters
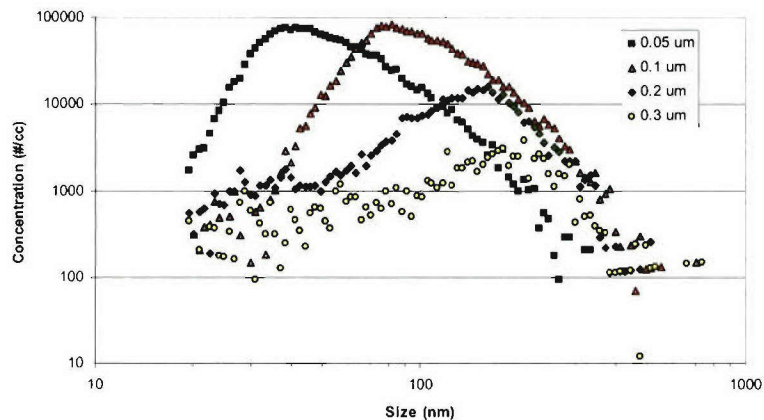
Figure C-5. Measured Particle Size Distributions of DOP Aerosol Used to Challenge P100 Filters

Figures C-6 and C-7 compare the measured size distributions of the 0.2, 0.3, and 0.4 μm aerosols at constant flow rates of 85 and 360 L/min, respectively. Note the similarity between the distributions of the 0.3 and 0.4 μm aerosols. Both distributions tend to shift toward smaller

particles as the flow rate is increased from 85 to 360 L/min. This is potentially due to increased evaporation caused by the additional dilution air, and could account for the increase in penetration observed with increasing particle size over 0.2 μm for the P100 filtering facepiece as discussed in Section 3.5.2.1 of the report. Figures C-8 and C-9 compare the up- and downstream distributions measured for the 0.4 μm aerosol at 85 and 360 L/min. Note that only a small fraction of the particles penetrating are greater than 0.3 μm. This shift in particle size could account for the increase in penetration with increased particle size observed for the filtering facepieces.
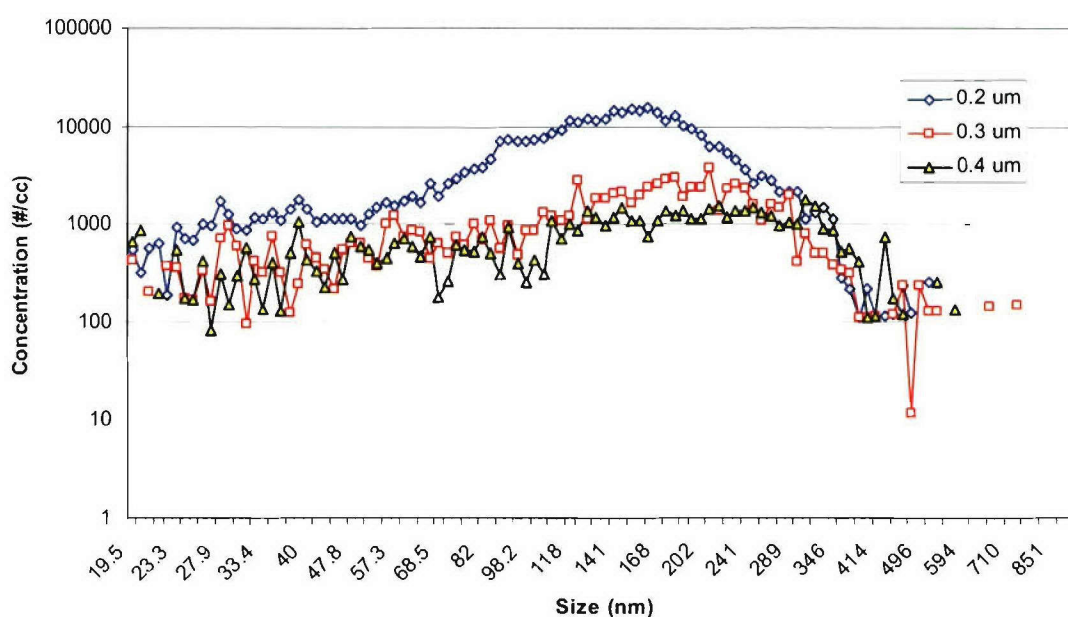
Figure C-6. Measured Size Distributions of the 0.2, 0.3, and 0.4 μm DOP Challenges at Flow Rate of 85 L/min
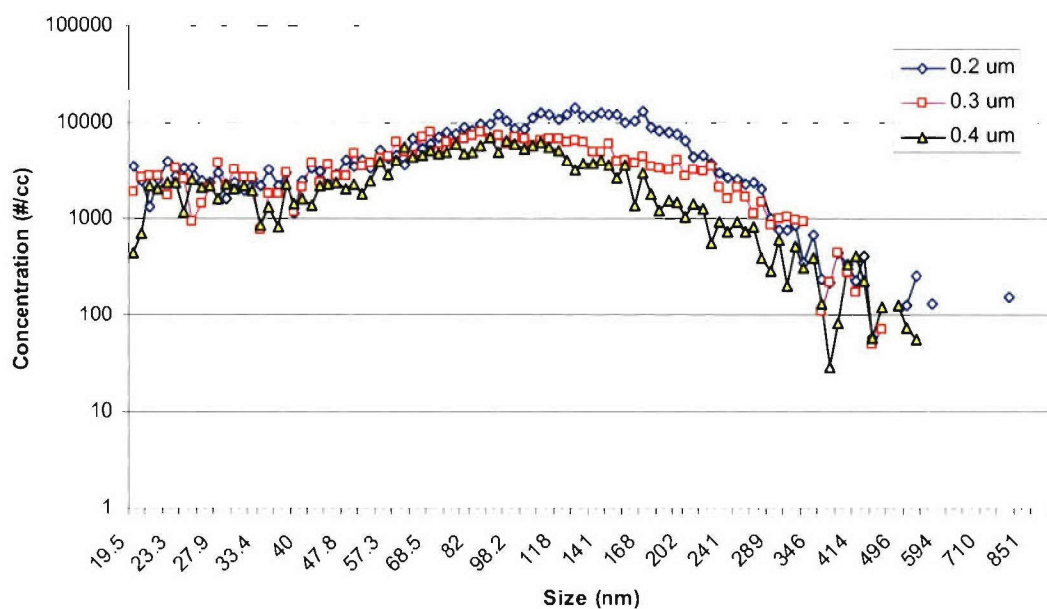
Figure C-7. Measured Size Distributions of the 0.2, 0.3, and 0.4 μm DOP Challenges at Flow Rate of 360 L/min
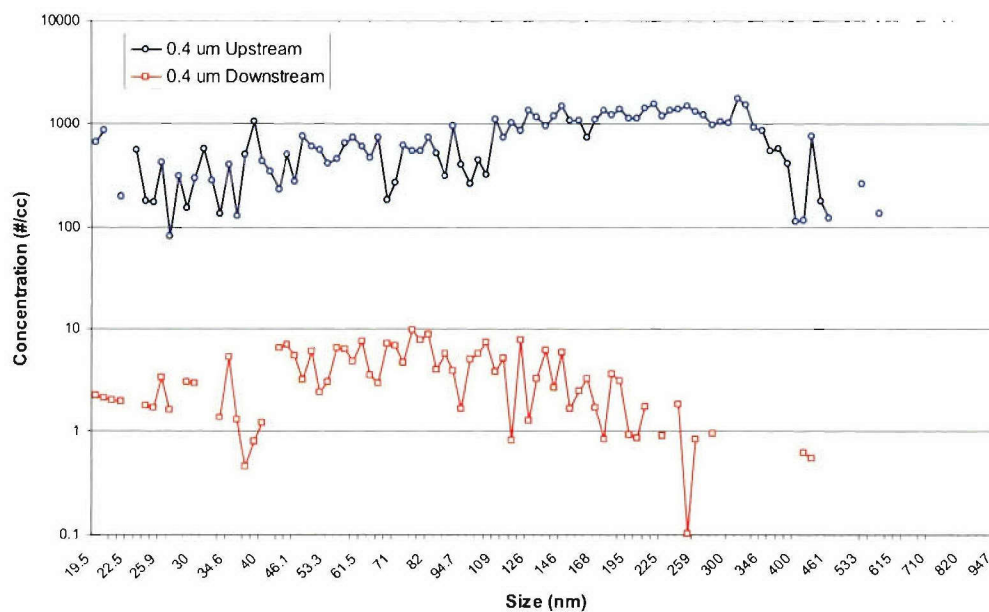
Figure C-8. Comparison of Measured Size Distributions Upstream and Downstream of Moldex P100 Filter at a Flow Rate of 85 L/min
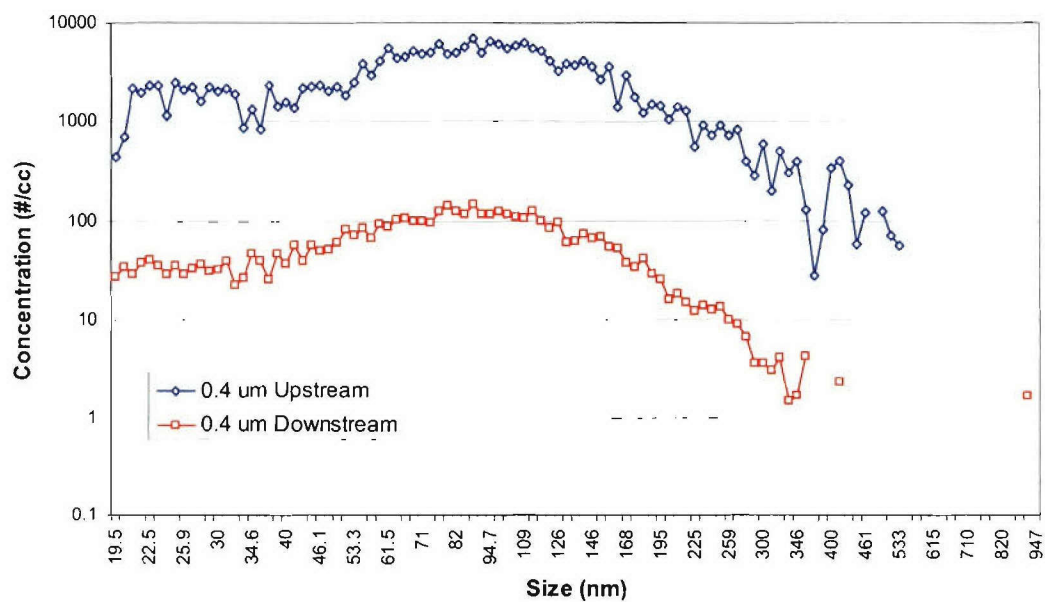
Figure C-9. Comparison of Measured Size Distributions Upstream and Downstream of Moldex P100 Filter at a Flow Rate of 360 L/min

Blank

APPENDIX D

SHAKEDOWN OF TEST SYSTEM FOR LARGE PARTICLE INERT TESTING

D.1 Large Particle Shakedown Testing

Shakedown tests were completed to verify the proper operating conditions of the system. This included both no-filter testing to identify any potential sampling bias between the up- and downstream samples, and characterizing the challenge aerosol.

D.2 No Filter Testing

Shakedown tests without a filtering facepiece or cartridge in the system were completed to identify any potential sampling bias between the up- and downstream measurements. The PSL with nominal diameters of 0.7, 1.3 and 2.9 μm were generated at three different constant flow rates. The measured no-filter penetrations are provided in Figure D-1. The results are based on the average of three independent trials at each test condition. The error bars represent one standard deviation. A penetration of 100 percent would represent agreement between the upstream and downstream measurements and no sampling bias. For the 0.7 and 1.3 μm particles, the measured penetrations ranged between 90 and 110 percent. However, the measured penetration of the 2.9 μm particle tended to decrease with increased flow rate indicating a sampling bias downstream for this particle size. Similar trends are observed under the cyclic flow conditions as shown in Figure D-2.
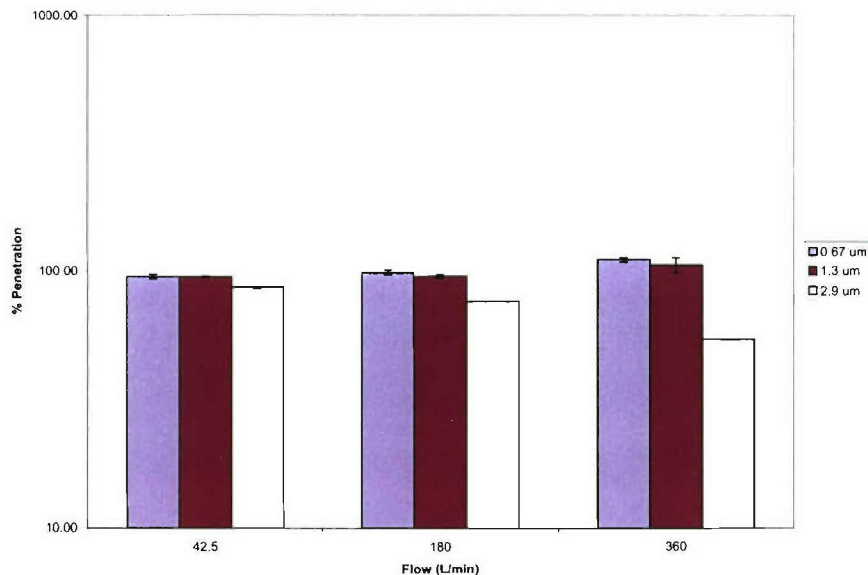

Figure D-1. Penetrations Measured Without Test Filter at Constant Flow Conditions
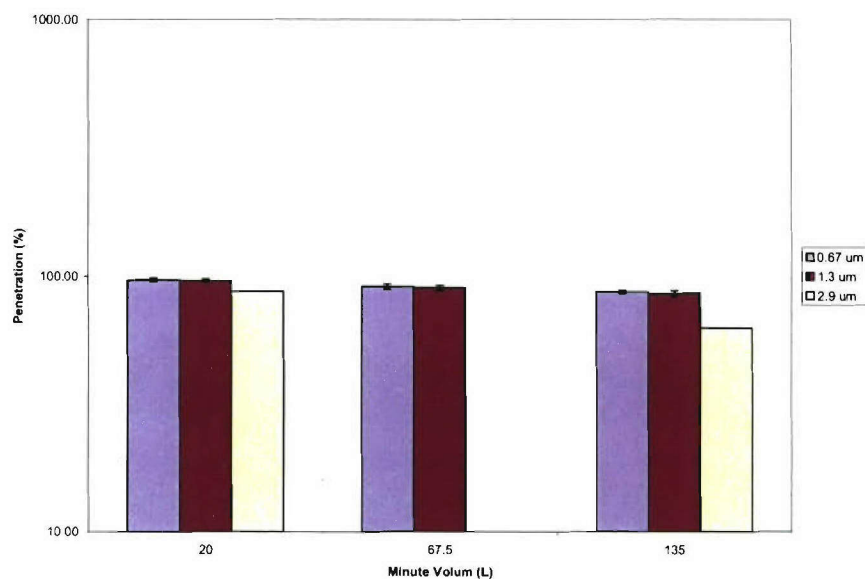
Figure D-2. Penetrations Measured Without Test Filter at Cyclic Flow Conditions

The no-filter penetrations with the 2.9 μm PSL are also shown in Figure D-3 as a function of flow rate. Each data point represents the mean of at least two trials and the error bars represent one standard deviation. The data points are connected by lines to emphasize the trends. These results were used to generate correction factors that could be applied to the 2.9 μm PSL results specific to each flow condition. However, the measured penetrations were below detectable limits in all cases (<0.001%), so it was not necessary to correct the data.
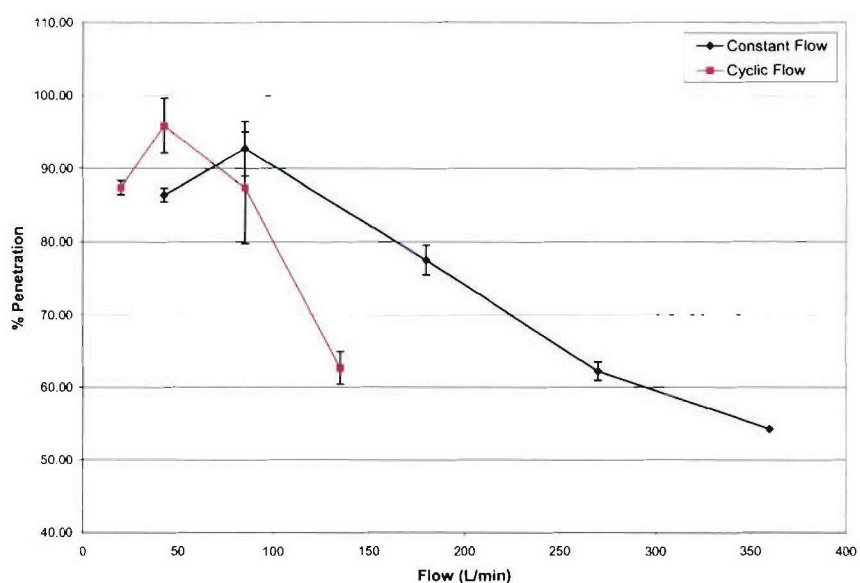
Figure D-3. 2.9 μm PSL No Filter Penetration for Cyclic and Constant Flows

Further experiments were performed to characterize the sampling technique for the 2.9 μm aerosol. The downstream expansion chamber was removed and replaced with a tee fitting (with an approximate diameter of 2.5 cm) that allowed the insertion of isokenetic sampling probes with various inlet diameters, as summarized in Table D-1. Each probe was used to sample downstream during no-filter testing at a constant flow rate of 360 L/min. The results, shown in Figure D-4, indicated that the measured penetration tended to increase as the probe inlet diameter increased. Penetrations ranging from 90 to 95 percent were measured using probes 6 through 8.

Table D-1. Summary of Isokinetic Probe Inlet Dimensions

Probe Number	Inlet ID (in)	Inlet ID (cm)
2	1/16	0.16
4	1/8	0.32
5	5/32	0.40
6	3/16	0.48
7	7/32	0.56
8	1/4	0.64
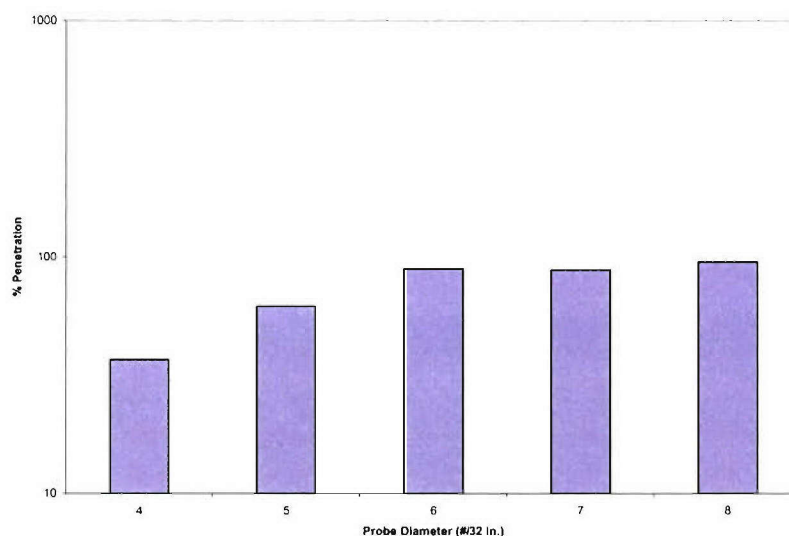
Figure D-4. Penetrations Measured Without a Test Filter at 360 L/min With Probes of Various Inlet Diameters

Probe 6 and a 0.3 cm ID probe located near the inlet of the downstream tubing, directly underneath the filter holder, were used to sample a 2.9 μm challenge downstream at different flow rates. The results are shown in Figure D-5. The percent penetration measured at each

sample location and flow rate represents a single trial. The measurements were all between 85 and 115 percent. From a practical perspective, the differences are not expected to have a significant impact on measured penetrations.
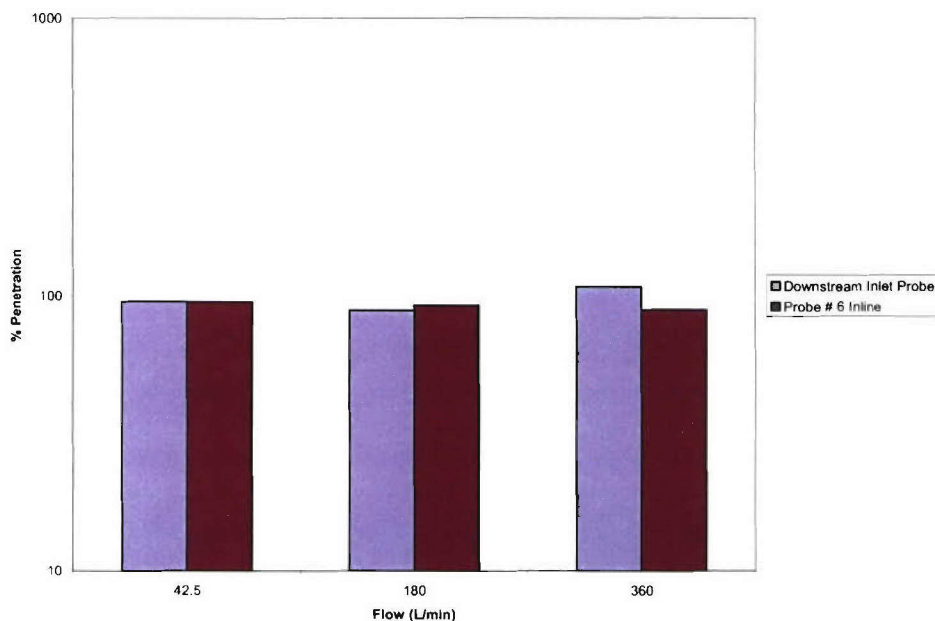
**Figure D-5. Comparison of Measured Penetrations Made
Using Two Different Sampling Probes**

D.3 Challenge Aerosol Characterization

Shakedown testing was also completed to assess the stability of the challenge concentration, which is required to sequentially make aerosol measurements between up- and downstream. Figure D-6 illustrates the length of time required for the challenge to reach steady state at various constant flow conditions. The challenge aerosol was 1.3 µm PSL generated using a 6-jet Collison nebulizer. As expected, the required duration to reach steady state increased with decreased flow rate. The challenge concentration reached steady-state within 5 minutes at the 180 and 360 L/min flow conditions. It took approximately 10 minutes at 135 L/min and 20 minutes at 42.5 L/min. These times are consistent with those expected based on the flow rate and test chamber volume. Recall, the test filter is bypassed during startup to prevent loading of the filter. Note that the aerosol concentration decreased as the flow rate increased, due to the additional dilution air.
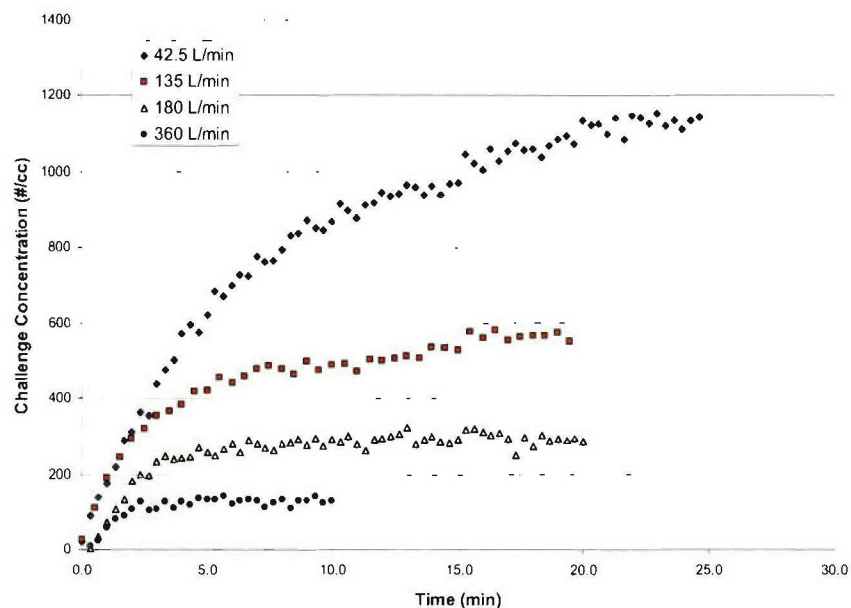
Figure D-6. Challenge Aerosol Concentration During System Startup

The same test was also performed with the 2.9 µm PSL at a flow rate of 135 L/min. The measured challenge concentration as a function of time is shown in Figure D-7. It took approximately 5 minutes for the chamber to reach steady state. Figure D-7 also compares concentration measurements made using the APS with and without the diluter (Model 3302A, TSI). Measurements made without the diluter were more consistent and, thus, the 2.9 µm challenge tests were not diluted prior to measurement. Note that the challenge concentration was only 20 particles/cc. The challenge concentration was increased by using a 24-jet Collison nebulizer and removing the charge neutralizer (Model 3012, TSI) from the test system. Figure D-8 shows the challenge concentration as a function of time at a flow rate of 135 L/min after the modifications. The concentration reached approximately 160 particles/cc after 5 minutes.
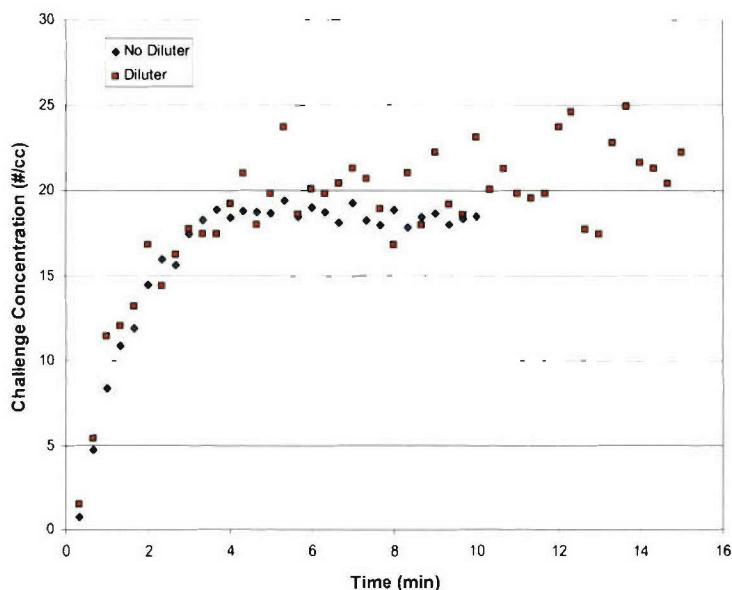
Figure D-7. Comparison of 2.9 μm Challenge Aerosol Concentration Measured Using the APS With and Without the Diluter
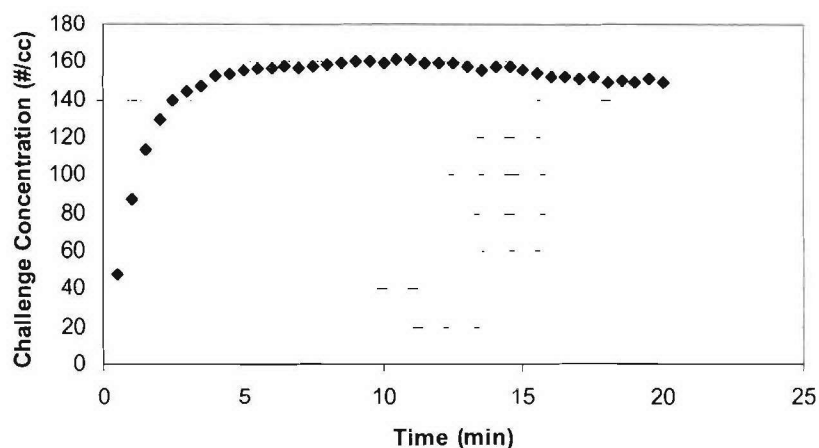
Figure D-8. Measured Challenge Concentration of 2.9 μm PSL During System Startup at a Flow Rate of 135 L/min

Due to the large test matrix, conducting 0.67 and 1.3 μm PSL tests simultaneously was considered advantageous. The mixture was aerosolized using the 6-jet Collison nebulizer. Figure D-9 illustrates the challenge concentration as a function of time for both particle sizes. The size distribution measured using the APS is shown in Figure D-10 and indicates two distinct peaks at the desired particle sizes. Aerosol penetrations through the MSA Flexi-Filter® were made using each particle size individually and as a mixture. Similar penetrations were measured

with both approaches, as shown in Table D-2. Thus, testing 0.67 and 1.3 μm PSL simultaneously was performed to reduce the number of tests. The 2.9 μm particles could not be included in the mixture since the diluter was required to measure the 0.67 and 1.3 μm challenge concentrations.
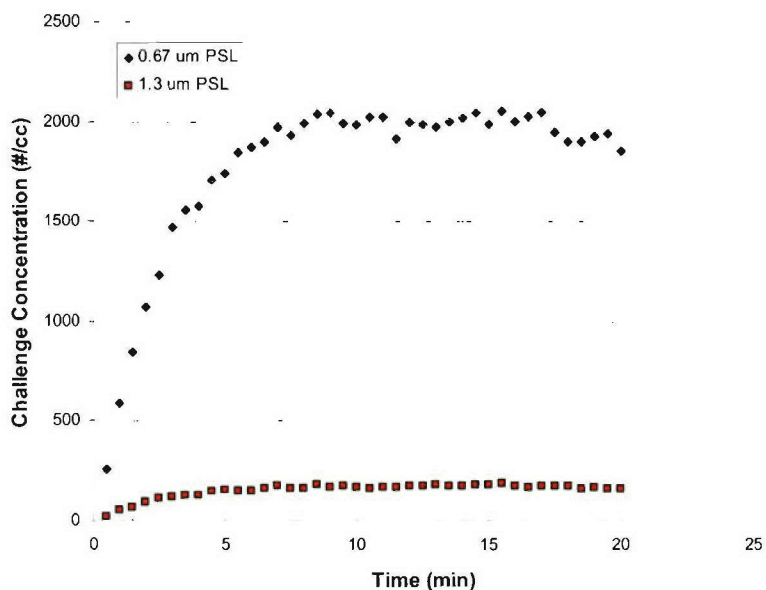
Figure D-9. Challenge Concentration of 0.67 and 1.3 μm PSL Generated from a Mixture Using Collison Nebulizer
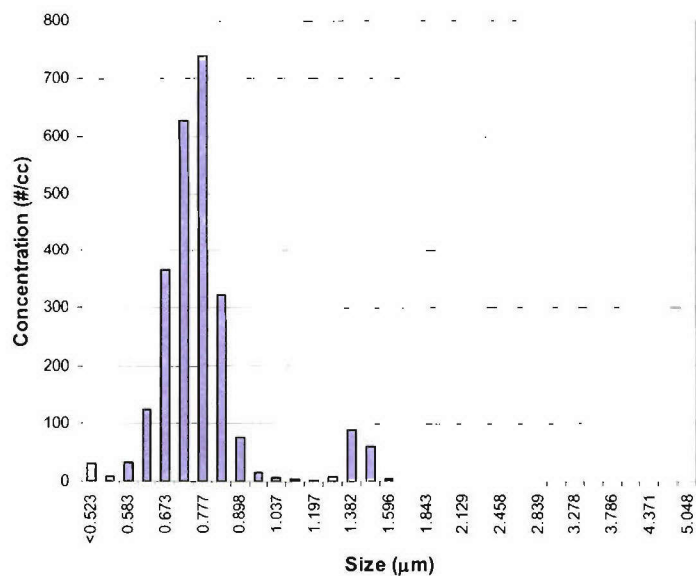
Figure D-10. Particle Size Distribution Measured Using APS of 0.67 and 1.3 μm PSL Mixture Generated Using Collison Nebulizer

Table D-2. Comparison of Measured Penetrations through MSA Flexi-Filter Using 0.67 and 1.3 μm PSL Aerosolized Individually and as Mixture

Challenge	Measured Penetration (%)	
	0.67 μm	1.3 μm
0.67 μm PSL	0.358	-
0.67 μm PSL	0.289	-
1.3 μm PSL	-	0.0263
1.3 μm PSL	-	0.0254
Mixed (0.67 and 1.3 μm PSL)	0.378	0.0263
Mixed (0.67 and 1.3 μm PSL)	0.351	0.0284

As mentioned previously, it would be beneficial to conduct 0.7, 1.3, and 2.9 μm filter tests simultaneously. A 6-jet Collison nebulizer was used to aerosolize Emery 3004 oil. The size distribution based on number concentration as measured using the APS is shown in Figure D-11. Adequate concentrations of 0.7, 1.3, and 2.9 μm particles were generated to measure oil efficiencies with all three particle sizes during a single trial. Thus, the 0.7, 1.3, and 2.9 μm oil tests were performed simultaneously.
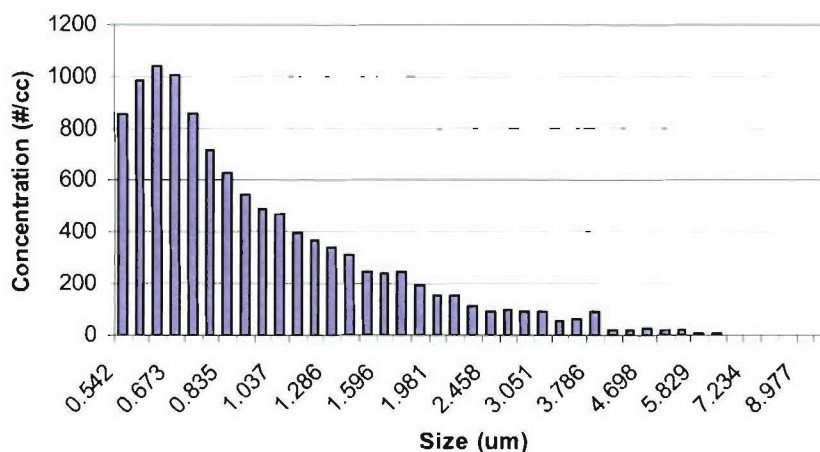
Figure D-11. Distribution of Emery 3004 Aerosol Generated Using Collison Nebulizer

Shakedown testing was performed to verify the assumption that the supermicron test system was well mixed. An oil challenge was generated with a 6-jet Collison Nebulizer. The aerosol exiting the nebulizer mixed with dry, filtered house air and passed through a charge neutralizer (Model 3012, TSI) before entering the chamber. An exhaust flow of 180 L/min was

drawn through a filter mounted in a filter holder. A significant amount of 0.67 and 1.3 μm oil particles was generated. Two tests were completed using two different probes. The first test used a long straight sample probe to sample from the left side of the chamber, center of the chamber, and right side of the chamber. The second test used a curved probe to sample from the front of the chamber, the center of the chamber, and the back of the chamber. Both probes were inserted through the center of the chamber's left side panel. The combined results of both tests showed a slight concentration increase from right to left and little difference from front to back for both particle sizes tested. A top view of the chamber, with a comparison of the 1.3 μm concentrations, is shown in Figure D-12. The percentages shown were calculated by dividing the concentration found from each section by the concentration found in the center and multiplying by 100 percent.

	106 %	
113 %	100 %	86 %
	107 % Front	

Figure D-12. Top View of Supermicron Test System with 1.3 μm Concentrations Shown as a Percentage of the Center Concentration

APPENDIX E

SUMMARY OF MEASURED INERT FILTRATION EFFICIENCIES

Table E-1. Summary of Measured Penetrations through SEA HE-T Cartridge

Flow Rate (L/min)	Trial	Particle Size (μm)							
		0.02	0.05	0.1	0.2	0.3	0.7	1.3	2.9
		Penetration (%)							
42.5	1	<0.0001	<0.0001	0.0002	0.0004	0.0003	<0.0001	<0.0001	<0.0001
	2	<0.0001	<0.0001	0.0003	0.0006	0.0003	<0.0001	<0.0001	<0.0001
	3	<0.0001	<0.0001	0.0002	0.0003	0.0002	<0.0001	<0.0001	(a)
	x	<0.0001	<0.0001	0.0002	0.0004	0.0003	<0.0001	<0.0001	<0.0001
	σ	-	-	0.0000	0.0001	0.0001	-	-	-
135	1	0.0001	0.002	0.009	0.012	0.006	<0.0001	<0.0001	<0.0001
	2	0.0001	0.002	0.008	0.011	0.005	<0.0001	<0.0001	<0.0001
	3	0.0001	0.002	0.010	0.012	0.006	<0.0001	<0.0001	(a)
	4	(b)	(b)	(b)	(b)	(b)	<0.0001	<0.0001	(b)
	x	0.0001	0.002	0.0091	0.012	0.006	<0.0001	<0.0001	<0.0001
	σ	0.0000	0.0004	0.0010	0.0009	0.0008	-	-	-
180	1	0.005	0.008	0.029	0.030	0.019	<0.0001	<0.0001	<0.0001
	2	0.002	0.009	0.027	0.021	0.012	<0.0001	<0.0001	<0.0001
	3	0.001	0.005	0.030	0.018	0.010	<0.0001	<0.0001	<0.0001
	x	0.003	0.007	0.029	0.023	0.014	<0.0001	<0.0001	<0.0001
	σ	0.002	0.002	0.001	0.006	0.005	-	-	-
20[c]	1	<0.0001	<0.0001	0.0002	0.0003	0.0002	<0.0001	<0.0001	<0.0001
	2	0.0001	<0.0001	0.0001	0.0003	0.0002	<0.0001	<0.0001	<0.0001
	3	<0.0001	<0.0001	0.0002	0.0003	0.0002	<0.0001	<0.0001	(a)
	x	0.0001	<0.0001	0.0001	0.0003	0.0002	<0.0001	<0.0001	<0.0001
	σ	-	-	0.0000	0.0000	0.0000	-	-	-
42.5[c]	1	0.0002	0.001	0.006	0.009	0.003	0.0001	<0.0001	<0.0001
	2	0.0001	0.0009	0.005	0.007	0.005	<0.0001	<0.0001	<0.0001
	3	0.0001	0.0003	0.002	0.002	0.002	<0.0001	<0.0001	(a)
	x	0.0001	0.0008	0.004	0.006	0.003	0.0001	<0.0001	<0.0001
	σ	0.0000	0.0004	0.002	0.003	0.002	-	-	-
57.5[c]	1	0.0004	0.002	0.010	0.013	0.007	0.0012	<0.0001	<0.0001
	2	0.0005	0.001	0.005	0.006	0.004	<0.0001	<0.0001	<0.0001
	3	0.0006	0.001	0.005	0.006	0.006	<0.0001	<0.0001	(a)
	4	(b)	(b)	(b)	(b)	(b)	<0.0001	<0.0001	(b)
	x	0.0005	0.002	0.006	0.008	0.006	0.0004	<0.0001	<0.0001
	σ	0.0001	0.0007	0.003	0.004	0.002	-	-	-
67.5[c]	1	0.001	0.004	0.016	0.018	0.010	<0.0001	<0.0001	<0.0001
	2	0.001	0.002	0.007	0.009	0.008	<0.0001	<0.0001	<0.0001
	3	0.002	0.002	0.008	0.010	0.010	<0.0001	<0.0001	(a)
	x	0.001	0.003	0.010	0.012	0.010	<0.0001	<0.0001	<0.0001
	σ	0.0003	0.001	0.005	0.005	0.001	-	-	-

(a) Only two tests planned
(b) Test not planned
(c) Cyclic flow minute volume

E-2

Table E-2. Summary of Measured Penetrations through Survivair 1050 Cartridge

Flow Rate (L/min)	Trial	Particle Size (μm)							
		0.02	0.05	0.1	0.2	0.3	0.7	1.3	2.9
		Penetration (%)							
42.5	1	0.0003	0.003	0.008	0.009	0.006	<0.0001	<0.0001	<0.0001
	2	0.0001	0.002	0.006	0.008	0.004	<0.0001	<0.0001	<0.0001
	3	0.0001	0.002	0.007	0.008	0.004	<0.0001	<0.0001	(a)
	x	0.0002	0.002	0.007	0.008	0.005	<0.0001	<0.0001	<0.0001
	σ	0.0001	0.0005	0.0007	0.0010	0.001	-	-	-
135	1	0.003	0.037	0.093	0.059	0.035	<0.0001	<0.0001	<0.0001
	2	0.004	0.043	0.10	0.064	0.038	<0.0001	<0.0001	<0.0001
	3	0.005	0.048	0.10	0.063	0.039	<0.0001	<0.0001	(a)
	x	0.004	0.043	0.098	0.062	0.037	<0.0001	<0.0001	<0.0001
	σ	0.001	0.005	0.005	0.003	0.002	-	-	-
180	1	0.025	0.12	0.23	0.12	0.086	0.0001	<0.0001	<0.0001
	2	0.021	0.097	0.19	0.10	0.068	0.0001	<0.0001	<0.0001
	3	0.008	0.029	0.046	0.030	0.034	<0.0001	<0.0001	(a)
	x	0.018	0.084	0.16	0.086	0.063	0.0001	<0.0001	<0.0001
	σ	0.009	0.050	0.097	0.049	0.027	0.0000	-	-
20[b]	1	0.0002	0.002	0.016	0.010	0.008	0.0001	<0.0001	<0.0001
	2	0.0002	0.002	0.008	0.010	0.006	<0.0001	<0.0001	<0.0001
	3	0.0003	0.003	0.010	0.013	0.007	0.0011	<0.0001	(a)
	x	0.0002	0.003	0.011	0.011	0.007	0.0006	<0.0001	<0.0001
	σ	0.0001	0.0005	0.004	0.002	0.0008	0.0008	-	-
42.5[b]	1	0.003	0.019	0.049	0.036	0.018	<0.0001	<0.0001	<0.0001
	2	0.003	0.019	0.046	0.036	0.014	<0.0001	<0.0001	<0.0001
	3	0.003	0.021	0.049	0.033	0.016	<0.0001	<0.0001	(a)
	x	0.003	0.020	0.048	0.035	0.016	<0.0001	<0.0001	<0.0001
	σ	0.0003	0.001	0.001	0.002	0.002	-	-	-
57.5[b]	1	0.005	0.029	0.066	0.041	0.020	<0.0001	<0.0001	<0.0001
	2	0.004	0.030	0.076	0.051	0.022	<0.0001	<0.0001	<0.0001
	3	0.010	0.044	0.097	0.072	0.035	<0.0001	<0.0001	<0.0001
	x	0.006	0.034	0.080	0.055	0.026	<0.0001	<0.0001	<0.0001
	σ	0.004	0.008	0.016	0.016	0.008	-	-	-
67.5[b]	1	0.013	0.064	0.13	0.078	0.032	<0.0001	<0.0001	<0.0001
	2	0.009	0.047	0.097	0.059	0.041	<0.0001	<0.0001	<0.0001
	3	0.016	0.063	0.12	0.083	0.044	<0.0001	<0.0001	<0.0001
	x	0.013	0.058	0.12	0.074	0.039	<0.0001	<0.0001	<0.0001
	σ	0.003	0.010	0.018	0.013	0.007	-	-	-

(a) Only two tests planned
(b) Cyclic flow minute volume

Table E-3. Summary of Measured Penetrations through North 7506 Cartridge

Flow Rate (L/min)	Trial	Particle Size (µm)							
		0.02	0.05	0.1	0.2	0.3	0.7	1.3	2.9
		Penetration (%)							
42.5	1	4.9	8.5	3.2	1.9	1.0	0.0	0.00	0.0001
	2	5.9	9.0	3.3	1.8	1.0	0.2	0.03	<0.0001
	3	5.8	9.0	3.5	1.9	1.1	0.2	0.03	(a)
	x	5.5	8.8	3.4	1.9	1.0	0.2	0.02	0.0000
	σ	0.6	0.3	0.2	0.1	0.0	0.1	0.01	0.0000
135	1	16.3	18.6	9.9	8.4	5.9	2.7	0.07	0.0002
	2	14.6	17.9	9.7	8.8	5.9	2.4	0.08	<0.0001
	3	9.8	14.7	9.1	5.9	3.8	2.8	0.09	(a)
	x	13.6	17.1	9.6	7.7	5.2	2.6	0.08	0.0001
	σ	3.4	2.0	0.4	1.5	1.2	0.2	0.01	0.0001
180	1	17.6	21.5	14.2	13.8	9.9	3.7	0.07	0.0002
	2	20.5	21.6	14.9	14.2	9.8	1.8	0.06	0.0004
	3	16.8	19.5	11.9	14.2	9.8	2.9	0.05	(a)
	x	18.3	20.8	13.7	14.1	9.9	2.8	0.06	0.0003
	σ	1.9	1.2	1.6	0.2	0.0	1.3	0.01	0.0002
20[b]	1	6.8	6.1	2.9	2.2	1.5	0.4	0.04	<0.0001
	2	6.6	6.4	2.7	2.2	1.9	0.7	0.07	<0.0001
	3	7.4	8.6	2.9	2.2	1.2	0.6	0.06	(a)
	x	6.9	7.0	2.9	2.2	1.5	0.5	0.06	<0.0001
	σ	0.5	1.3	0.1	0.0	0.4	0.1	0.02	-
42.5[b]	1	11.3	13.0	6.0	5.4	3.7	2.0	0.09	<0.0001
	2	12.4	14.3	7.9	7.0	5.0	1.7	0.08	<0.0001
	3	8.1	9.2	4.3	3.0	1.7	0.5	0.01	(a)
	x	10.6	12.2	6.1	5.1	3.5	1.4	0.06	<0.0001
	σ	2.2	2.6	1.8	2.0	1.6	0.8	0.05	-
57.5[b]	1	15.5	18.3	9.4	8.2	5.8	3.5	0.13	<0.0001
	2	15.3	17.0	9.5	8.7	7.4	2.6	0.09	0.0004
	3	14.1	16.5	9.4	8.4	7.1	2.7	0.09	(a)
	x	15.0	17.3	9.4	8.5	6.8	2.9	0.10	0.0003
	σ	0.7	0.9	0.1	0.3	0.8	0.5	0.03	-
67.5[h]	1	18.4	21.7	12.3	11.0	7.9	0.9	0.01	0.0028
	2	19.2	15.9	10.2	11.0	6.4	2.6	0.07	0.0005
	3	18.8	18.8	10.9	11.0	8.3	2.6	0.07	(a)
	x	18.8	18.8	11.2	11.0	7.5	2.0	0.05	0.0016
	σ	0.4	2.9	1.1	0.0	1.0	1.0	0.03	0.0016

(a) Only two tests planned
(b) Cyclic flow minute volume

E-4

Table E-4. Summary of Measured Penetrations through MSA Flexi-Filter

Flow Rate (L/min)	Trial	Particle Size (µm)							
		0.02	0.05	0.1	0.2	0.3	0.7	1.3	2.9
		Penetration (%)							
42.5	1	0.2	0.4	0.1	0.0	0.0	0.00	0.00	<0.0001
	2	0.2	0.8	0.3	0.1	0.0	0.01	0.00	<0.0001
	3	0.2	0.8	0.4	0.1	0.1	0.00	0.00	(a)
	x	0.2	0.7	0.3	0.1	0.0	0.00	0.00	<0.0001
	σ	0.0	0.2	0.1	0.1	0.0	0.00	0.00	-
135	1	2.2	5.3	2.7	1.8	1.0	0.25	0.03	<0.0001
	2	2.1	3.1	1.7	1.0	0.5	0.29	0.02	<0.0001
	3	2.0	5.2	2.8	1.9	1.2	0.40	0.02	(a)
	x	2.1	4.6	2.4	1.6	0.9	0.31	0.02	<0.0001
	σ	0.1	1.2	0.6	0.5	0.4	0.08	0.00	-
180	1	2.6	2.8	2.1	1.7	1.1	0.65	0.04	<0.0001
	2	3.7	5.7	4.2	3.4	2.9	0.90	0.03	<0.0001
	3	4.6	9.4	6.9	5.2	3.3	0.53	0.03	(a)
	x	3.7	6.0	4.4	3.4	2.4	0.69	0.03	<0.0001
	σ	2.6	2.8	2.1	1.7	1.1	0.26	0.00	-
20[c]	1	0.5	0.9	0.5	0.3	0.2	0.01	0.00	<0.0001
	2	0.8	1.2	0.6	0.6	0.6	0.02	0.00	<0.0001
	3	0.7	1.0	0.6	0.6	0.8	0.01	0.00	(a)
	x	0.7	1.0	0.6	0.5	0.6	0.01	0.00	<0.0001
	σ	0.1	0.2	0.1	0.2	0.3	0.01	0.00	-
42.5[c]	1	2.0	2.0	1.1	0.8	0.7	0.14	0.01	<0.0001
	2	3.3	3.8	2.0	1.4	1.3	0.09	0.01	<0.0001
	3	2.9	4.2	2.5	2.4	2.9	0.15	0.01	(a)
	x	2.7	3.3	1.9	1.5	1.6	0.13	0.01	<0.0001
	σ	0.7	1.2	0.7	0.8	1.2	0.03	0.00	-
57.5[c]	1	5.5	7.9	5.8	5.1	4.5	0.27	0.02	<0.0001
	2	2.0	4.2	2.1	1.4	0.8	0.26	0.02	<0.0001
	3	7.8	10.5	8.2	8.0	7.4	0.22	0.02	(a)
	4	3.6	7.2	3.9	2.7	1.9	(b)	(b)	(b)
	x	4.7	7.5	5.0	4.3	3.6	0.25	0.02	<0.0001
	σ	2.5	2.6	2.6	2.9	3.0	0.03	0.00	-
67.5[c]	1	4.3	8.0	4.8	3.8	3.1	0.52	0.05	<0.0001
	2	4.6	7.0	4.8	5.0	5.9	0.29	0.02	<0.0001
	3	4.4	9.2	6.4	5.0	3.8	0.48	0.03	(a)
	x	4.4	8.1	5.3	4.6	4.3	0.43	0.03	<0.0001
	σ	3.2	2.4	2.7	2.9	2.9	0.12	0.01	-

(a) Only two tests planned
(b) Test not planned
(c) Cyclic flow minute volume

Table E-5. Summary of Measured Penetrations through 3M 8293

Flow Rate (L/min)	Trial	Particle Size (µm)							
		0.02	0.05	0.1	0.2	0.3	0.7	1.3	2.9
		Penetration (%)							
85	1	0.006	0.009	0.004	0.004	0.004	<0.0001	<0.0001	<0.0001
	2	0.007	0.008	0.002	0.001	0.0008	0.0011	0.0004	<0.0001
	3	0.011	0.014	0.005	0.005	0.006	<0.0001	<0.0001	<0.0001
	x	0.008	0.010	0.004	0.003	0.004	0.0004	0.0002	<0.0001
	σ	0.003	0.003	0.002	0.002	0.002	-	-	-
270	1	0.17	0.20	0.041	0.019	0.045	0.002	0.0001	0.0002
	2	0.23	0.21	0.039	0.012	0.035	0.004	0.001	<0.0001
	3	0.26	0.26	0.049	0.012	0.033	0.001	0.0002	<0.0001
	x	0.22	0.22	0.043	0.014	0.038	0.002	0.0005	0.0001
	σ	0.047	0.035	0.005	0.004	0.007	0.001	0.0005	-
360	1	0.61	0.52	0.17	0.12	0.30	0.002	0.0001	0.0001
	2	0.43	0.33	0.11	0.19	0.37	0.002	0.0002	0.0001
	3	0.58	0.31	0.17	0.11	0.27	0.002	<0.0001	0.0001
	x	0.54	0.39	0.15	0.14	0.31	0.002	0.0001	0.0001
	σ	0.098	0.12	0.035	0.04	0.055	0.0002	0.0001	0.0000
40[b]	1	0.014	0.030	0.004	0.0003	0.0003	0.002	0.001	0.0006
	2	0.010	0.025	0.003	0.0004	0.0004	0.0004	0.0003	0.0003
	3	0.021	0.028	0.006	0.003	0.003	0.001	0.0008	0.0001
	x	0.015	0.028	0.005	0.001	0.001	0.001	0.0008	0.0003
	σ	0.005	0.003	0.001	0.002	0.002	0.0006	0.0005	0.0003
85[b]	1	0.21	0.30	0.051	0.006	0.007	0.0001	<0.0001	<0.0001
	2	(a)	(a)	(a)	(a)	(a)	0.0008	0.0005	0.0001
	3	(a)	(a)	(a)	(a)	(a)	0.0006	0.0003	0.0001
	x	0.21	0.30	0.051	0.006	0.007	0.0008	0.0005	0.0001
	σ	-	-	-	-	-	0.0003	0.0001	0.0000
115[b]	1	0.45	0.43	0.086	0.012	0.018	0.0003	<0.0001	<0.0001
	2	0.41	0.44	0.081	0.013	0.021	0.0002	<0.0001	<0.0001
	3	0.42	0.52	0.094	0.017	0.021	0.0005	0.0002	0.0001
	x	0.42	0.47	0.087	0.014	0.020	0.0003	0.0002	0.0001
	σ	0.022	0.045	0.007	0.003	0.002	0.0002	-	-
135[b]	1	(a)	(a)	(a)	(a)	(a)	0.004	0.001	0.0003
	2	(a)	(a)	(a)	(a)	(a)	0.001	0.0004	<0.0001
	3	(a)	(a)	(a)	(a)	(a)	0.003	0.001	0.0001
	x	-	-	-	-	-	0.002	0.0009	0.0002
	σ	-	-	-	-	-	0.001	0.0005	0.0001

(a) Test not planned
(b) Cyclic flow minute volume

Table E-6. Summary of Measured Penetrations through Moldex 2360

Flow Rate (L/min)	Trial	Particle Size (µm)							
		0.02	0.05	0.1	0.2	0.3	0.7	1.3	2.9
		Penetration (%)							
85	1	0.014	0.061	0.035	0.004	0.002	0.0002	<0.0001	<0.0001
	2	0.007	0.026	0.010	0.0006	0.0002	0.0001	<0.0001	<0.0001
	3	0.012	0.058	0.022	0.006	0.002	<0.0001	<0.0001	<0.0001
	x	0.011	0.048	0.022	0.003	0.001	0.0002	<0.0001	<0.0001
	σ	0.004	0.019	0.012	0.003	0.001	0.0001	-	-
270	1	1.5	1.3	0.67	0.52	0.72	0.037	0.0003	0.0002
	2	0.36	0.61	0.33	0.42	0.58	0.063	0.0001	0.0005
	3	0.36	0.91	0.54	0.37	0.20	0.025	0.0017	0.0001
	4	(a)	(a)	(a)	(a)	(a)	0.022	(a)	0.0001
	x	0.75	0.94	0.51	0.43	0.50	0.037	0.0007	0.0002
	σ	0.67	0.35	0.17	0.075	0.27	0.016	0.0009	0.0002
360	1	0.33	0.64	1.1	0.17	0.29	0.056	0.019	0.001
	2	0.38	0.70	0.34	0.15	0.24	0.047	0.0001	0.004
	3	1.9	2.2	1.6	1.4	1.6	0.04	0.0002	0.0006
	4	(a)	(a)	(a)	(a)	(a)	(a)	(a)	0.0004
	x	0.86	1.2	1.0	0.57	0.71	0.0490	0.0064	0.0014
	σ	1.1	1.0	0.89	0.89	0.96	0.0023	0.0001	0.0015
40[b]	1	0.009	0.081	0.032	0.004	0.059	0.0008	0.0005	0.0001
	2	0.026	0.11	0.053	0.018	0.014	0.0005	0.0003	<0.0001
	3	0.014	0.10	0.047	0.015	0.004	0.0002	<0.0001	<0.0001
	4	(a)	(a)	(a)	(a)	(a)	(a)	(a)	0.0002
	x	0.016	0.096	0.044	0.013	0.026	0.0005	0.0004	0.0001
	σ	0.009	0.013	0.011	0.007	0.029	0.0003	0.0001	0.0000
85[b]	1	0.18	0.70	0.30	0.047	0.016	0.009	0.0009	<0.0001
	2	0.16	0.69	0.32	0.055	0.020	0.003	<0.0001	<0.0001
	3	0.14	0.79	0.37	0.059	0.029	0.003	0.0001	<0.0001
	x	0.16	0.73	0.33	0.054	0.022	0.005	0.0005	<0.0001
	σ	0.023	0.057	0.037	0.006	0.007	0.003	0.0006	-
115[b]	1	(a)	(a)	(a)	(a)	(a)	0.020	0.006	0.001
	2	(a)	(a)	(a)	(a)	(a)	0.028	0.005	0.0001
	3	(a)	(a)	(a)	(a)	(a)	0.013	0.0003	<0.0001
	4	(a)	(a)	(a)	(a)	(a)	0.031	(a)	(a)
	x	-	-	-	-	-	0.023	0.004	0.0007
	σ	-	-	-	-	-	0.008	0.003	0.0008
135[b]	1	(a)	(a)	(a)	(a)	(a)	0.016	0.001	0.0007
	2	(a)	(a)	(a)	(a)	(a)	0.026	<0.0001	0.0001
	3	(a)	(a)	(a)	(a)	(a)	0.014	<0.0001	<0.0001
	x	-	-	-	-	-	0.019	0.001	0.0004
	σ	-	-	-	-	-	0.007	-	0.0005

(a) Test not planned
(b) Cyclic flow minute volume

Table E-7. Summary of Measured Penetrations through MSA Affinity Plus

Flow Rate (L/min)	Trial	Particle Size (µm)							
		0.02	0.05	0.1	0.2	0.3	0.7	1.3	2.9
		Penetration (%)							
85	1	1.0	2.7	1.9	1.3	0.9	0.86	0.20	0.0006
	2	1.3	3.3	2.4	1.8	1.4	1.1	0.21	<0.0001
	3	0.6	2.4	1.6	1.2	1.0	0.81	0.19	(a)
	x	1.0	2.8	2.0	1.4	1.1	0.92	0.20	0.0004
	σ	0.4	0.5	0.4	0.3	0.3	0.16	0.01	-
270	1	1.8	5.1	3.8	3.4	2.5	5.9	0.18	0.0026
	2	5.4	9.1	8.3	7.8	6.0	2.0	0.04	0.0017
	3	2.2	5.5	4.2	3.5	2.5	3.7	0.17	(a)
	4	4.2	9.7	8.5	7.7	5.5	(b)	(b)	(b)
	5	4.8	8.8	7.2	5.7	4.0	(b)	(b)	(b)
	x	3.7	7.6	6.4	5.6	4.1	3.8	0.13	0.0022
	σ	1.6	2.2	2.2	2.2	1.6	2.0	0.08	0.0006
360	1	4.8	7.9	7.6	7.1	5.6	3.82	0.13	0.0013
	2	3.4	6.1	6.4	6.2	5.0	3.39	0.08	0.0007
	3	3.1	6.8	6.8	6.4	5.2	5.86	0.15	(a)
	4	6.0	10.7	10.1	9.1	7.1	(b)	(b)	(b)
	5	5.9	10.4	10.4	9.2	7.4	(b)	(b)	(b)
	6	5.1	9.6	8.7	8.0	6.3	(b)	(b)	(b)
	x	4.7	8.6	8.3	7.7	6.1	4.36	0.12	0.0010
	σ	1.2	1.9	1.7	1.3	1.0	1.32	0.04	0.0004
40[c]	1	1.3	3.1	2.0	1.6	1.1	1.04	0.16	0.0004
	2	1.3	2.8	1.9	1.7	1.0	1.42	0.23	0.0004
	3	1.7	3.4	2.6	2.3	1.8	2.07	0.28	(a)
	x	1.4	3.1	2.2	1.8	1.3	1.51	0.22	0.0004
	σ	0.2	0.3	0.4	0.4	0.5	0.52	0.06	0.0000
85[c]	1	3.3	7.8	5.1	4.2	3.0	1.02	0.13	0.0001
	2	4.6	7.6	6.1	5.4	3.7	2.14	0.16	0.0014
	3	4.7	10.7	9.1	8.2	5.9	2.47	0.19	(a)
	x	4.2	8.7	6.7	5.9	4.2	1.87	0.16	0.0008
	σ	0.8	1.7	2.1	2.0	1.5	0.76	0.03	0.0009
115[c]	1	7.2	14.1	13.1	12.5	8.6	1.45	0.02	0.0002
	2	8.5	13.3	12.5	11.2	8.5	3.67	0.15	<0.0001
	3	6.5	12.8	11.9	10.3	7.2	4.32	0.24	(a)
	x	7.4	13.4	12.5	11.3	8.1	3.14	0.14	0.0002
	σ	1.0	0.7	0.6	1.1	0.7	1.51	0.11	-
135[c]	1	(b)	(b)	(b)	(b)	(b)	3.28	0.09	0.0006
	2	(b)	(b)	(b)	(b)	(b)	2.64	0.07	0.0004
	3	(b)	(b)	(b)	(b)	(b)	2.52	0.05	(a)
	x	-	-	-	-	-	2.81	0.07	0.0005
	σ	-	-	-	-	-	0.41	0.02	0.0001

(a) Only two tests planned
(b) Test not planned
(c) Cyclic flow minute volume

Table E-8. Summary of Measured Penetrations through Gerson 1730

Flow Rate (L/min)	Trial	Particle Size (μm)							
		0.02	0.05	0.1	0.2	0.3	0.7	1.3	2.9
		Penetration (%)							
85	1	2.2	4.2	3.0	2.5	1.7	0.47	0.12	0.0059
	2	2.0	4.1	2.7	2.0	1.4	0.39	0.07	0.0036
	3	2.3	4.4	3.0	2.1	1.4	0.38	0.07	(a)
	x	2.1	4.2	2.9	2.2	1.5	0.41	0.09	0.0048
	σ	0.2	0.2	0.2	0.2	0.2	0.05	0.03	0.0016
270	1	7.2	10.9	10.1	9.1	7.8	2.78	0.09	0.0003
	2	4.4	8.4	8.4	7.2	4.8	2.77	0.27	0.0050
	3	5.4	9.9	8.7	7.1	5.3	3.27	0.18	(a)
	x	5.6	9.7	9.1	7.8	6.0	2.94	0.18	0.0027
	σ	1.4	1.3	0.9	1.1	1.6	0.29	0.09	0.0033
360	1	6.8	8.9	9.0	7.9	6.0	3.46	0.11	0.0014
	2	6.0	8.9	9.1	7.7	6.6	3.37	0.10	0.0010
	3	4.9	7.5	7.7	6.5	5.2	3.29	0.09	(a)
	x	5.9	8.4	8.6	7.4	5.9	3.37	0.10	0.0012
	σ	1.0	0.8	0.8	0.8	0.7	0.08	0.01	0.0003
40[c]	1	4.4	8.7	6.3	5.9	5.1	0.58	0.11	0.0013
	2	3.4	7.2	4.8	4.0	3.1	0.57	0.11	0.0016
	3	4.0	7.7	5.5	5.6	5.1	0.58	0.14	(a)
	x	3.9	7.9	5.5	5.2	4.4	0.58	0.12	0.0015
	σ	0.5	0.8	0.8	1.0	1.1	0.01	0.02	0.0002
85[c]	1	7.5	13.6	11.3	9.5	6.5	1.63	0.16	0.0010
	2	9.9	15.9	14.6	11.9	8.0	2.18	0.22	0.0026
	3	7.7	13.7	11.4	10.2	7.4	1.89	0.37	(a)
	x	8.4	14.4	12.5	10.5	7.3	1.90	0.25	0.0018
	σ	1.4	1.3	1.9	1.2	0.7	0.28	0.11	0.0011
115[c]	1	12.6	18.7	16.8	14.6	10.1	1.99	0.11	0.0015
	2	9.1	15.1	14.3	12.1	8.2	1.74	0.16	0.0021
	3	11.4	15.3	15.5	13.1	8.8	2.42	0.08	(a)
	x	11.0	16.4	15.5	13.2	9.0	2.05	0.11	0.0018
	σ	1.8	2.0	1.3	1.2	1.0	0.34	0.04	0.0004
135[c]	1	(b)	(b)	(b)	(b)	(b)	2.70	0.10	<0.0001
	2	(b)	(b)	(b)	(b)	(b)	2.43	0.15	0.0021
	3	(b)	(b)	(b)	(b)	(b)	2.29	0.08	(a)
	x	-	-	-	-	-	2.47	0.11	0.0011
	σ	-	-	-	-	-	0.21	0.03	-

(a) Only two tests planned
(b) Test not planned
(c) Cyclic flow minute volume

Blank

APPENDIX F

ESTIMATION METHOD FOR CYCLIC FLOW PENETRATIONS

F.1 Introduction

The results summarized in Section 3.5 demonstrated that the mean inhalation flow is a key parameter when comparing penetrations measured under constant and cyclic flow conditions. To further understand the relationship, a method was developed to predict cyclic flow penetrations based on penetrations measured over a range of constant flow rates. The method is described in Section F.2 and compared to the experimental results that were discussed in Section 3.0.

F.2 Approach

Initially, the effect of flow rate on penetration for a specific particle size must be determined experimentally. A regression analysis of this data provides the penetration as a function of flow rate:

$$P_i(F_C) = A \times F_C^{\,B}$$

where P_i is the penetration of the specific particle size (%), F_C the constant flow rate (L/sec), and A and B the regression coefficients. An example is provided in Figure F-1 for the SEA P100 cartridge tested against a 0.2 µm particle at flow rates of 42.5, 135, and 180 L/min. For cyclic flow, the flow rate through the filter is time dependent and, thus, the penetration will also be time dependent. Assuming sinusoidal flow, the time dependent flow rate F(t) is given by:

$$F(t) = F_{Peak} \sin\left(\frac{2\pi}{\omega}t\right)$$

where F_{Peak} is the peak inhalation flow rate (L/sec), ω is the breathing flow cycle time (sec), and t is the time (sec). The flow rate over the inhalation cycle is provided in Figure F-2 for the four cyclic flow conditions used in cartridge testing. Combining the above expressions gives the penetration as a function of time over the inhalation cycle:

$$P_i(F(t)) = A \times \left[F_{Peak} \sin\left(\frac{2\pi}{\omega}t\right)\right]^{B}$$

which is shown in Figure F-3 for each of the four flow conditions.

$$P_i(F(t)) = A \times F_i(t)^B$$

$y = 0.0011x^{2.8267}$

$R^2 = 0.9989$

◆ 0.2 um
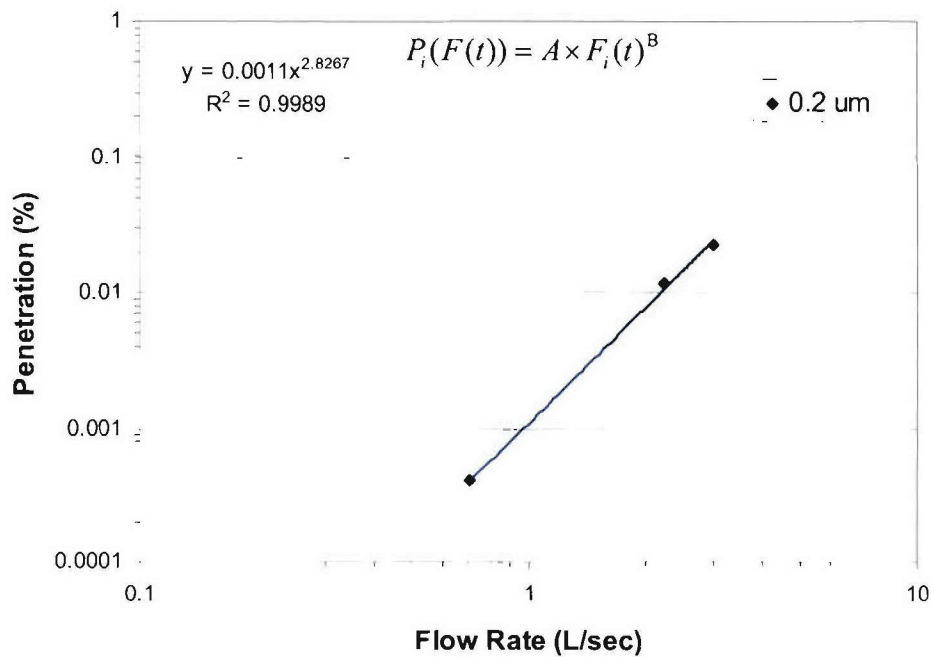
Figure F-1. Effect of Flow Rate and Particle Size on Measured Penetration Through the Survivair® P100 Cartridge

- 0.8 L, 25 breaths/min
- 1.15 L, 37 breaths/min
- 1.35 L, 42 breaths/min
- 1.55 L, 44 breaths/min
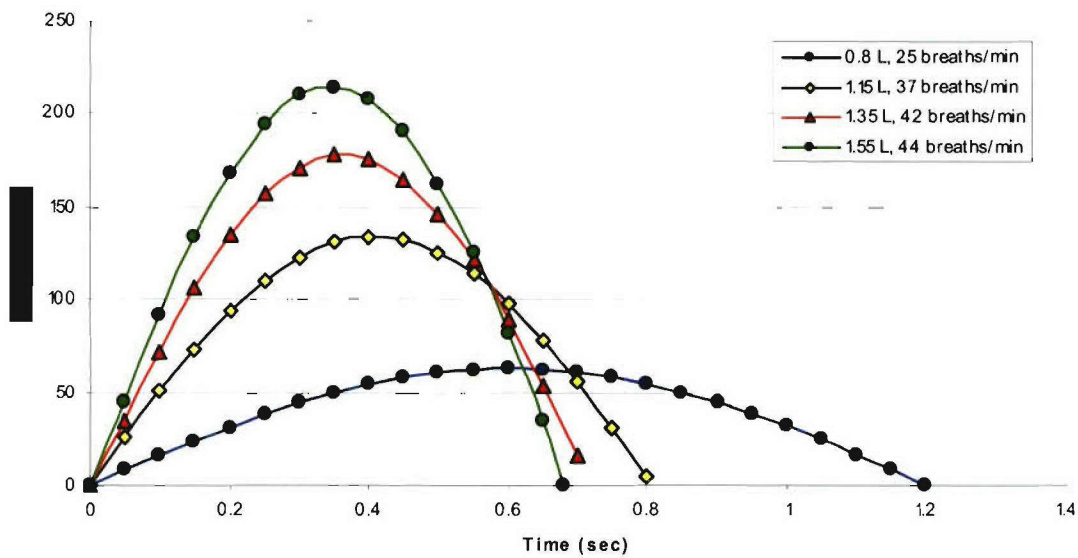
Figure F-2. Instantaneous Flow Rates During Inhalation Cycle Assuming Ideal Sinusoidal Waveform
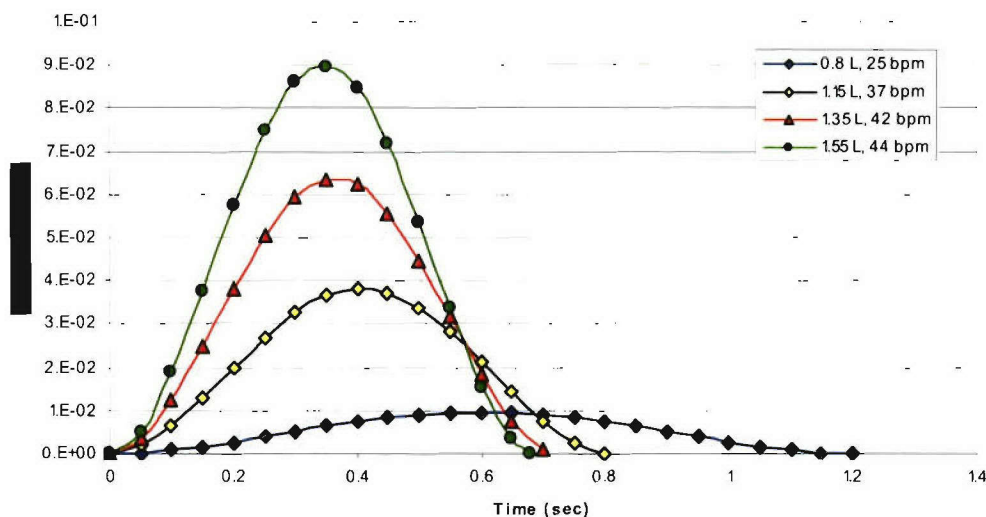
Figure F-3. Predicted Instantaneous Penetrations During Inhalation Cycle Based on Measured Constant Flow Penetrations for the SEA Cartridge

The average penetration over the inhalation cycle was then determined for each cyclic flow condition using the following expression:

$$P_{Avg} = \frac{\int_0^{\varpi/2} P_i(F(t))dt}{\int_0^{\varpi/2} dt}$$

The integral was estimated using a numerical technique. The predicted cyclic flow penetrations using this method are compared with the measured cyclic flow penetrations measured for the cartridges and filtering facepieces in Figures F-4 and F-5. The figures include a variety of particle sizes and flow conditions. The flow rates in the legend represent cyclic flow minute volumes. The dashed line is the one-to-one line, and represents agreement between the predicted and measured penetrations. The results show that the penetration measured during breathing flow conditions can be accurately estimated from the constant flow conditions, as all data points tend to lie on the one-to-one line.
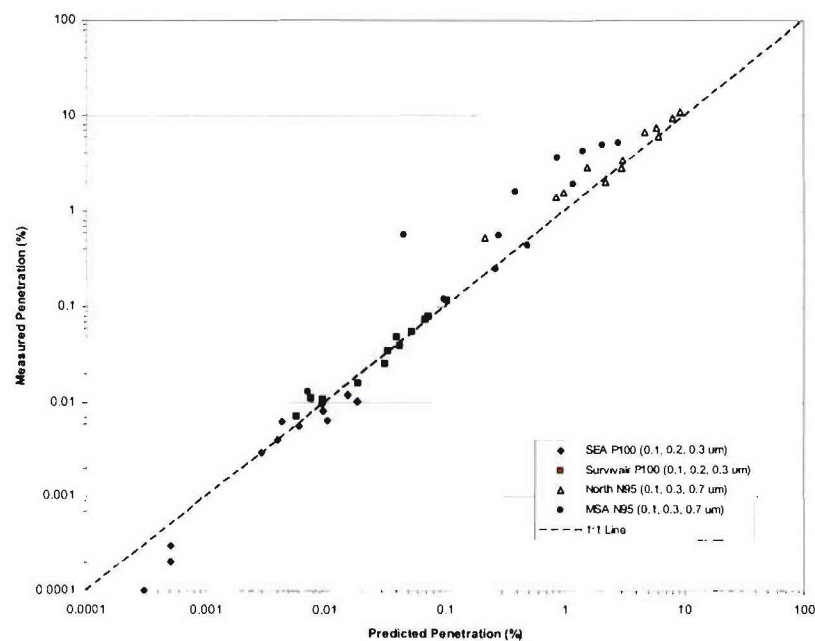
Figure F-4. Comparison of Measured and Predicted Cyclic Flow Penetrations Through Cartridges
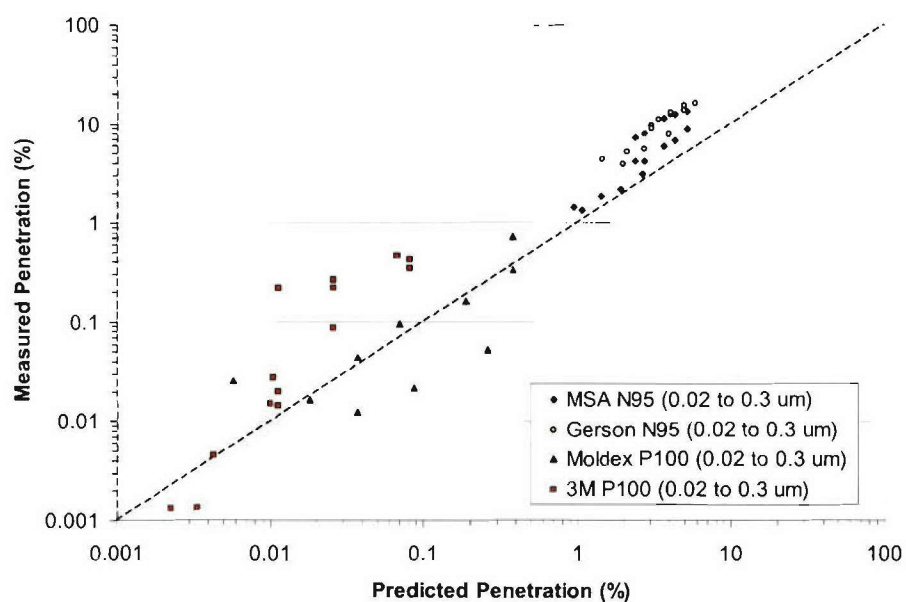
Figure F-5. Comparison of Measured and Predicted Cyclic Flow Penetrations Through Filtering Facepieces

Blank

APPENDIX G

MICROBIOLOGICAL METHODS

G.1 Bg Spores

G.1.1 Growth/Harvest of Bg

The Bg spores were purchased from the U.S. Army's Dugway Proving Ground (Dugway, UT) in powder form.

G.1.2 Quantification of Bg Spores

The concentration of Bg spores was determined by the standard plate and count method. Samples collected on mixed cellulose ester filters were removed from their respective filter holders using decontaminated forceps and placed in 50 mL conical tubes containing 10 mL pH=7.4 phosphate buffered saline (PBS). Extraction was then performed by vortexing each tube at the maximum setting for 30 seconds each. Bg samples were serially diluted in PBS per standard microbiological protocols. Samples were then plated in triplicate on Tryptic Soy Agar (TSA) using the Spiral Biotech Autoplate® 4000 (Figure G-1). The plates were incubated overnight at 30°C. Colony forming units per mL (cfu/mL) were determined by counting the resulting colonies with the Spiral Biotech QCount® colony counter Figure G-2.

Figure G-1. Spiral Biotech Autoplate 4000®
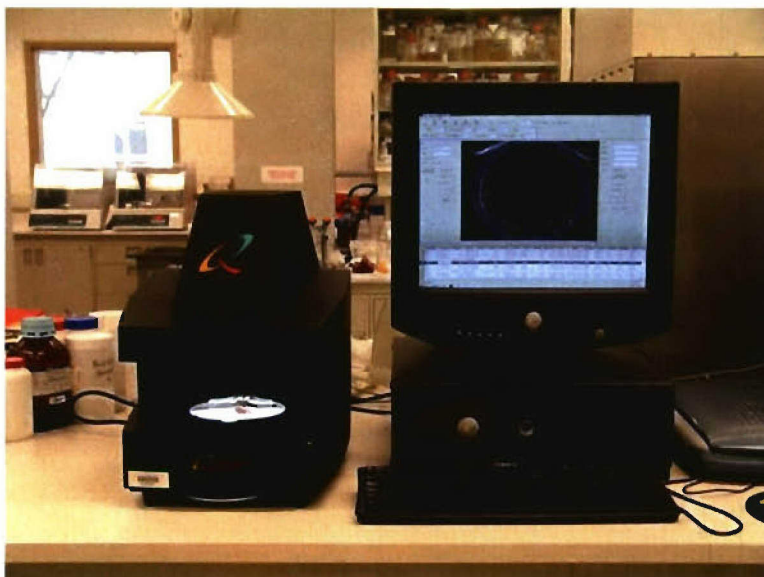
Figure G-2. Spiral Biotech QCount® Colony Counter

G.2 MS2 Phage

G.2.1 Growth of *E. coli*

E. coli serves as the host for MS2 replication and was needed for the MS2 quantification assay. Before culturing, the E. coli (American Type Culture Collection [ATCC] No. 15597, Rockville, MD) stock was tested for purity by streaking on a tryptic soy agar (TSA) plate, incubating at 37°C for 12 hours, and examining the plate for contaminating colonies. After verifying the stock was pure, a working solution of E. coli was prepared by inoculating nutrient broth (NB) media and incubating in a shaking incubator at 37°C and 150 revolutions per minute (rpm).

G.2.2 Growth/Harvest of MS2

MS2 was prepared according to the U.S. Army Dugway Proving Ground Draft SOP: MS2 Growth and Purification (March, 1996). Two 50 mL overnight cultures of *Escherichia coli* A/λ in LB-Miller broth were prepared by inoculating each 50 mL aliquot of LB-Miller in 250 mL flasks with one colony each of E. coli A/λ. The cultures were incubated approximately

12 hours at 37 °C with shaking at 200 rpm. After the incubation period was complete, each 50 mL culture was used to inoculate 500 mL of LB-Miller broth in 2800 mL fernbach flasks. The cultures were incubated at 37°C until a cellular density of 10^8 to 10^9 cells was achieved indicated by an optical density at 600 nm of 0.2 to 0.3. Once this density was achieved, each culture was inoculated with 3 mL of a 5.0E+11 pfu/mL MS2 suspension to achieve a multiplicity of infection of approximately 0.5. The cultures were incubated at 37°C with shaking at 200 rpm until lysis occurred, which was indicated by a drop in optical density. To aid in release of phage from the cells, 500 µL of 0.05 g lysozyme/mL was added to each culture and incubated at 37°C with shaking at 200 rpm for 30 minutes. After the incubation, 1.0 mL of 0.5 M EDTA and 1.0 mL of chloroform were added to each culture and incubated at 37°C with shaking at 200 rpm for 30 minutes. The suspensions were then centrifuged at 8000 rpm at 4°C for 30 minutes in 250 mL centrifuge bottles to remove cell debris. The supernatant was filtered through a 0.22 µm cellulose acetate filter. This crude preparation was stored at 2 - 8°C.

The MS2 phage stock solution was from the ATCC (No. 15597-B1). MS2 was grown by adding 0.1 mL of the MS2 stock and 0.2 mL of the E. coli working solution to 3 mL of molten top agar and then pouring the mixture onto a TSA plate. Plates were incubated for 24 hours at a temperature of 37°C to allow virus growth. After incubation, 3 mL of filtered, de-ionized water was added to plates which had 10^3 to 10^4 plaques and the surface of the plate agitated for five minutes to facilitate transfer of MS2 from the agar to the water. The liquid was removed from the plates, centrifuged at 8000 rpm for 15 minutes and filtered through a 0.2 µm filter to remove any cellular debris. MS2 remained in suspension throughout centrifugation and filtration. This clarified virus suspension became the working solution for bioaerosol generation and its infectivity was determined as described in section G.2.4. Previous experience has shown that this working solution will have > 10^9 infectious virus particles per mL of solution.

A precipitation procedure was used to further purify the crude MS2 preparations. The crude MS2 suspensions were added to a sterile 2000 mL flask containing a sterile stir bar. Sodium chloride was added to a final concentration of 0.5 M (29.2 g/L). Polyethylene glycol 8000 was added to a final concentration of 10% (100 g /L). The suspension was stirred at the lowest setting for 12 hours while incubating at 4°C. The precipitation suspension was then centrifuged in 250 mL centrifuge bottles at 10,000 rpm for 30 minutes at 4°C. The resulting

supernatant was discarded and the pellets were resuspended in one liter of 0.22 μm-filtered distilled water. This purified suspension was the stored at 2 – 8°C.

G.2.3 Dry MS2 Preparation

Dry MS2 was prepared by adding 500 mL of the purified MS2 suspension to 500 mL of 20% skim milk solids. The resulting suspension was mixed thoroughly and divided equally among three 500 mL bottles. The MS2 suspensions were then frozen at -70°C for three hours. The surface area of the MS2 was maximized by incubating the bottles at a slant during freezing. The frozen MS2 suspensions were then placed uncapped in freeze flasks and connected to a Labconco Lyph-Lok 6 freeze dry system. The samples were dried for 6 days. After the samples were completely dry, they were removed from the lyophilizer and large pieces were broken up with a spatula. Particle size was further reduced by light grinding with a mortar and pestle. The dry MS2 was then placed in a US Stoneware milling jar with 16 pieces of 0.5 inch milling media. The milling jar was placed on an automated roller and the MS2 was milled for three hours. The dry MS2 was removed from the milling jar and stored in a sterile Nalgene bottle. Final particle size reduction was achieved using a jet mill (Model 00 Jet-O-Mizer, Fluid Energy Processing and Equipment Company, Telford, PA) operated at 120 psig. The crude MS2 was fed to the jet mill using an electromagnetic vibrating feeder (Model F-TO-C, FMC Technologies, Homer City, PA). The feed material to the jet mill is entrained by the stream of circulation fluid within the jet mill. The violent jet action breaks up individual particles through particle to particle impaction. The jet mill is shown in Figures G-3 and G-4. After milling, the dry MS2 was mixed with 10 percent Aerosil by weight.
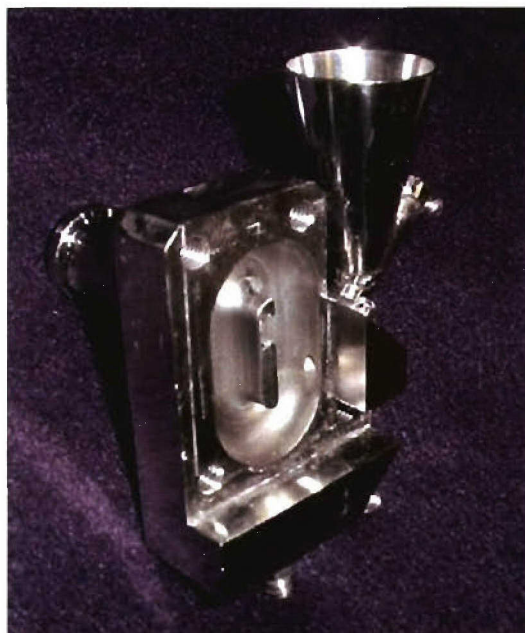
Figure G-3. Jet Mill Used for Processing Dry MS2

Figure G-4. Jet Mill and Vibrating Feeder Used for Processing Dry MS2

G.2.4 Enumeration of MS2

The number of infective virus particles was determined by plaque assay. Plaque assays are done by infecting a monolayer of host cells. When light is passed through a Petri dish containing a monolayer of cells the dish appears cloudy. As the virus grows and lyses the host, the area where cells are dying becomes clear. This is called a plaque. Ideally, the virus sample

is diluted so that each plaque is made by a single virus particle and the concentration of infectious virus in a sample is given as the number of pfu per mL of solution.

Sampled gelatin filters were removed from their respective filter holders using decontaminated forceps and placed in 50 mL conical tubes containing 10 mL pH=7.4 phosphate buffered saline (PBS). The filters were then solubilized by incubating at 37°C with shaking at 200 rpm for 15 minutes. MS2 samples were then serially diluted in PBS per standard microbiological protocols and plated following the method described by U.S. Army Dugway Proving Ground Draft SOP: MS2 Growth and Purification (March, 1996). Using this method, a 0.1 mL aliquot of diluted MS2 suspension was transferred to an empty Petri dish, along with a 0.2 mL aliquot of *Escherichia coli* A/λ host cells in the logarithmic phase of growth. Approximately 20 mL of TSA with a decreased percentage of agar (0.75%) was then poured into each dish and the contents were thoroughly mixed. Each sample was plated in triplicate and the plates were incubated overnight at 37°C. Plaques, areas of clearing caused by lysis of the *E.coli* host cell lawn, were counted and used to calculate the plaque forming units per mL (pfu/mL).

Blank

APPENDIX H

SHAKEDOWN TESTING OF THE BIOAEROSOL TEST SYSTEM

H.1 Bioaerosol Test System Shakedown

Prior to efficiency testing, shakedown testing was performed to establish proper operating conditions. This included inert testing to compare with the ECBC test system, characterization of the challenge aerosol, flow calibrations, and characterization of the viable particle samplers. The system shakedown results are provided in this Appendix.

H.2 Comparison with ECBC Test System

An objective of this task is to compare efficiencies measured using the inert and biological aerosols. Since the inert testing was performed at ECBC and the biological testing at Battelle, shakedown tests were performed with inert aerosols to compare the two test systems. Inert testing was completed at Battelle with the North N95 cartridge filter and challenge aerosols of 0.3 and 1.0 μm PSL. The upstream and downstream concentrations were measured using the LAS-X. The results are provided in Table H-1 and graphically compared in Figure H-1. In general, the measured penetrations at both facilities were similar with the exception of the 1.3 μm results at a constant flow of 180 L/min. The penetration measured at Battelle under these conditions was approximately an order of magnitude higher than that measured at ECBC. The trends in measured penetration are similar for both facilities.

Table G-1. Comparison of Inert Filtration Efficiencies Measured at Battelle and ECBC

Filter	Particle Size (μm)	Flow Condition	Flow Rate (L/min)	Average Penetration (%)	ECBC Penetration (%)
North N95	0.3	Constant	42.5	1.6 ± 0.04	1.0 ± 0.02
North N95	0.3	Constant	180	13 ± 2.8	10 ± 0.02
North N95	1.3[a]	Constant	42.5	0.03 ± 0.04	0.03 ± 0.01
North N95	1.3[a]	Constant	180	0.3 ± 0.06	0.06 ± 0.01
North N95	0.3	Cyclic	42.5[b]	3.9 ± 2.7	3.5 ± 1.7
North N95	0.3	Cyclic	68[c]	4.3 ± 6.2	7.5 ± 1.0
North N95	1.3[a]	Cyclic	42.5	0.08 ± 0.02	0.06 ± 0.05
North N95	1.3[a]	Cyclic	68	0.05	0.05 ± 0.03

(a) 1.0 um PSL used in Battelle testing
(b) 1.15 L tidal volume, 37 breaths/min
(c) 1.55 L tidal volume, 44 breaths/min
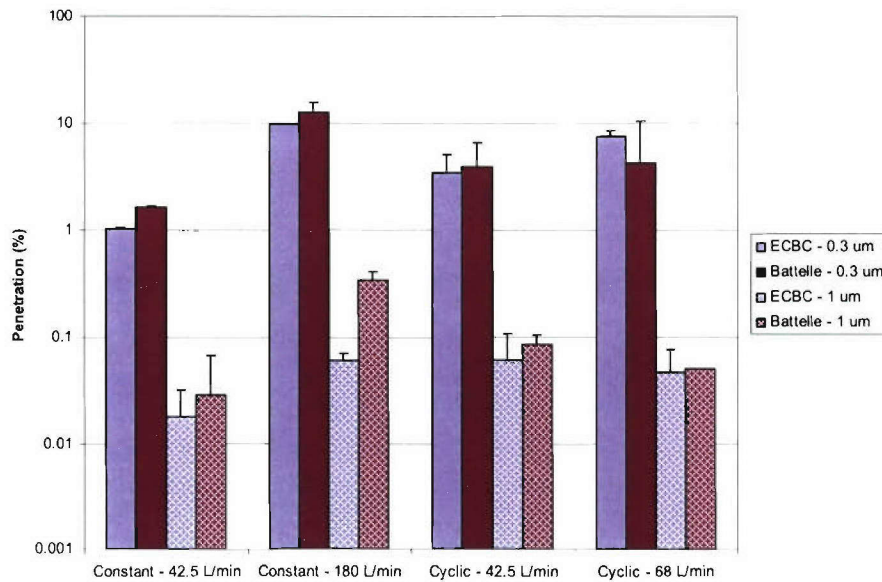
Figure H-1. Comparison of Inert Filtration Efficiencies Measured at Battelle and ECBC

H.3 Challenge Aerosol Characterization

Shakedown testing was completed to measure the size distribution of the Bg spores and to verify the generator maintained a stable output. The aerosol concentration as a function of test duration as measured by the Aerosizer is shown in Figure H-2. The bioaerosol particle size distributions were measured using either a laser aerosol spectrometer, Aerosizer, or cascade impactor as was described in the report. Attempts to measure the particle size distributions of the bioaerosols using the Andersen impactor were unsuccessful due to the high challenge concentration which resulted in overloading of the stages.
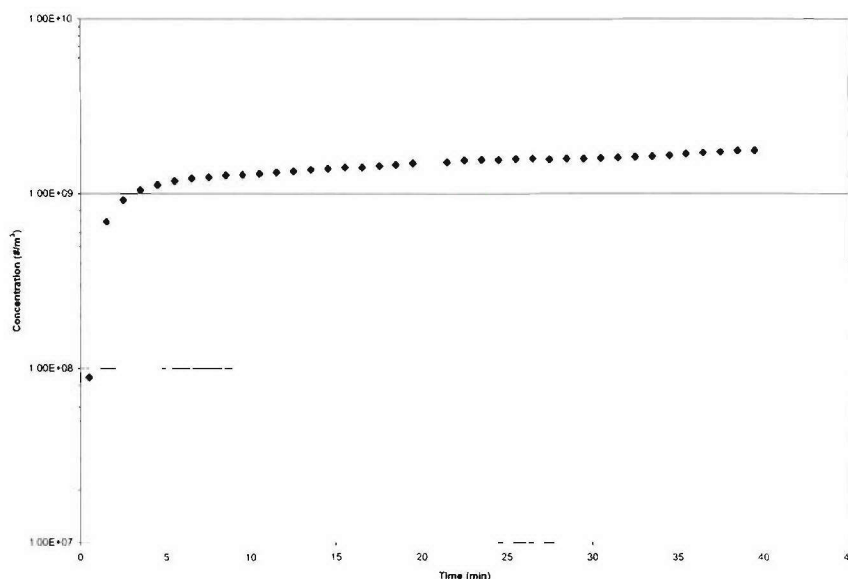
Figure H-2. Concentration of Bg Spore Aerosol Challenge as a Function of Test Time

H.4 Bioaerosol Sampling

Tests were completed to characterize the collection efficiencies of the cellulose ester filters. The collection efficiencies were measured by collecting samples with two filters operated in series and performing a bioassay on each. The initial filter typically collected over 99.99 percent of the total spores collected.

Tests were also completed without a respirator filter to compare samples collected up- and downstream. Tests were performed at constant flow rates of 42.5 and 180 L/min and resulted in measured penetrations of 97.3 and 93.3 percent, respectively. Similar tests at cyclic flows with minute volumes of 40 and 135 L/min resulted in penetrations of 93 and 103 percent. Thus, the upstream and downstream measurements were within 10 percent for all tests.

Following a test with a Bg spore challenge, the test system was flushed with HEPA filtered air and a negative control test was performed. Samples were collected from the downstream chamber and bioassayed. No viable particles were detected. This demonstrated the procedure for sterilization of the system and 47-mm filter holders was successful and there was no carryover between tests. The minimum detection limit of the bioassay technique was set at 20 cfu or pfu/L air sampled. A typical challenge concentration was 1×10^5 cfu/L air sampled. Thus, the minimum measurable penetration was typically 0.005 percent. This was nearly an order-of-magnitude lower than the P100 penetration requirement (<0.03 percent).

APPENDIX I

SUMMARY OF BIOAEROSOL PENETRATION RESULTS

Table I-1. Summary of Measured Penetrations through SEA HE-T

| Flow Rate (L/min) | Trial | Bioaerosol Challenge | | | |
| | | Bg "Wet" | Bg "Dry" | MS2 "Wet" | MS2 "Dry" |
		Penetration (%)			
42.5 Constant	1	<0.005	<0.001	<0.002	<0.001
	2	<0.003	<0.001	<0.004	<0.001
	3	<0004	<0.001	<0.001	-
	x	0.004	0.001	0.002	0.001
	σ	0.001	-	0.002	-
135 Constant	1	<0.004	<0.002	<0.013	<0.001
	2	<0.004	<0.003	<0.008	<0.002
	3	<0.004	<0.003	<0.005	-
	x	0.004	0.003	0.009	0.002
	σ	-	0.001	0.004	0.001
42.5 Cyclic[a]	1	<0.001	<0.005	<0.001	<0.001
	2	<0.001	<0.002	<0.013	<0.001
	3	<0.003	<0.001	<0.006	-
	x	0.002	0.003	0.007	0.001
	σ	0.001	0.002	0.006	-
67.5 Cyclic[a]	1	<0.001	<0.001	0.015	<0.002
	2	<0.002	<0.002	<0.010	<0.005
	3	<0.003	<0.002	<0.020	-
	x	0.002	0.002	0.015	0.004
	σ	0.001	0.001	0.005	0.002

(a) Cyclic flow minute volume

Table I-2. Summary of Measured Penetrations through Survivair 1050

| Flow Rate (L/min) | Trial | Bioaerosol Challenge | | | |
| | | Bg "Wet" | Bg "Dry" | MS2 "Wet" | MS2 "Dry" |
		Penetration (%)			
42.5 Constant	1	<0.004	0.008	0.059	<0.030 [b]
	2	<0.003	<0.001	0.005	<0.002
	3	<0.002	<0.001	0.002	-
	x	0.003	0.003	0.022	0.002
	σ	0.001	0.004	0.032	-
135 Constant	1	<0.005	0.086	<0.008	<0.001
	2	<0.004	<0.002	0.035	<0.002
	3	<0.004	<0.002	<0.012	-
	x	0.004	0.030	0.018	0.002
	σ	0.001	0.048	0.016	0.001
42.5 Cyclic[a]	1	0.001	<0.002	0.017	<0.008
	2	0.002	<0.003	<0.007	<0.001
	3	0.001	<0.001	<0.012	-
	x	0.001	0.002	0.012	0.005
	σ	0.001	0.001	0.005	0.005
67.5 Cyclic[a]	1	<0.001	<0.003	<0.047	<0.015
	2	0.006	<0.003	0.013	<0.009
	3	0.013	<0003	<0.32 [b]	-
	x	0.006	0.003	0.030	0.012
	σ	0.006	-	0.024	0.004

(a) Cyclic flow minute volume
(b) Not included in average due to low challenge concentration

Table I-3. Summary of Measured Penetrations through MSA Flexi-Filter

| Flow Rate (L/min) | Trial | Bioaerosol Challenge | | | |
| | | Bg "Wet" | Bg "Dry" | MS2 "Wet" | MS2 "Dry" |
		Penetration (%)			
42.5 Constant	1	<0.002	<0.001	1.4	<0.001
	2	<0.002	0.012	0.24	<0.016
	3	<0.002	<0.001	0.012	-
	x	**0.002**	**0.005**	**0.55**	**0.009**
	σ	-	**0.007**	**0.75**	**0.010**
135 Constant	1	<0.004	0.013	2.7	0.010
	2	0.006	0.018	0.80	0.004
	3	0.005	0.011	0.43	-
	x	**0.005**	**0.014**	**1.3**	**0.007**
	σ	**0.001**	**0.004**	**1.2**	**0.004**
42.5 Cyclic[a]	1	0.003	0.014	1.0	<0.002
	2	<0.002	0.010	0.16	<0.004
	3	<0.003	0.014	2.1	-
	x	**0.003**	**0.013**	**1.1**	**0.003**
	σ	**0.001**	**0.002**	**1.0**	**0.002**
67.5 Cyclic[a]	1	0.003	0.036	0.68	0.022
	2	0.080	0.017	0.81	0.029
	3	0.019	0.037	0.13	-
	x	**0.034**	**0.030**	**0.54**	**0.025**
	σ	**0.041**	**0.011**	**0.36**	**0.005**

(a) Cyclic flow minute volume
(b) Low challenge, not included in average

Table I-4. Summary of Measured Penetrations through North 7506

| Flow Rate (L/min) | Trial | Bioaerosol Challenge | | | |
| | | Bg "Wet" | Bg "Dry" | MS2 "Wet" | MS2 "Dry" |
		Penetration (%)			
42.5 Constant	1	0.008	0.003	0.39	0.001
	2	<0.004	0.003	0.32	0.002
	3	<0.003	0.012	0.19	-
	x	**0.005**	**0.006**	**0.30**	**0.001**
	σ	**0.003**	**0.005**	**0.10**	**0.001**
135 Constant	1	0.009	0.16	0.78	0.022
	2	<0.005	0.018	2.1	0.021
	3	0.013	0.042	2.9	-
	x	**0.009**	**0.074**	**1.9**	**0.022**
	σ	**0.004**	**0.075**	**1.1**	**0.001**
42.5 Cyclic[a]	1	0.004	0.030	0.53	0.004
	2	0.010	0.026	4.0	0.007
	3	0.004	0.110	0.54	-
	x	**0.006**	**0.055**	**1.7**	**0.005**
	σ	**0.004**	**0.047**	**2.0**	**0.002**
67.5 Cyclic[a]	1	0.021	0.039	1.0	0.006
	2	0.013	0.023	4.3	0.018
	3	0.008	0.035	2.1	-
	x	**0.014**	**0.032**	**2.5**	**0.012**
	σ	**0.007**	**0.001**	**1.7**	**0.009**

(a) Cyclic flow minute volume

Table I-5. Summary of Measured Penetrations through 3M 8293

Flow Rate (L/min)	Trial	Bioaerosol Challenge			
		Bg "Wet"	Bg "Dry"	MS2 "Wet"	MS2 "Dry"
		Penetration (%)			
85	1	<0.003	0.018	<0.001	<0.002
	2	<0.003	<0.003	<0.001	<0.002
	3	<0.003	<0.001	<0.001	-
	x	0.003	0.008	0.001	0.002
	σ	-	0.009	-	-
270	1	<0.008	<0.002	<0.012	<0.004
	2	<0.012	<0.003	<0.014	<0.004
	3	<0.009	<0.004	<0.015	-
	x	0.010	0.003	0.014	0.004
	σ	0.002	0.001	0.002	-
85[a]	1	<0.009	<0.002	<0.004	<0.005
	2	<0.004	<0.001	<0.001	0.014
	3	<0.003	<0.001	<0.001	-
	x	0.005	0.001	0.002	0.009
	σ	0.003	0.001	0.002	0.006
135[a]	1	<0.005	<0.001	<0.001	<0.003
	2	<0.007	<0.001	<0.001	<0.002
	3	<0.003	0.008	<0.008	-
	x	0.005	0.003	0.003	0.003
	σ	0.002	0.004	0.004	0.001

(a) Cyclic flow minute volume
(b) Low challenge, not included in average

Table I-6. Summary of Measured Penetrations through Moldex 2396

Flow Rate (L/min)	Trial	Bioaerosol Challenge			
		Bg "Wet"	Bg "Dry"	MS2 "Wet"	MS2 "Dry"
		Penetration (%)			
85 Constant	1	0.056	0.034	0.008	<0.004
	2	<0.008	0.004	<0.002	<0.004
	3	<0.004	0.015	0.006	-
	x	0.023	0.017	0.005	0.004
	σ	0.029	0.015	0.003	-
270 Constant	1	<0.007	<0.004	0.057	<0.005
	2	0.015	0.004	0.043	<0.003
	3	<0.014	<0.005	0.051	-
	x	0.012	0.004	0.050	0.004
	σ	0.004	0.001	0.007	0.001
85 Cyclic[a]	1	0.008	<0.001	<0.002	<0.002
	2	0.005	<0.001	<0.001	0.026
	3	0.007	0.006	0.001	-
	x	0.006	0.003	0.001	0.014
	σ	0.002	0.003	0.001	0.017
135 Cyclic[a]	1	0.010	<0.002	0.014	<0.007
	2	<0.006	0.001	0.013	<0.002
	3	0.010	0.007	<0.003	-
	x	0.009	0.003	0.010	0.004
	σ	0.002	0.003	0.006	0.04

(a) Cyclic flow minute volume

I-4

Table I-7. Summary of Measured Penetrations through MSA Affinity Plus

| Flow Rate (L/min) | Trial | Bioaerosol Challenge | | | |
| | | Bg "Wet" | Bg "Dry" | MS2 "Wet" | MS2 "Dry" |
		Penetration (%)			
85 Constant	1	0.25	0.016	0.64	0.010
	2	0.12	0.069	0.10	<0.004
	3	0.008	0.019	0.80	-
	x	**0.13**	**0.035**	**0.51**	**0.007**
	σ	**0.12**	**0.030**	**0.37**	**0.004**
270 Constant	1	0.071	0.029	3.0	0.011
	2	0.11	0.059	0.35	0.006
	3	0.28	0.038	0.34	-
	4	0.075	-	-	-
	x	**0.13**	**0.042**	**1.7**	**0.009**
	σ	**0.099**	**0.016**	**1.8**	**0.004**
85 Cyclic[a]	1	0.19	0.087	0.18	0.028
	2	0.52	0.18	0.89	0.016
	3	0.48	0.13	1.6	-
	4	0.19	-	1.1	-
	x	**0.35**	**0.13**	**0.93**	**0.022**
	σ	**0.18**	**0.048**	**0.60**	**0.009**
135 Cyclic[a]	1	0.032	0.13	1.2	0.060
	2	0.021	0.52	0.31	0.10
	3	0.069	1.28	1.1	-
	4	0.065	-	1.8	-
	x	**0.047**	**0.64**	**1.1**	**0.082**
	σ	**0.024**	**0.59**	**0.61**	**0.030**

(a) Cyclic flow minute volume
(b) Low challenge, not included in average

Table I-8. Summary of Measured Penetrations through Gerson 1730

| Flow Rate (L/min) | Trial | Bioaerosol Challenge | | | |
| | | Bg "Wet" | Bg "Dry" | MS2 "Wet" | MS2 "Dry" |
		Penetration (%)			
85 Constant	1	0.062	0.034	0.30	0.028
	2	0.022	0.030	0.72	0.40
	3	0.024	0.020	-	-
	x	**0.036**	**0.028**	**0.51**	**0.22**
	σ	**0.023**	**0.007**	**0.30**	**0.27**
270 Constant	1	0.39	0.25	1.6	1.0
	2	0.22	0.22	1.3	0.037
	3	0.60	0.12	2.4	-
	x	**0.40**	**0.20**	**1.8**	**0.52**
	σ	**0.18**	**0.064**	**0.55**	**0.69**
85 Cyclic[a]	1	0.28	0.096	0.43	0.60
	2	0.13	0.13	0.77	6.8[b]
	3	0.24	0.36	0.53	-
	x	**0.21**	**0.20**	**0.48**	**0.60**
	σ	**0.077**	**0.14**	**0.07**	-
135 Cyclic[a]	1	0.17	0.32	0.90	0.099
	2	0.30	1.6	0.35	0.051
	3	0.30	5.2	1.4	-
	4	-	-	0.89	-
	x	**0.26**	**2.4**	**0.89**	**0.075**
	σ	**0.074**	**2.5**	**0.43**	**0.034**

(a) Cyclic flow minute volume
(b) Probable leak in seal to system, not included in average

Blank

APPENDIX J

SUMMARY OF REAEROSOLIZATION RESULTS

Table J-1. Summary of Reaerosolization Trials with 0.8 µm PSL Aerosol

| Filter Type | Trial | Filtering Facepiece Loading | | Collection Filter | | Reaerosolization (%) | Average (%) | St Dev |
		Density (#/cm²)	Number (#)	Pre-Cough (#)	Post-Cough (#)			
MSA Affinity Plus (No Valve)	1	1.3x10⁴	2.2 x10⁶	0	3	0.0001		
	2	1.7x10⁴	3.0 x10⁶	12	66	0.002	0.001	0.001
	3	-	-	-	-	-		
MSA Affinity Plus (No Valve)	1	1.4x10⁵	2.4 x10⁷	350	200	0.0008		
	2	1.4x10⁵	2.5 x10⁷	95	205	0.0008	0.0006	0.0003
	3	1.6x10⁵	2.8 x10⁷	0	75	0.0003		
MSA Affinity Plus (No Valve)	1	8.2x10⁵	1.4 x10⁸	20	175	0.0001		
	2	8.2x10⁵	1.4 x10⁸	50	700	0.0005	0.0005	0.0003
	3	8.2x10⁵	1.4 x10⁸	145	1070	0.0007		
MSA Affinity Plus (With Valve)	1	1.8x10⁴	2.8 x10⁶	35	200	0.007		
	2	2.5x10⁴	3.9 x10⁶	50	362	0.009	0.007	0.002
	3	1.7x10⁴	2.6 x10⁶	58	150	0.006		
Gerson 1730 (No Valve)	1	1.4x10⁴	2.4 x10⁶	25	65	0.003		
	2	1.5x10⁴	2.6 x10⁶	100	70	0.003	0.003	0.0003
	3	2.4x10⁴	4.1 x10⁶	25	85	0.002		
Gerson 1740 (With Valve)	1	3.3x10⁴	4.9 x10⁶	410	600	0.012		
	2	4.6x10⁴	7.0 x10⁶	30	775	0.011	0.009	0.005
	3	2.9x10⁴	4.3 x10⁶	15	120	0.003		
Gerson 1740 (Valve Protected During Loading)	1	2.2x10⁴	3.4 x10⁶	15	145	0.004		
	2	2.5x10⁴	3.8 x10⁶	25	155	0.004	0.004	0.0002
	3	2.2x10⁴	3.3 x10⁶	165	130	0.004		

Table J-2. Summary of Reaerosolization Trials with 2.2 µm PSL Aerosol

| Filter Type | Trial | Filtering Facepiece Loading | | Collection Filter | | Reaerosolization (%) | Average (%) | St Dev |
		Density (#/cm²)	Number (#)	Pre-Cough (#)	Post-Cough (#)			
Gerson 1730 (No Valve)	1	1.7x10³	2.9 x10⁵	85	20	0.006		
	2	2.7x10³	4.6 x10⁵	35	35	0.008	0.009	0.005
	3	2.1x10³	3.6 x10⁵	30	50	0.015		
Gerson 1740 (With Valve)	1	1.9x10³	2.9 x10⁵	130	20	0.006		
	2	1.7x10³	2.5 x10⁵	80	35	0.014	0.012	0.005
	3	2.1x10³	3.2 x10⁵	35	52	0.016		

Table J-3. Summary of Reaerosolization Trials with Bg Spore Aerosol

Filter Type	Wet/Dry	Trial	Filtering Facepiece Loading Density (#/cm²)	Number (#)	Collection Filter Pre-Cough (#)	Post-Cough (#)	Reaerosolization (%)	Average (%)	St Dev
MSA Affinity Plus (No Valve)	Wet	1	9.2×10^2	1.6×10^5	100	55	0.034		
		2	9.0×10^2	1.6×10^5	262	60	0.037	0.035	0.002
		3	-	-	-	-	-		
MSA Affinity Plus (With Valve)	Wet	1	6.8×10^2	1.2×10^5	20	55	0.046		
		2	6.8×10^2	1.2×10^5	10	25	0.019	0.040	0.018
		3	6.5×10^2	1.1×10^5	10	60	0.054		
Gerson 1730 (No Valve)	Wet	1	1.2×10^3	2.1×10^5	30	140	0.065		
		2	2.2×10^3	3.8×10^5	30	170	0.045	0.056	0.012
		3	1.0×10^3	1.8×10^5	35	105	0.058		
Gerson 1740 (With Valve)	Wet	1	3.8×10^2	2.4×10^6	8	115	0.18		
		2	8.0×10^2	2.6×10^6	0	20	0.012	0.094	0.13
		3	-	-	-	-	-		
Gerson 1730 (No Valve)	Dry	1	1.2×10^4	2.1×10^6	-	2670	0.13		
		2	-	-	-	-	-	0.13	-
		3	-	-	-	-	-		
Gerson 1740 (With Valve)	Dry	1	1.5×10^4	2.3×10^6	-	3550	0.16		
		2	-	-	-	-	-	0.16	-
		3	-	-	-	-	-		

Table J-4. Summary of Reaerosolization Trials with MS2 Phage Aerosol

Filter Type	Wet/Dry	Trial	Filtering Facepiece Loading Density (#/cm²)	Number (#)	Collection Filter Pre-Cough (#)	Post-Cough (#)	Reaerosolization (%)	Average (%)	St Dev
MSA Affinity Plus (No Valve)	Wet	1	1.1×10^4	2.0×10^6	1090	765	0.038		
		2	1.7×10^4	2.9×10^6	35	3610	0.124	0.066	0.050
		3	1.7×10^4	2.9×10^6	175	1050	0.035		
MSA Affinity Plus (With Valve)	Wet	1	9.3×10^3	1.5×10^6	1300	890	0.06		
		2	8.9×10^3	1.5×10^6	0	300	0.02	0.11	0.12
		3	1.1×10^4	1.7×10^6	610	4300	0.3		
Gerson 1730 (No Valve)	Wet	1	1.8×10^4	1.3×10^6	35	200	0.007		
		2	2.5×10^4	1.6×10^6	50	362	0.009	0.007	0.002
		3	1.7×10^4	2.2×10^6	58	150	0.006		
Gerson 1730 (No Valve)	Dry	1	7.8×10^4	1.3×10^7	730	42,000	0.32		
		2	6.8×10^4	1.1×10^7	0	61,000	0.53	0.46	0.13
		3	6.4×10^4	1.0×10^7	60	59,000	0.54		
Gerson 1740 (With Valve)	Dry	1	4.1×10^4	6.2×10^6	1900	43,000	0.69		
		2	1.3×10^4	2.0×10^6	960	9,700	0.49	0.51	0.18
		3	8.9×10^3	1.3×10^6	880	4,500	0.30		

DEPARTMENT OF THE ARMY
CDR USARDECOM
ATTN AMSRD CII
5183 BLACKHAWK ROAD
APG MD 21010-5424

OFFICIAL BUSINESS

FIRST CLASS